UNIVERSITY OF ADELAIDE
FACULTY OF SCIENCES
School of Biological Sciences

LINKING CHEMISTRY AND SCLEROCHRONOLOGY TO PHYSIOLOGICAL PROCESSES IN FISH

Jasmin Carmel Amina Martino
This thesis is presented towards the degree of
Doctor of Philosophy
January 2019

DECLARATION

I certify that this work contains no material which has been accepted for the award of any other degree or diploma in my name, in any university or other tertiary institution and, to the best of my knowledge and belief, contains no material previously published or written by another person, except where due reference has been made in the text. In addition, I certify that no part of this work will, in the future, be used in a submission in my name, for any other degree or diploma in any university or other tertiary institution without the prior approval of the University of Adelaide and where applicable, any partner institution responsible for the joint-award of this degree.

I acknowledge that copyright of published works contained within this thesis resides with the copyright holder(s) of those works.

I also give permission for the digital version of my thesis to be made available on the web, via the University's digital research repository, the Library Search and also through web search engines, unless permission has been granted by the University to restrict access for a period of time.

I acknowledge the support I have received for my research through the provision of an Australian Government Research Training Program Scholarship.

Jasmin Carmel Amina Martino

TABLE OF CONTENTS

PUBLICATIONS AND CONTRIBUTIONS

CHAPTER TWO: Using otolith chronologies to understand long-term trends and extrinsic drivers of growth in fisheries.

Authors: *Martino JC, Fowler AJ, Doubleday ZA, Grammer GL, Gillanders BM.*

Status: Published in *Ecosphere* 10, e02553.

CHAPTER THREE: Metabolic effects on carbon isotope biomarkers in fish tissues

Authors: *Martino JC, Doubleday ZA, Gillanders BM.*

Status: Published in *Ecological Indicators 97:10-16.*

CHAPTER FOUR: Biominerals track metabolic rates in fish

Authors: *Martino JC, Doubleday ZA, Gillanders BM.*

Status: Prepared for submission.

CHAPTER FIVE: Disentangling intrinsic and extrinsic drivers of otolith chemistry in a coastal marine fish

Authors: *Martino JC, Fowler AJ, Doubleday ZA, Gillanders BM.*

Status: Prepared for submission.

CO-AUTHOR AFFILIATIONS

Bronwyn M Gillanders
School of Biological Sciences
University of Adelaide
Adelaide, South Australia, Australia

Zoë A Doubleday
School of Biological Sciences
University of Adelaide
Adelaide, South Australia, Australia

Anthony J Fowler
South Australian Research and Development
Institute (Aquatic Sciences)
West Beach, South Australia, Australia

Gretchen L Grammer
South Australian Research and Development
Institute (Aquatic Sciences)
West Beach, South Australia, Australia

ABSTRACT

Physiology underpins how species survive, reproduce and interact with their environment. Many fish populations are difficult to directly monitor due to the vastness and complexity of aquatic habitats. Retrospective tracking using intrinsic biomarkers is a powerful alternative that is both effective and inexpensive. This thesis investigates physical and chemical biomarkers for reconstructing physiological processes (growth and metabolic rate) in fish. Physiological histories can uncover health and physical performance of individuals, reveal biological responses to external environments and are key in understanding the functioning, movement and biomass of wild fish populations.

My study species was the iconic and valuable fishery species, Australasian snapper (*Chrysophrys auratus*). Recent changes and downturns in commercial catch of snapper have provoked concerns about long-term sustainability and spatial structure of the fishery in South Australia. Exposing physiological mechanisms behind the population and fishery dynamics will assist to understand contributing factors to the changes.

Somatic growth rate is a primary predictor for a wide-range of biological and ecological processes. Using otolith sclerochronology and mixed-effects modelling, I reconstructed nearly four decades (37 years) of growth in snapper across four oceanographically diverse regions and investigated the influence of extrinsic factors. Growth was found to decline in the two most productive regions. Across all regions, snapper growth was influenced by primary productivity, temperature, extreme climatic episodes, and population density.

In experiemental settings, I investigated the link between stable isotopes in fish tissues and physiology. Juvenile snapper were reared in four temperature treatments and carbon isotopes ($\delta^{13}C$) were measured in hard-tissues (otoliths), soft-tissues (muscle and liver) and potential carbon sources (water and diet). Intermittent-flow respirometry was then used to calculate metabolic rates. Metabolic effects significantly influenced the incorporation of carbon isotopes in all tissues. A significant negative linear relationship was found between carbon isotopes and metabolic rates. However, with increasing stress (heat and exertion), this negative relationship switched to an increasingly positive relationship. This research validates the use of carbon isotopes as metabolic biomarkers and is an important precursor to using otolith chemistry to track metabolic rates in the field.

The relationships between otolith chemistry, intrinsic properties, and environmental conditions were then investigated in wild snapper. I analysed lifetime profiles of stable isotopes of carbon and oxygen ($\delta^{18}O$), and elemental signatures of magnesium (Mg:Ca), strontium (Sr:Ca), barium (Ba:Ca), manganese (Mn:Ca) and lithium (Li:Ca) in snapper across two oceanographically diverse regions (northern Spencer Gulf and the South-East in South Australia) and three cohorts (1979, 1991, 2006) to examine regional and temporal variation. Mixed-effects modelling was used to investigate the influence of intrinsic properties (age, otolith growth, fish length, sex) and environmental factors (sea surface temperature and chlorophyll-*a*) on chemical markers. Carbon isotopes, magnesium and, to a lesser extent, strontium were found to relate to intrinsic characteristics and their utility in reconstructing lifetime physiological trends is suggested. The chemical chronologies also improved our understanding of movement histories in wild snapper populations. Our results highlight the use of isotopic and elemental chemistry in otoliths for reconstructing environmental, migration and physiological histories in wild fish populations.

In this thesis, I demonstrate the potential of physical and chemical tags in otoliths as physiological biomarkers. The developed techniques are transferable to other fish species to address a widerange of ecological questions. The long-term growth, chemical and metabolic histories developed for snapper help to understand the processes driving population dynamics and productivity. Intrinsic biomarkers are powerful tools and will help sustainable management of wild fish into the future.

ACKNOWLEDGMENTS

I would still be a floundering fingerling lost in the blue abyss if not for the exhaustive encouragement from my incredible support network.

First and foremost, thank you to my generous and extraordinary supervisors. Thank you for always being there when I needed you, with positive attitudes and open-doors.

Bronwyn Gillanders, thank you for taking a huge chance on unexperienced newcomer. The learning curve was steep but rewarding and I am very grateful for your patience, encouragement and confidence in my abilities.

Zoë Doubleday, thank you for always finding interesting project avenues and narrative angles. You have taught me how to tell a story and that science writing does not have to be dull! I am sure you have shaped my writing for years to come.

Anthony Fowler, thank you for sharing your invaluable knowledge on fisheries and snapper. You helped ground my project in reality and taught me the significance of details. I know I am a better scientist because of you.

Thank you Gretchen Grammer and John Morrongiello for your valuable help with mixed-effects modelling, Mark Rollog and Kristine Nielson for your enthusiastic assistance in isotope analysis, and Rob Michael for help with obtaining juvenile snapper from the wild.

I am grateful for the intellectual and emotional support from my marine science peers. Thank you in particular - Troy Rogers, Matt McMillan, Shannon Lauchlan, Nina Wootton, Koster Sarakinis, Jackson Stockbridge, Alice Jones, Sophie Dolling, Kayla Gilmore, and James Walker.

Most importantly, I am forever grateful for the love and understanding from my family. Thank you for endlessly encouraging and supporting me through this journey. Thank you to my grandparents, your sacrifices and hard-work will never be forgotten.

CHAPTER ONE

INTRODUCTION

Fish and physiological histories

Fish are ecological staples of aquatic environments. Fish populations are also a primary source of protein and income for billions of people worldwide (Worm, 2016). However, fish currently face increasing environmental and anthropogenic stressors which has led to global declines in fish stocks (Bell et al. 2017, Pauly and Zeller 2016, Worm 2016). For example, climate change is expected to increase ocean temperatures by up to 3°C by 2100 and increase frequencies of extreme climatic events (Cai et al. 2014, IPCC 2014). Concurrently, large-scale fishing continues to exert biological and ecological selective pressures on fish populations worldwide (Audzijonyte et al. 2013, Swain et al. 2007). Climate change and fishing are predicted to act as cumulative stressors, with the loss of biodiversity and truncation of age and geographic structuring due to fishing increasing the sensitivity of fish populations and marine ecosystems to environmental change (Berkeley et al. 2004, Brander 2007, Ottersen et al. 2006). Documenting long-term ecological trends is an important step in understanding responses to cumulative stressors and to enable us to enact effective countermeasures to protect and recover populations into the future.

Intrinsic biomarkers

Direct monitoring of fish populations can be expensive, labour-intensive and is often susceptible to sampling bias. Retrospective reconstructions using intrinsic biomarkers offer a cost-effective and efficient alternative. Chemical signatures in tissues provide valuable insights into short and long-term biological histories. Animal tissues exhibit varying rates of chemical turnover and incorporation, reflecting a range of time periods from decades to ‘snapshots’ of dietary inputs. Soft-tissues such as muscle and liver tissues, exhibit relatively rapid metabolic turnover but can provide valuable snapshots into recent biological trends. Carbon isotope signatures ($\delta^{13}C$) in softtissues have been used extensively to track dietary sources and uncover trophic structures and nutrient pathways (Boecklen et al. 2011, Pasquaud et al. 2007, Rau et al. 1983). However, diet-totissue carbon fractionation can vary between species, diets and tissues with recorded values from bulk isotope analysis ranging from 1‰ (DeNiro and Epstein 1978) to 5‰ (Bloomfield et al. 2011, Gaston and Suthers 2004).

In contrast, hard calcified structures, such as bones or shells, exhibit low metabolic activity and slow turn-over rates, and thus can incorporate long-term isotopic signatures. Hard calcified structures also show minimal degradation through time and extensive archives exist in research institutes and museums world-wide, providing easy access to a wide range of species, locations and year classes. Ear stones (otoliths) in teleost fish are valuable chemical and physical repositories of information that can be used to reconstruct the lifetime histories of fish. Otoliths are calcium carbonate ($CaCO_3$) structures which are acellular and metabolically inert, creating lifetime chemical profiles that are permanently locked into the structure (Campana 1999). Otoliths also have annually-forming translucent and opaque bands which correspond with somatic growth and provide age estimates, allowing for growth and chemical signatures to be matched to age and calendar years (Campana and Thorrold 2001). Otoliths have previously been used to identify past movements (Elsdon et al. 2008, Miles et al. 2018) and nursery habitats (Kitchens et al. 2018, Wright et al. 2018); track past environmental histories (Crook et al. 2017, Elsdon and Gillanders 2005); and distinguish between populations or clarify stock structure (Bastow et al. 2002, Fowler et al. 2017). To effectively apply otolith chemistry for reconstructing past histories, it is important to understand the sources of chemical signatures and the influences on their incorporation into otoliths. Generally ions are taken up from the environmental water via the gills or intestines into the blood plasma, then into the endolymphatic fluid to be accreted onto the surface of the otolith (Campana 1999). However, chemical discrimination can occur at each physiological barrier along this pathway with varying degrees of discrimination among elements (Campana 1999). Chemical signatures with high physiological regulation may reflect fish physiology and individual genetic makeup (Gronkjaer 2016), whereas chemical signatures with little physiological discrimination are more strongly likely to reflect environmental conditions (Izzo et al. 2018, Thomas et al. 2017).

Otoliths may reconstruct long-term physiological histories in fish. Physiology is an important indicator of health and physical performance, revealing important biological responses to external environments and is key in understanding the functioning, movement and biomass of wild fish populations. Otolith chronologies may track growth trends (Doubleday et al. 2015, Morrongiello and Thresher 2015, Weisberg et al. 2010), identify metabolic activity (Kalish 1991, Sherwood and Rose 2003, Wurster et al. 2005, Trueman et al. 2016), and provide further insights in physiological activity (Gronkjaer 2016, Limburg et al. 2018). Consequently, long-term physiological histories reconstructed from otoliths can address a wide-range of ecological questions for use in conservation and management of wild populations. However, further method development and validation is needed to improve the accuracy of otolith chronologies for reconstructing physiological histories in fish.

Physiological processes

Somatic growth in fish

Somatic growth is a primary predictor of a wide-range of biological and ecological processes. Faster growth rates increase the sizes of individual fish which leads to higher stock biomass and reproductive output; lower natural mortality (Barneche et al. 2018, Hixon et al. 2014); as well as increased success in ecological interactions such as predator-prey relationships and interspecific competition (Lewin et al. 2006, Rose et al. 2001). Even small changes in fish size can significantly alter rates of mortality, biomass and catch (Audzijonyte et al. 2013). As such, growth models are used extensively in stock assessments to determine size-related population processes, performance measures and reference points (Lorenzen 2016). Consequently, there is value in mapping trends in growth and the influences of growth to identify key population parameters to inform fishery management. Fish typically have indeterminate growth (Sebens 1987) that is subject to high degrees of genetic variation and responds rapidly to external selection pressures (Bœuf and Payan 2001). Genetic make-up can shape growth potential and the extent of phenotypic-plasticity, which are the adaptive physical responses (e.g. changes of morphometrics, behaviour, physiology) of a specific genotype to environmental conditions (Fusco and Minelli 2010, Price et al. 2003). Fish growth can also be influenced by broad climatic shifts that alter ocean climates (Gillanders et al. 2012, Macfarlane et al. 2005, Ong et al. 2018); ocean productivity, which affects the availability of food (Do Souto et al. 2018, Rosenfeld et al. 2005); and population densities and intra-specific competition (Lewin et al. 2006, Rose et al. 2001; Stephens and Sutherland 1999). While there are inherent genetic differences between individuals, extrinsic pressures play a key role in shaping lifetime fish growth and need to be considered in fishery strategies.

Long-term growth histories can be developed from otoliths. Growth trends and influences on growth can be established by measuring bands in otoliths that reflect annual somatic growth and matching these to age, calendar years and corresponding extrinsic factors (Campana and Thorrold 2001, Morrongiello et al. 2012). Otolith sclerochronology has been combined with statistical approaches such as: fixed-effects modelling (Weisberg 1993); dendrochronology (Black et al. 2011); and Bayesian hierarchical modelling (Helser et al. 2012). Mixed-effects modelling is a powerful alternative which captures multiple biological (intrinsic) and environmental or anthropogenic (extrinsic) effects and provides detailed comparisons and interactions between them (Morrongiello and Thresher 2015, Weisberg et al. 2010). Mixed effects modelling overcomes limitations associated with many other approaches, such as overlooking within-fish or within-year correlations, and uniquely facilitate straightforward comparisons between different studies, locations or time periods (Weisberg et al. 2010).

Metabolic rates in fish

Metabolic rate is a key driver of physiological functioning in individuals and a propellant of ecosystem dynamics. Metabolic rate represents total energy use and influences biology at an individual (e.g. performance, growth, maintenance, physical activity, reproduction, and excretion), population (e.g. population dynamics and intra-specific competition) and ecosystem (e.g. ecological processes, trophic dynamics, and drain of resources) level (Brown et al. 2004, Chabot et al. 2016). Proxies for metabolic variation can be translated to quantitative population level predictions which aid in fishery and environmental planning. Bioenergetic models are an example of the application of physiological proxies and stem from calculating energy balance equations from independent estimates of physiological factors (Kitchell et al. 1977). Bioenergetic models are used extensively in large-scale ecosystem management to understand species and ecosystem-specific food consumption and predation morality, which can be used to set stocking quotas or harvest goals, to predict the effect of extrinsic changes (such as climate change) or to compare feeding habits between populations (Hansen et al. 1993, Chipps and Wahl 2008). Metabolic proxies have also been used to predict population-level growth trends or reproductive output. Consequently, estimates of metabolic rates greatly enhance our understanding of the functioning and dynamics of wild fish populations.

Laboratory experiments are a key step towards understanding field ecology. Physiological experiments derive important insights under controlled conditions, which assists to identify and isolate biological responses and their influences (Cooke et al. 2017). Direct calorimetry measures of metabolic rate involve measuring heat released during metabolic energy transformation, but are expensive and technically challenging to measure in fish (Nelson 2016, Treberg et al. 2016). Consequently, indirect calorimetry involving measurements of oxygen uptake are commonly used (Alexandre and Palstra 2017, Regan and Richards 2017). Indirect calorimetry can measure a range of metabolic attributes spanning from baseline to upper limit derivations, such as standard metabolic rates, maximum metabolic rates, and aerobic scope. Standard metabolic rate is a key physiological trait representing the minimum amount of energy to sustain life and has important implications for maximum performance, growth rate and lifestyle, and social interactions (Chabot et al. 2016). Maximum metabolic rate measures the upper limit of metabolic capacity and highlights potential energy usage (Norin and Clark 2016, Treberg et al. 2016). Absolute aerobic scope is the difference between standard and maximum metabolic rate, and illustrates energy niches and fitness/performance windows (Clark et al. 2013). Measuring metabolic rates in experimental conditions establishes baseline understandings on biological responses and their influences and is an important precursor for understanding metabolic rates in the field.

Stable carbon isotopes in otoliths may track metabolic rates but experimental validation is needed. Carbon isotopes in otoliths arise from two sources: (1) dissolved inorganic carbon in environmental water incorporated via gill or intestinal interfaces and (2) metabolically sourced carbon via the cellular respiration of food (Kalish 1991, McConnaughey et al. 1997, Sherwood and Rose 2003, Wurster et al. 2005). As metabolic demand increases, there is a concurrent increase in respiration and metabolic carbon dioxide (CO_2) which increases the proportion of the metabolic carbon in the blood and endolymph, which is subsequently deposited onto the otolith (Trueman et al. 2016). Metabolic carbon has a significantly depleted carbon signature (values are more negative) compared to water so changes in otolith carbon signatures are thought to be driven by metabolic shifts. The influence of other carbon sources is considered minimal as carbon signatures typically remain within a narrow range in marine waters, whilst considerable changes to diet are required to significantly alter values of otolith carbon (Kroopnick 1985, Schmittner et al. 2013, Trueman et al. 2016). Previous research establishes that carbon isotopes negatively correlate with estimates of standard metabolic rate predicted by metabolic theory in Atlantic cod (Chung et al. 2019b). Further experimental work is needed to validate this relationship in other species, particularly in warmer temperature ranges.

Elemental chemistry in otoliths may also uncover insights into fish physiology. No relationship has been found between magnesium concentrations (Mg:Ca) and factors such as water or diet, whilst there are suggestions that magnesium is taken up in proportion to metabolic activity (Limburg et al. 2018, Woodcock et al. 2012). Magnesium concentrations likely have high physiological regulation during incorporation into otoliths and may have potential to provide retrospective insights into physiological processes. Furthermore, strontium concentrations (Sr:Ca) have been related to both environment and physiology. While water sources likely contribute 59 - 83% of strontium in marine fish (Doubleday et al. 2013, Walther and Thorrold 2006, Webb et al. 2012), it has also been shown to be controlled by physiological processes

(Grammer et al. 2017, Izzo et al. 2016, Sturrock et al. 2015). Consequently, magnesium and strontium concentrations in otoliths may reveal understandings into past physiology in fish, particularly when considered in conjunction with carbon isotopes.

Study Species

Australasian snapper (*Chrysophrys auratus*) is an iconic and valuable fishery species that is broadly distributed in the Australasia and Indo-Pacific regions. Snapper dwell in diverse habitats including shallow bays and estuaries to the edge of the continental shelf (≤200 m). Australian snapper live up to 40 years (Norriss and Crisafulli 2010) and while slow growing, can reach 1.3 m and 20 kg (Gomon et al. 2008). Snapper are serial spawners that reach sexual maturity at 3-5 years (20-30cm FL; Fowler 2000, Francis and Pankhurst 1988). South Australia represents three biological stocks which are each dependent on a primary nursery area located in large coastal embayments (Fowler et al. 2017). There is high regional variability in oceanography and ecology among snapper habitats in South Australia and this has led to differences in population size, size at-age and commercial catch between regional populations (Fowler et al. 2016). Record snapper catches in South Australia were recorded from 2007 to 2012 followed by a considerable downturn. Management concerns were raised about long-term sustainability and changes to the spatial structure for the fishery (Fowler et al. 2017). Physiological histories will enhance our understanding of the processes that drive the population and fishery dynamics.

Objectives and thesis structure

This thesis investigates chemical and sclerochronology approaches to reconstruct physiological processes in fish. The thesis is organised as 4 data chapters (Chapters 2 – 5) that are written in the form of a stand-alone scientific paper suitable for publication in a peer-reviewed journal. Chapter one is a general introduction that presents and evaluates the published current literature on the thesis topic. Chapter 6 is a general discussion that consolidates and reviews the outcomes from the data chapters. Brief overview of each chapter is detailed below.

CHAPTER ONE: Introduction

This chapter is a literature review of the relevant information and past studies.

CHAPTER TWO: Using otolith chronologies to understand stressors of growth in fisheries

Objective: Use otolith sclerochronology and mixed-effects modelling to generate long-term growth chronologies and identify primary drivers in Australasian snapper growth across four oceanographically and ecologically diverse regions in southern Australia.

Growth is a primary predictor for a wide-range of biological and ecological processes and as such, growth models are used extensively in fishery management and stock assessments. This chapter used otolith sclerochronology and mixed-effects modelling to reconstruct nearly four decades (37 years) of growth across four oceanographically diverse regions in an iconic fishery species, snapper (*Chrysophrys auratus*). Growth was related to environmental factors (sea surface temperature, chlorophyll-*a* and Southern Oscillation Index) and population performance indicators (recruitment and commercial catch).

This chapter has been published in *Ecosphere* 10, e02553.

CHAPTER THREE: Metabolic effects on carbon isotope biomarkers in fish

Objective: Experimentally investigate the relationships between carbon isotopes in carbon sources, otoliths and soft-tissues and assess metabolic effects.

Carbon isotopes in otoliths may track metabolic rates in fish, while carbon isotopes in soft-tissues have been used to uncover trophic structures and nutrient pathways. I laboratory-reared juvenile snapper at four temperatures and then measured carbon isotopes in otolith, liver, muscle, ambient water and diet using isotope-ratio mass spectrometry (IRMS). Carbon composition in tissues were then compared to diet and water to investigate metabolic effects and the proportional contributions of carbon sources. This chapter was an important precursor to chapters four and five to investigate the influence of metabolic effects on carbon isotopes.

This chapter has been published in *Ecological Indicators* 97: 10-16.

CHAPTER FOUR: Biominerals track metabolic rates in fish

Objective: Under experimental conditions, measure and investigate the relationship between isotopes in otoliths (carbon and oxygen) and metabolic parameters (standard metabolic rate, maximum metabolic rate and absolute aerobic scope).

A geochemical tracer of metabolic rate in fish would allow development of long-term metabolic histories. A relationship may exist between carbon isotopes in otoliths and metabolic rates, but this relationship needs to be experimentally validated. I laboratory-reared juvenile snapper in three temperatures and then used intermittent-flow respirometry to calculate standard metabolic rates, maximum metabolic rates and absolute aerobic scope. Carbon isotopes in otoliths were then analysed and compared to metabolic rates to validate their potential as metabolic biomarkers.

CHAPTER FIVE: Disentangling intrinsic and extrinsic drivers of otolith chemistry in a coastal marine fish

Objective: Investigate intrinsic and extrinsic influences on otolith chemistry in wild Australasian snapper; assess the potential of chemical markers as metabolic proxies; and use chemical chronologies to reconstruct temporal and spatial patterns of South Australian snapper.

Lastly, the results derived from chapters 2-4 were applied to wild fish populations. Otolith samples were chosen from two regions characterised by significantly different growth patterns (chapter 2) and across three cohorts to investigate and incorporate spatial and temporal variation. Carbon and oxygen isotopes were analysed using IRMS and magnesium, strontium, barium, manganese and lithium concentrations were analysed using a laser ablation system coupled with an Inductively Coupled Plasma-Mass Spectrometer (ICP-MS). Mixed-effects modelling was then used to investigate the influence of age, physiological characteristics (otolith growth, fish size, sex) and environmental factors (sea surface temperature and chlorophyll-*a*) on otolith chemical markers. Chemical histories provided insights into the physiological and environmental histories of snapper within and among populations.

CHAPTER SIX: Discussion

This chapter provides a general discussion of the key thesis results from the data chapters and suggestions for future directions. The suitability and benefits of intrinsic markers were considered versus other approaches. I then discussed their ability to improve the understanding of wild fish populations and how they can help in fishery management.

Statement of Authorship

Title of Paper	Using otolith chronologies to understand long-term trends and extrinsic drivers of growth in fisheries		
Publication Status	☑ Published	☐ Accepted for Publication	
	☐ Submitted for Publication	☐ Unpublished and Unsubmitted work written in manuscript style	
Publication Details	Martino, J.C., Fowler, A.J., Doubleday, Z.A., Grammer, G.L., Gillanders, B.M., 2019. Using otolith chronologies to understand long-term trends and extrinsic drivers of growth in fisheries. Ecosphere 10, e02553.		

Principal Author

Name of Principal Author (Candidate)	Jasmin Martino		
Contribution to the Paper	Collected, analysed and interpretated data, wrote manuscript and acted as corresponding author.		
Overall percentage (%)	85%		
Certification:	This paper reports on original research I conducted during the period of my Higher Degree by Research candidature and is not subject to any obligations or contractual agreements with a third party that would constrain its inclusion in this thesis. I am the primary author of this paper.		
Signature		Date	

Co-Author Contributions

By signing the Statement of Authorship, each author certifies that:

i. the candidate's stated contribution to the publication is accurate (as detailed above);
ii. permission is granted for the candidate in include the publication in the thesis; and
iii. the sum of all co-author contributions is equal to 100% less the candidate's stated contribution.

Name of Co-Author	Anthony Fowler		
Contribution to the Paper	Supervised development of work, helped in data interpretation and manuscript evaluation.		
Signature		Date	25/1/19

Name of Co-Author	Zoe Doubleday		
Contribution to the Paper	Supervised development of work, helped in data interpretation and manuscript evaluation.		
Signature		Date	24/1/2019

Name of Co-Author	Gretchen Grammer		
Contribution to the Paper	Helped conduct analyses and data interpretation and manuscript evaluation.		
Signature		Date	25 Jan 2019

Name of Co-Author	Bronwyn Gillanders		
Contribution to the Paper	Supervised development of work, helped in data interpretation and manuscript evaluation.		
Signature		Date	24 Jan 2019

CHAPTER TWO

Using otolith chronologies to understand long-term trends and extrinsic drivers of growth in fisheries.

This research is published as:

Martino JC, Fowler AJ, Doubleday ZA, Grammer GL, Gillanders BM (2019) Using otolith chronologies to understand long-term trends and extrinsic drivers of growth in fisheries. Ecosphere 10, e02553.

ABSTRACT

Identifying trends and drivers of fish growth in commercial species is important for ongoing sustainable management, but there is a critical shortage of long-term datasets in marine systems. Using otolith (ear stone) sclerochronology and mixed-effects modelling, we reconstructed nearly four decades (37 years) of growth across four oceanographically diverse regions in an iconic fishery species, snapper (*Chrysophrys auratus*). Growth was then related to environmental factors (sea surface temperature, chlorophyll-*a* and Southern Oscillation Index) and population performance indicators (recruitment and commercial catch). Across the decades, growth rates declined in the two most productive fishery regions. Chlorophyll-*a* (a measure of primary productivity) was the best predictor of growth for all regions but direction and magnitude of the relationships varied, indicating regional-specific differences in intra-specific competition. Sea surface temperature was positively correlated with fish growth, but negatively correlated after temperature reached optimum thermal maxima, which suggests individuals in warmer regions may be under thermal stress. Growth also decreased at the extremes of the Southern Oscillation Index, indicating fish growth is impeded in significant climatic events. Contrasting relationships between growth, catch and recruitment indicated regional-specific density-dependent effects, with growth positively correlated with population size in one region but negatively correlated in another. Our results indicate that under future ocean warming and increased frequency of extreme climate events, fish growth and fisheries productivity is likely to be affected. Furthermore, the interactive effects of extrinsic factors also indicated that stressors on fisheries should be managed collectively. We show that otolith chronologies are an effective method to assess long-term trends and drivers of growth in fishery species. Such informed ecological predictions will help shape the sustainable management of fisheries under future changing climates.

INTRODUCTION

Sustainable management of natural resources necessitates accounting for long-term ecological change. Many fisheries worldwide are declining (Bell et al. 2017, Pauly and Zeller 2016), and it is vital to develop methods to detect potential stressors. Long-term ecological datasets establish baseline conditions, which can be used to identify and isolate possible causes of change from the baseline and provide context for natural variability (Hobbie et al. 2003, Reid and Ogden, 2006). Contextualising baseline conditions can also help in setting targets for restoration efforts (Reid and Ogden, 2006). Therefore, documenting historical change assists in understanding the present in order to anticipate the future. This is particularly important in relation to climate change, with the ocean forecast to warm by up to 3°C by 2100 and increasing occurrences of extreme climatic events, which will likely impact population functionality and productivity (Brander, 2010, Cai et al. 2014, IPCC, 2014). Understanding long-term trends and stressors can contribute to guiding the sustainable management of fisheries to the benefit of fish populations, the fishing industry and general community.

Fishery scientists are tasked with estimating individual sizes of fish and the factors that influence them so as to inform fishery management. Fish growth is a primary predictor used in this process. Faster growth rates increase the sizes of individual fish which leads to higher stock biomass and reproductive output; lower natural mortality (Barneche et al. 2018, Hixon et al. 2014); as well as increased success in ecological interactions such as predator-prey relationships and interspecific competition (Lewin et al. 2006, Rose et al. 2001). As such, growth models are used extensively in stock assessments to determine size-related population processes, performance measures and reference points (Lorenzen 2016). Furthermore, changes in growth can indicate physiological responses to changing environments or density-dependent responses to harvesting, which can have important implications for future planning. Consequently, there is value in mapping trends in growth to identify key population parameters to inform fishery management.

Fish typically have indeterminate growth (Sebens 1987) that is influenced by high genetic variation. Genetic make-up can shape growth potential and the extent of phenotypic-plasticity, which are the adaptive physical responses (e.g. changes of morphometrics, behaviour, physiology) of a specific genotype to environmental conditions (Fusco and Minelli 2010, Price et al. 2003). Multi-generational exposure to environmental pressures can also select for adapted genotypes in populations (Dingemanse and Wolf 2013). Genetically-determined growth rates are then mediated by the environmental conditions, with fish growth responding rapidly to immediate external selection pressures (Bœuf and Payan 2001). For example, ocean temperatures (within optimum thermal ranges) can increase growth rates as fish are ectothermic and available somatic energy reflects water temperatures (Barrow et al. 2017, Neuheimer et al. 2011, Smoliński and Mirny 2017). Fish growth can also be influenced by broad climatic shifts that alter ocean climates (Bruce Macfarlane et al. 2005, Gillanders et al. 2012, Ong et al. 2015); ocean productivity, which affects the availability of food (Do Souto et al. 2018, Rosenfeld et al. 2005); and population densities and intra-specific competition (Lewin et al. 2006, Rose et al. 2001, Stephens and Sutherland 1999). While there are inherent genetic influences between individuals, extrinsic pressures play a key role in shaping lifetime fish growth.

Many fish populations are difficult to monitor by direct observational methods, due to high costs and logistical difficulties associated with the vastness and complexity of oceanic environments. Historical reconstructions using otolith (ear stone) proxies offer a cost-effective and efficient alternative. Otoliths are metabolically-inert calcified structures that retain chemical and physical signatures that correspond to biological and environmental histories throughout a fish’s life (Campana 1999). Growth histories can be created through measuring translucent and opaque zones in otoliths that reflect yearly somatic growth and can be matched with age, calendar years and corresponding extrinsic factors (Campana and Thorrold 2001, Morrongiello et al. 2012). Otolith sclerochronology combined with mixed-effects modelling is a powerful approach for capturing multiple biological (intrinsic) and environmental or anthropogenic (extrinsic) effects (Morrongiello and Thresher 2015, Weisberg et al. 2010). Limited work has investigated the application of these sclerochronological approaches on temporal scales smaller than annual measurements. Consequently, there is potential to investigate the value of finer scale (such as seasonally or monthly-resolved) growth histories, which may offer a higher-resolution approach and capture small-scale, inter-annual variation relating to environmental fluctuations (Grammer et al. 2017, Izzo et al. 2016).

Here we use otolith chronologies to assess long-term growth variation and drivers of growth for an iconic fishery species of Australasia, snapper (*Chrysophrys auratus*). Our otolith samples represented a number of regional snapper populations that have demonstrated different trends in population biomass. We aimed to investigate the growth histories of snapper by 1) using a mixed-effects modelling approach to generate long-term growth chronologies from four distinctive regions; and 2) identify primary extrinsic drivers of the growth trends for each region.

METHODS

Study species

Snapper (*Chrysophrys auratus*) is a long-lived demersal finfish species that is broadly distributed in the Australasia and Indo-Pacific regions. Snapper dwell in diverse habitats including shallow bays and estuaries to the edge of the continental shelf (≤200 m). Australian snapper live up to 40 years (Norriss and Crisafulli 2010) and while slow growing, can reach 1.3 m and 20 kg (Gomon et al. 2008). Each mainland Australian state supports commercial and recreational fisheries, and it is one of Australia's most important and iconic fishery resources (Fowler et al. 2017). Record snapper catches in South Australia (SA) were recorded from 2007 to 2012 followed by a considerable downturn. Management concerns were raised about long-term sustainability and changes to the spatial structure for the fishery (Fowler et al. 2017). Growth histories of snapper from four key fishery regions will enhance our understanding of the processes that drive the population and fishery dynamics.

Snapper otoliths form a single annual increment that consist of an opaque and translucent zone (Ferrell et al. 1992, Fowler and McGlennon 2011). The theoretical 'birth-date' is 1 January, which is near the peak of the spawning season (Saunders et al. 2012). The opaque zone begins to form in September (austral spring) but is not generally delineated until January (Fowler et al. 2004, Wakefield et al. 2017). Furthermore, somatic growth of snapper strongly correlates with otolith width (Figure S2.1).

Study Regions

This study involved four oceanographically and ecologically diverse marine regions along the South Australian coastline (Figure 2.1). Northern Gulf St Vincent (NGSV) and Northern Spencer Gulf (NSG) are semi-enclosed reverse-estuaries which experience warm semi-arid/Mediterranean climates (Edyvane 1999). Both regions are hypersaline and display high variation in temperatures between summer and winter. In contrast, the South East (SE) and West Coast (WC) regions are open ocean ecosystems. The SE experiences the lowest oceanic temperatures with a temperate, meso-thermal climate and is also influenced by seasonal coldwater, coastal upwellings (Bonney Upwelling) which provide nutrients to surface waters

(Edyvane 1999). Some WC areas also get periodic coastal upwelling and are characterised by an ephemeral temperature inversion within the shelf waters, while other WC areas receive relatively nutrient poor, warm water from the Leeuwin Current (Edyvane 1999). Our samples represent three biological stocks which are each dependent on a primary nursery area (Fowler et al. 2016). NGSV supports its own primary nursery area and is a self-sustaining population. The biomass of snapper in the SE region is dependent on emigration and inter-annual variability in recruitment from primary nursery area in Port Phillip Bay, Victoria. NSG and WC comprise a single stock, where the primary nursery area is located in NSG from where fish migrate to the WC.

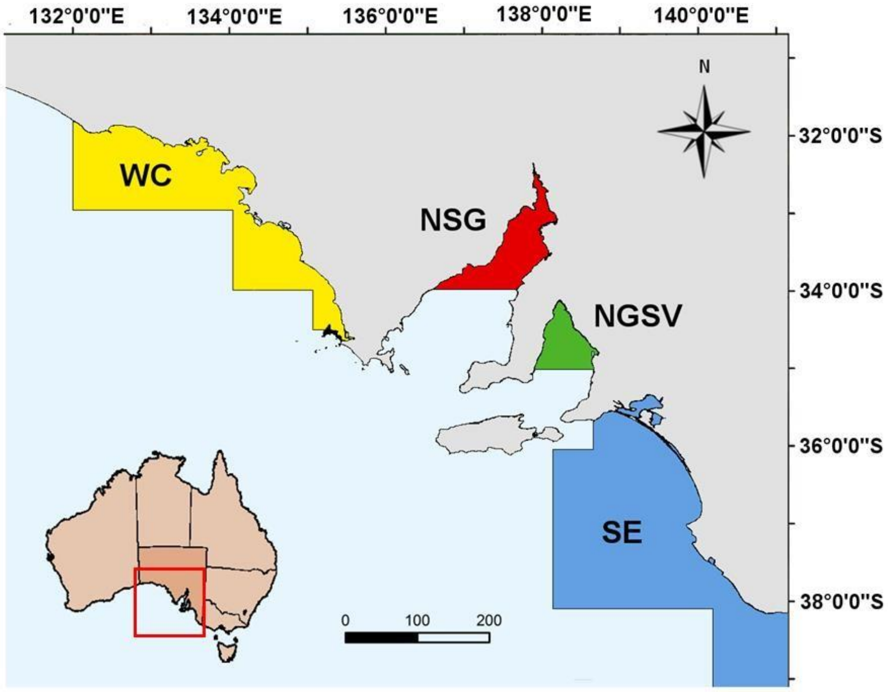

Figure 2.1 - Map of the South Australian coast showing the four study regions Northern Gulf St Vincent (NGSV), Northern Spencer Gulf (NSG), the South East (SE) and West Coast (WC).

Otolith preparation and increment measurement

An archived collection of sectioned snapper otoliths was provided by the South Australian Research and Development Institute (SARDI). These otoliths had been collected from fish between 2000 and 2017 by market sampling of commercial catches at Adelaide's wholesale fish market. Once a week, SARDI researchers visited the market to sample commercial catches from the South Australian regions. Individual fish were measured for caudal fork length (CFL) and weighed, and then both sagittal otoliths were removed. One otolith from each fish was embedded in clear setting epoxy resin (Struers Epofix), thinly sectioned (~400 µm) and then polished using lapping film. For this study, otoliths were selected for 541 mature fish from NGSV (*n* = 140), NSG (*n* = 142), SE (*n* = 152) and WC (*n* = 107). Ages ranged from 5 to 27 years. The previously prepared and aged transverse section from each fish was viewed with a stereo microscope (Olympus SZX7) and photographed using an attached digital camera (Olympus DP72). Annual increment widths were marked and measured (mm) along the dorsal antisulcus axis (core to marginal increment) using the imaging software Stream Basic (v1.9.1; Figure 2.2). A total of 4611 annual increments were measured.

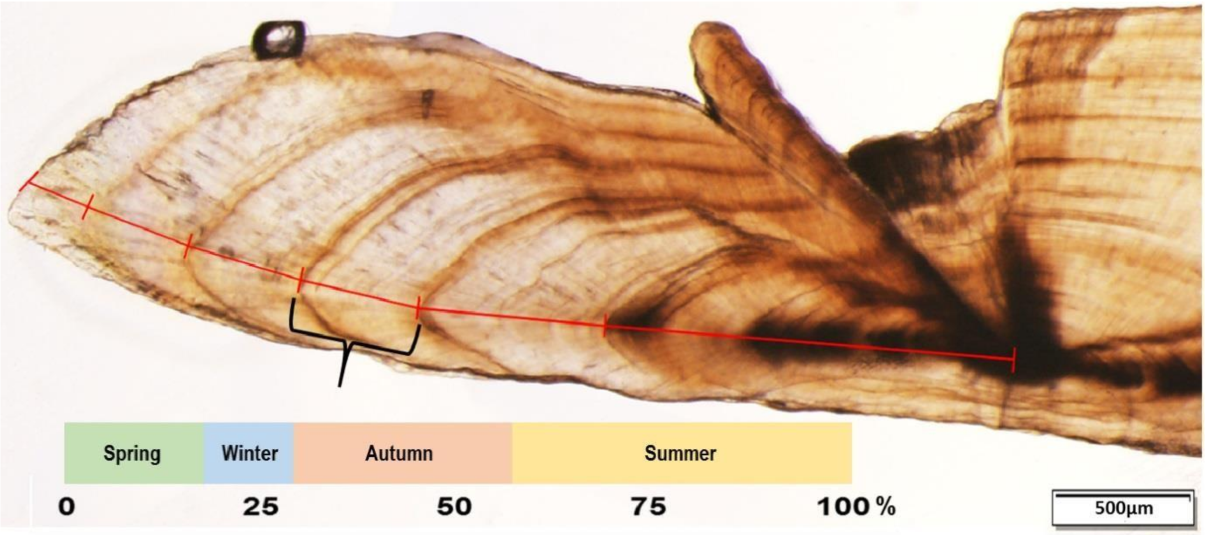

Figure 2.2 - Transverse section of snapper otolith showing the axis used for aging and growth measurements. The partitioning of the growth of one annual increment into seasonal percentages is shown.

Increments were assigned to a year by back-calculating from date of capture and accounting for marginal increment interpretation. Subsequently, estimates of yearly age (Age), age-at-capture (Age-at-capture) and year class (Cohort) were designated. The total number of increments measured spanned 36 years for NGSV (1980 – 2016), 37 years for NSG (1979 – 2016), 31 years for SE (1983 – 2014) and 24 years for WC (1992 – 2016; Figure 2.3). The first increment (core to first opaque zone) and marginal increment were removed from analysis, as they did not comprise a complete year of growth. The sample depth was at least five increment measurements per calendar year for each region. Annual increment measurements were separated into seasonal growth, based on percentages from a previous marginal increment analysis (Fowler et al. 2004; Figure 2.2). The values represented averages from fish aged 5/6 and 11/12. Minor variation occurred between year classes and ages but the overall trends across the large sample size (*n*=776) was consistent which provides evidence that these values are accurate proxies of seasonal growth in snapper.

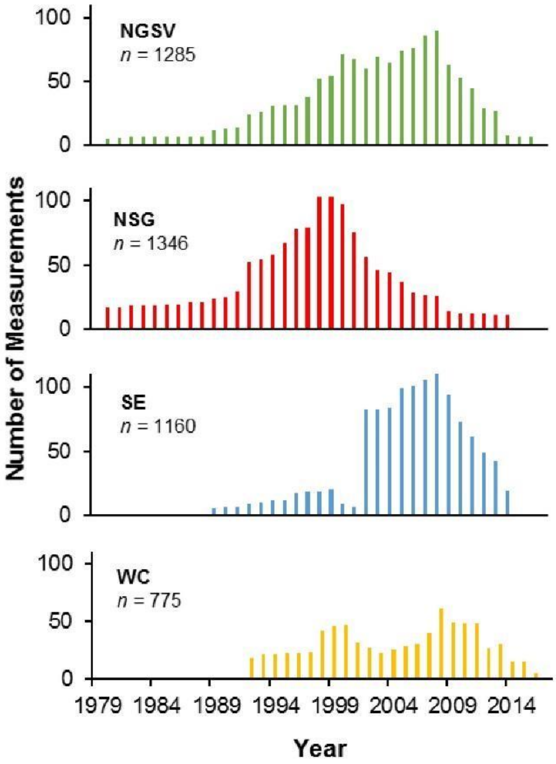

Figure 2.3 - Accumulated number of otolith annual increments in snapper measured for each calendar year for Northern Gulf St Vincent (NGSV), Northern Spencer Gulf (NSG), the South East (SE) and West Coast (WC). Total increment sample size (*n)* is indicated.

Growth predictors

Possible sources and drivers of growth variation were identified (Table 2.1). First, we investigated intrinsic variables, representing intra-population drivers (e.g. individual biology). Fixed intrinsic variables included Age and Age-at-capture, which account for expected age-related trends, bias and selectivity (Morrongiello et al. 2012). Fixed effects in seasonal models included Age and Age-at-capture as discrete values (e.g. one year = four seasons old).

We then examined extrinsic variables, representing external population drivers (e.g. environmental or population performance indicators), which included environmental covariates of Sea Surface Temperature (SST), Chlorophyll-*a* (Chl-*a*) and Southern Oscillation Index (SOI); biological estimates of Recruitment and commercial Catch (Table 2.1). Estimates of SST and Chl-*a* were accessed via the IMOS AODN (IMOS 2017). SST data were provided as a 72-hour, night-time composite from polar-orbiting satellites. Chl-*a* data, a representation of ocean productivity including phytoplankton biomass and abundance, were recorded from satellite daily images computed through OC3M algorithm. Localised values of SST and Chl-*a* were derived for each study region by defining boundary coordinates in AODN. SOI indicates large-scale climate events, specifically the intensity and direction of El Niño or La Niña episodes in the Pacific Ocean. Sustained negative SOI values (<-7) indicate warmer, lower-rainfall El Niño events, while sustained positive SOI values (>7) indicate cooler, higher-rainfall La Niña events. Climate effects can be experienced across Australia, including southern Australian oceans (Chiew et al. 1998). Estimates of SOI were accessed from an online database provided by the Australian Federal Government and calculated as a singular monthly data point that represents El Niño and La Niña events in the Pacific Ocean (Bureau of Meteorology 2017). Total commercial catches between 1984 and 2016 were determined from catch returns from commercial fishers reported through SARDI and stored in the Marine Scalefish Fisheries Information System. In this study, catch was used to indicate removal of biomass rather than being a measure of snapper abundance. Recruitment indices were calculated from regional age structures developed from estimates of fish age from market sampling and were available for all regions except WC (Fowler et al. 2016). For a number of annual age structures, annual estimates of Cohort strength were determined using catch curve regression that was fit to the natural log of the numbers of fish per age class (Maceina 1997). The residuals, representing the deviations from the abundances determined from the regression equation, were assumed to reflect the variation in Cohort strength (Fowler et al. 2016). Recruitment indicated the influx of young fish and increase to regional biomass, with strong cohorts represented by large positive values and weak cohorts by negative values.

For all extrinsic variables, significant temporal trends for the individual regions were assessed using linear regression in the statistical program R v3.4.1 (R Development Core Team 2014). Additionally, SST, Chl-*a* and SOI were grouped in 3-month averages for seasonal models. Lagged versions (offset by one month) of SST, Chl-*a* and SOI were included in both annual and seasonal models to accommodate potential delays in biological responses.

Table 2.1 - Descriptions of predictor variables used in mixed-effects modelling of snapper growth. Random (R) and fixed (F) effects are indicated. Also indicated is the source of the data and range in years for which data were available.

Parameter	**Description**	**Effects**	**Source**	**Data Range**
FishID	Unique fish identifier.	R		
Year	Year annual increment was formed (1 Jan – 31 Dec).	R, F		
Cohort	Class of fish born in the same year.	R		
Age	Age when increment was formed.	R,F		
Age-at-capture	Age when fish was sampled.	F		
Sea surface temperature	Surface temperature of ocean water body (°C).	F	IMOS†	1992 – 2017 *26 years*
Chlorophyll-*a*	Concentration of inferred chlorophyll from relative fluorescence per unit volume of the water body (mg/m³).	F	IMOS†	2002 – 2017 *16 years*
Southern Oscillation Index	Indication of development and intensity of El Niño or La Niña events in the Pacific Ocean.	F	BOM‡	1979 – 2017 *39 years*
Recruitment	Index of population recruitment to reflect the variation in year class strength centred on 0.	F	SARDI§	1979 – 2008 *30 years* (Intermittent)
Catch	Total commercial catch (tonnes).	F	SARDI§	1984 – 2016 *33 years*

† Integrated Marine Observing System

‡ Bureau of Meteorology

§ South Australian Research and Development Institute (Aquatic Sciences)

Statistical modelling

A series of hierarchical mixed-effects models were selected to investigate sources of growth variation based on Morrongiello and Thresher (2015). This approach overcomes limitations of other sclerochronological approaches, such as overlooking within-fish or within-year correlations, and uniquely facilitates straightforward comparisons between different studies, locations or time periods (Weisberg et al. 2010). Increasingly complex combinations of intrinsic and extrinsic covariates were added to establish optimal models to predict fish growth. Analyses were performed in R using packages lme4 (Bates et al. 2015), AICcmodavg (Mazerolle 2015) and effects (Fox 2003). Growth, Age and Age-at-capture were log-transformed to meet model assumptions. All intrinsic and extrinsic variables were mean-centred to assist model convergence and random slope interpretation (Morrongiello and Thresher 2015, Morrongiello et al. 2014). Random intercepts were added to unique fish identifiers (FishID), Year, Cohort and Region (in 'All regions' analyses) to allow for correlations among growth increments within individual fish, calendar year, year class, and region. Random intercepts allowed for higher or lower growth within each variable relative to the model average (intercept). Random age slopes were also investigated for both FishID and Year to facilitate detrending the age-related influences.

Optimal models were selected for each region. Best intrinsic models were developed by analysing all intrinsic fixed effects (Age and Age-at-capture) with a series of random effect structures (combinations of random slope and/or intercepts of FishID, Age, Year, Cohort and Region). Models were ranked using Akaike's Information Criterion (*AIC*) corrected for small sample sizes (*AICc*; Burnham and Anderson 2004). Best models were then fitted using restricted maximum likelihood estimation (REML; Zuur et al. 2009).

Growth chronologies were developed by extracting the random effect conditional models (best linear unbiased predictors, 'BLUPs') from an optimal Year-only model (Morrongiello and Thresher 2015). The growth chronologies represent an estimate of the mean inter-annual or inter-seasonal growth variation which centres around an overall chronology mean of zero. Next, temporal trends were determined by extracting the predicted effects of Year as a fixed effect in a linear or curvilinear (quadratic) form and comparing the fits against best intrinsic models using *AICc*.

To assess external influences on fish growth, extrinsic factors were added to the best intrinsic models. Best intrinsic models were compared to models with linear and curvilinear forms of the extrinsic covariate using *AICc*, then BLUPs and predicted effects were extracted. Interaction terms were fitted for environmental variables to assess synergistic effects. Interactive models that included highly correlated variables (Pearson's product-moment correlation $p<0.05$) were excluded. The best intrinsic model with the full range of extrinsic factors (including individual and interactive extrinsic structures) were ranked using *AICc* to determine the most important drivers of growth.

The model fit was assessed by calculating two R^2 metrics: marginal R^2 which describes the proportion of variance explained by fixed effects, and conditional R^2 which describes the variance explained by both fixed and random effects (Morrongiello and Thresher 2015).

Estimates of temporal growth synchrony, the correlation of growth increments among individuals through time, were extracted by calculating intra-class correlation coefficients (ICC) of optimal Year and Cohort random intercept-only models. ICC measures the relative similarity between quantitative observations as proportions between 0 (low) – 1 (high) (Cicchetti 1994, Koch 2004). Additionally, within-individual centring was used to determine whether population-level SST-growth relationships and variation were driven by individual phenotypic or environmental responses. SST was partitioned in R using packages *stats*, *plyr* (Bunn 2008) and *base* to derive an average SST experienced by an individual in their lifetime and the deviation of annual temperatures from this mean (Morrongiello and Thresher 2015, Van de Pol and Wright 2009). These variables were then fitted to and compared against optimal base models using *AICc*. Differences in within-individual and among-individual effects were derived by replacing the within-individual term with the original SST effect. Population-level variation was compared against within-individual variation (representing evolutionary fixed phenotypically-plastic responses) and among-individual variation (representing facultative environmental responses).

RESULTS

The growth chronologies for the four regions demonstrated substantial inter-annual variation. NSG experienced the steepest decline in growth (Figure 2.4f) with NGSV also experiencing significant decrease in growth predominantly from 2000 onwards (Figure 2.4e). In contrast, growth for the WC increased until 2005 and then decreased (Figure 2.4h) and for the SE, growth showed no significant trend through time (Figure 2.4g).

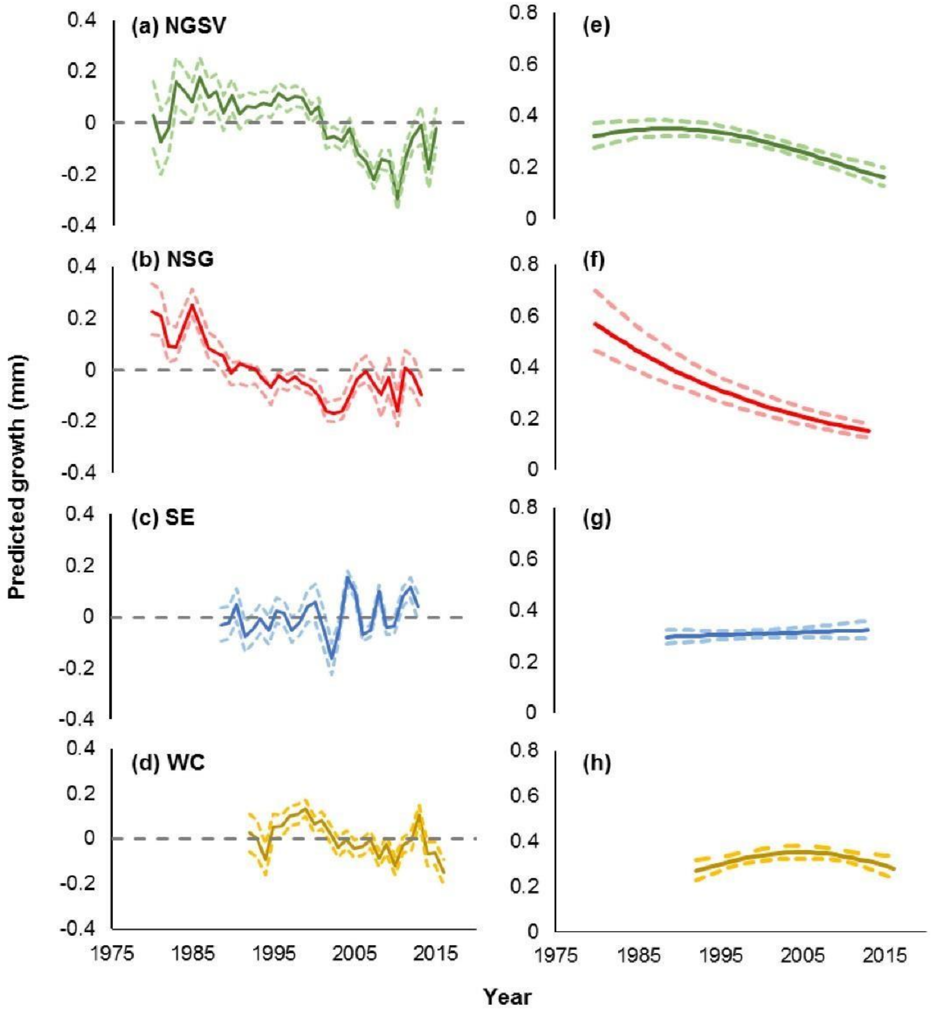

Figure 2.4 - Predicted variation and trends in growth of snapper in Northern Gulf St Vincent (NGSV), Northern Spencer Gulf (NSG), South East (SE) and West Coast (WC). Predicted inter-annual growth variation (a – d) was derived from Year random effect estimates. *Dashed lines* in the panels indicate average growth in each region across the chronology. Temporal trends (e - h) of snapper growth are indicated which were derived by examining a Years term as a fixed effect. Linear SE temporal growth has been included for comparison with other regions, however analysis indicated no significant temporal trend.

Intrinsic predictors

Different combinations of fixed and random effects made up the best intrinsic models for both annual and seasonal chronologies (Table 2.2). The best intrinsic models always included the full random-effects structure with random age slopes. Age was the best predictor of growth, with increment width declining as fish aged (Figure 2.5). WC had the highest growth rates at age, NSG had the lowest, while for NGSV and SE the growth rates were similar and fell in the middle of the two extremes. Temporal growth synchrony (ICC) for Year, which indicates growth similarity across individuals over a calendar year, was generally low and ranged from 3.9% for WC to 10.3% in SE (Table 2.3). Cohort ICC, indicating growth similarity across individuals from the same year class, was also generally low and ranged from 0.4% for WC to 13.7% in SE (Table 2.3). Year ICC had higher levels of growth synchrony than Cohort ICC, except for WC where this was reversed.

Table 2.2 - Optimal model structures derived by ranking a series of increasingly complex mixed-effects models. Optimal fixed effects structures, random effects structures and extrinsic predictors of snapper growth in NGSV, NSG, SE and WC is indicated and separated into Annual and Seasonal models. Optimal extrinsic predictors were derived by ranking optimal intrinsic models against models containing either individual extrinsic variables or combinations (indicating interactive effects) of extrinsic variables. Random slope term is indicated by x **|** y and inclusion of lagged (by one month) environmental variable is indicated by an asterisk. Seasonal models include Age and Age-at-capture as discrete seasonal values (e.g. one year = four seasons old).

Region	Fixed effects	Random effects	Best extrinsic covariate structure
Annual			
NGSV	Age	Age|FishID, Age|Year, Age|Cohort	Chl-*a* x Recruitment
NSG	Age	Age|FishID, Age|Year, Age|Cohort	Chl-*a** x Recruitment
SE	Age	Age|FishID, Age|Year, Age|Cohort	Chl-*a* x Recruitment
WC	Age	Age|FishID, Age|Year, Age|Cohort	Chl-*a*
Seasonal			
NGSV	Age, Age-at-capture	Age|FishID, Age|Year	Chl-*a** x SST*
NSG	Age, Age-at-capture	Age|FishID, Age|Year	Chl-*a** x SST
SE	Age	Age|FishID, Age|Year	Chl-*a* x SST
WC	Age	Age|FishID, Age|Year	Chl-*a* x SST*

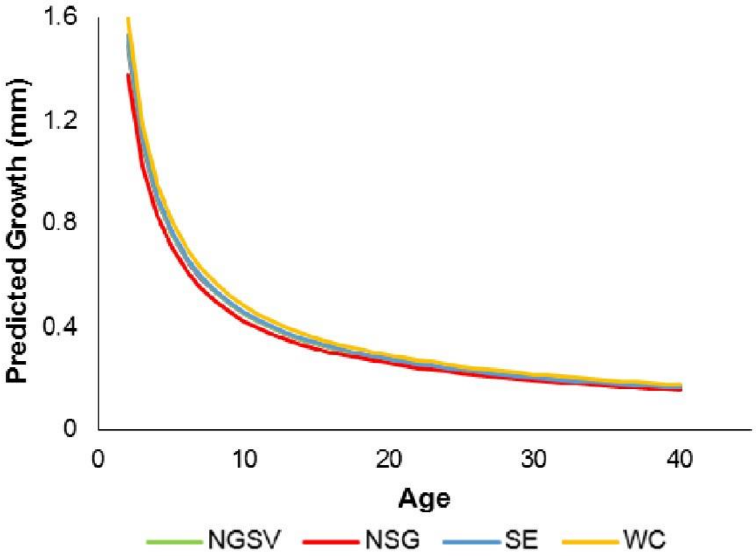

Figure 2.5 - Predicted growth of snapper at age 2 to 40 years of Northern Gulf St Vincent (NGSV), Northern Spencer Gulf (NSG), South East (SE) and West Coast (WC).

Extrinsic conditions

The magnitude and temporal trends in extrinsic parameters varied between regions (Figure 2.6). NSG experienced the highest levels of SST while SE had the lowest. Chl-*a* was 3-4 times higher in NGSV and NSG compared to the two open ocean regions. Catches were generally higher from NGSV and NSG. Linear regressions indicated there were no significant temporal trends for SST, Recruitment or SOI ($p>0.05$), but Chl-*a* significantly increased in NSG, SE and WC (Table S2.1**)**. Furthermore, Catch significantly increased in NGSV and SE and decreased for NSG ($p<0.05$). SOI fluctuated between a low of -13 and high of 13, with a higher overall percentage of negative troughs indicating more El Niño events.

Table 2.3 - Intra-class correlation coefficients (ICC) of snapper growth for Year and Cohort for NGSV, NSG, SE and WC.

Region	Year (%)	Cohort (%)
NGSV	5.7	3.3
NSG	5.5	1.0
SE	10.3	13.7
WC	3.9	0.4

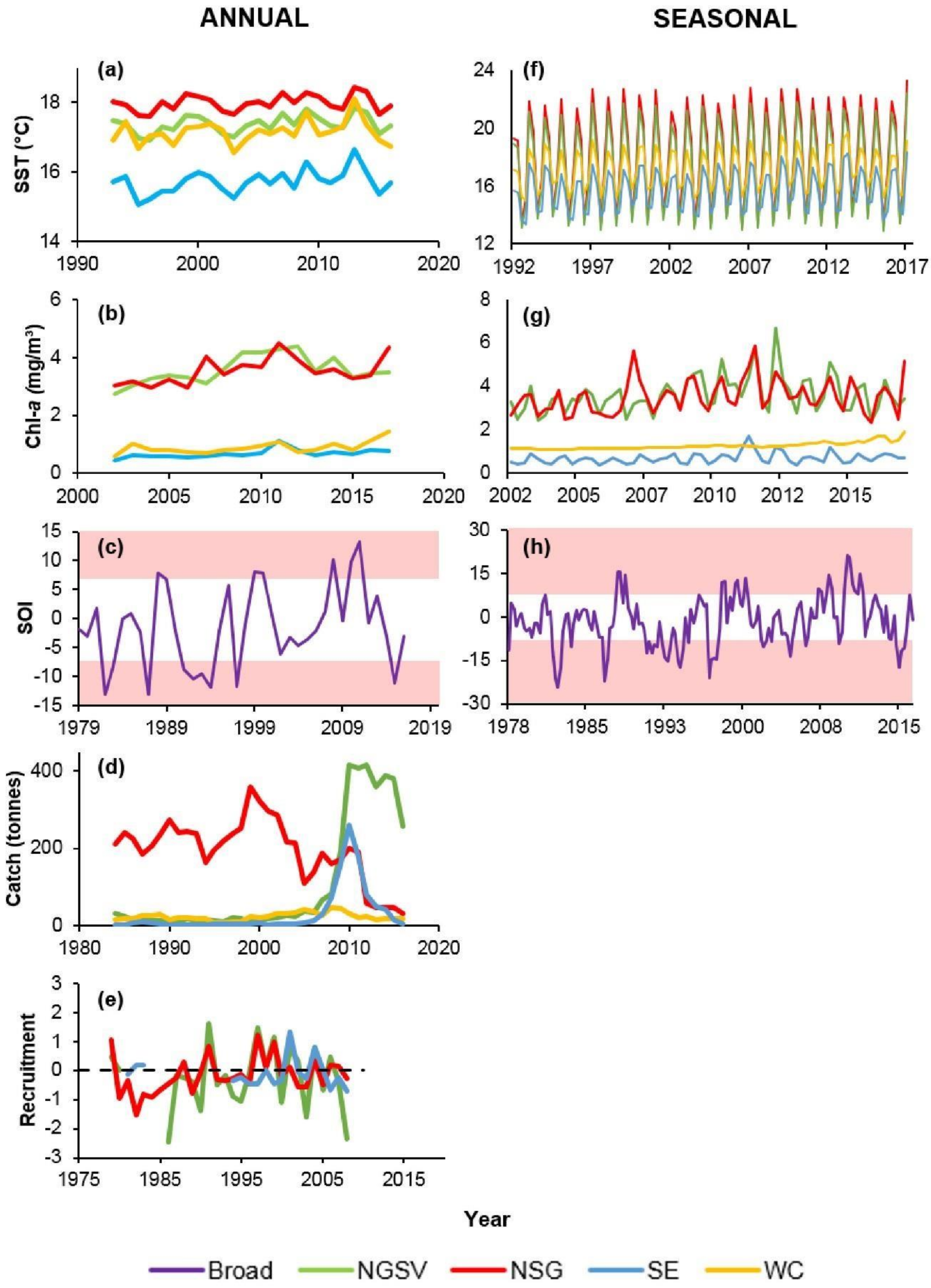

Figure 2.6 - Mean annual and seasonal values in Sea Surface Temperatures (a,f), Chlorophyll-*a* (b,g), Southern Oscillation Index (c,h), Catch (d) and Recruitment (e). Mean values are separated into the individual regions of Northern Gulf St Vincent (NGSV), Northern Spencer Gulf (NSG), South East (SE) and West Coast (WC). Shaded areas in (c,h) indicate El Niño events (<-7) and La Niña (>7) climate events.

Extrinsic predictors

The best drivers of snapper growth were examined by comparing the optimal model against individual and combined extrinsic variables. The best extrinsic predictors for annual NGSV, NSG and SE models were Recruitment and Chl-*a* combined, while for WC Chl-*a* alone was the best predictor (Table 2.2). For the seasonal models, the best extrinsic predictors included SST and Chl-*a* combined (Table 2.2). There were strong correlative relationships between individual extrinsic factors and growth for all regions. In models containing the best intrinsic model and SST as the singular extrinsic variable, SST (lagged) was a better fit for all regions except the WC.

SST was positively correlated with both annual and seasonal growth for all regions (Figure 2.7a, 7f; Table 2.4). The positive predicted effect on annual growth rate by SST was steepest in the SE (21.4 % per °C), and least in NSG (1.54 % per °C). Seasonal SST models for all regions, except the SE, showed strong positive curvilinear relationships that increased then plateaued and fell from 18.8-20.2°C (Figure 2.7f). For the SE there was a positive linear relationship, although its maximum temperature only reached 18.0°C. Compared to the annual SST predicted effects plots, seasonal SST plots encompassed a greater temperature range (about 5 times more), as well as a greater range of otolith-predicted growth, albeit at lower values (Figure 2.7a, 2.7f).

Table 2.4 - Indication of directional relationship of snapper growth with Sea Surface Temperature (SST), Chlorophyll-*a* (Chl-*a*), Southern Oscillation Index (SOI), Catch and Recruitment in four southern Australian regions. Symbols reflect the direction of extrinsic variable-growth relationships illustrated in Figure 2.6. Positive (+) and negative (-) relationships are indicated, as well as growth decreasing at the extremes of index values (°).

	Region	SST	Chl-*a*	SOI	Catch	Recruitment
Annual	NGSV	+	+	°	-	+
	NSG	+	-		+	-
	SE	+	+	°		+
	WC	+	-			
Seasonal	NGSV	+	+	-		
	NSG	+	+			
	SE	+	+			
	WC	+	-			

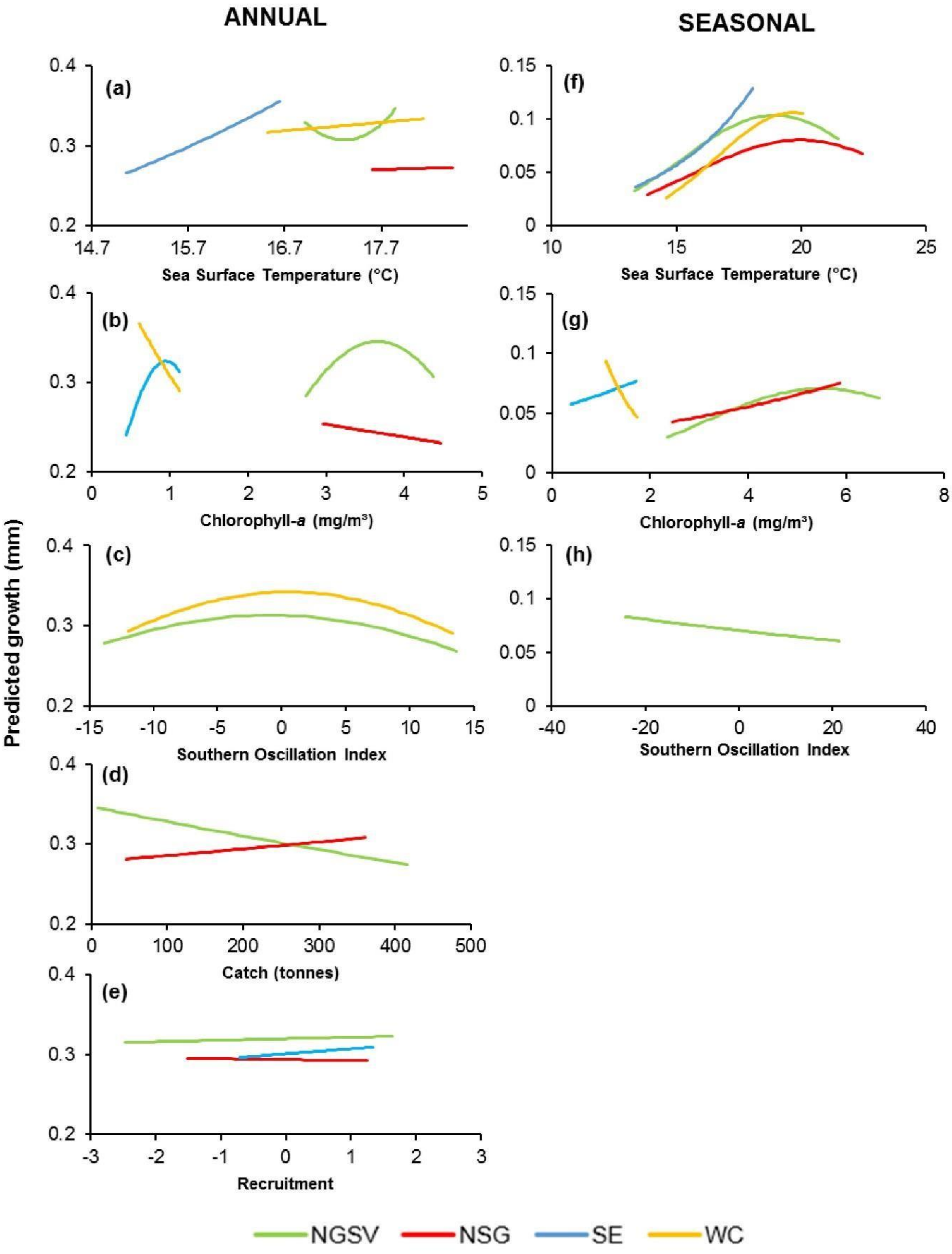

Figure 2.7 - Predicted annual and seasonal growth variation in snapper due to Sea Surface Temperature (a,f), Chlorophyll-*a* (b,g), Southern Oscillation Index (c), Catch (d) and Recruitment (e) in Northern Gulf St Vincent (NGSV), Northern Spencer Gulf (NSG), South East (SE) and West Coast (WC). Growth relationships are only presented when extrinsic factors improved fit over best intrinsic model. Note different scales on the x and y-axes. Standard errors can be found in Supplementary Information (Figures S3.4, S3.5, S3.6, and S3.7).

Growth was related to Chl-*a* concentrations in all regions, although the direction of the relationship varied (Figure 2.7b, 2.7g; Table 2.4). The annual growth relationship was negative for NSG and the WC. In contrast, NGSV and SE had positive curvilinear relationships. The predicted effects on annual growth by Chl-*a* was highest for SE, whilst for the WC there was a strong negative relationship. This was followed by NGSV and NSG. Seasonal models generally included a greater range of Chl-*a* but lower values of predicted growth than annual models (Figure 2.7b, Figure 2.7g). Seasonal models predicted positive effects of Chl-*a* on growth for all regions except WC, with positive linear relationships for NSG and SE and a positive curvilinear relationship with NGSV. Conversely, WC had a strong negative linear relationship. Seasonal snapper growth was most correlated with Chl-*a* in NGSV and least correlated in the SE (Table S3.3).

SOI correlated with growth for WC and NGSV (Figure 2.7c; Table 2.4). These regions had curvilinear growth relationships with SOI, which were highest centred on SOI = 0. The WC relationship had both the steepest incline and decline.

Catch correlated negatively with growth for NGSV and positively with NSG (Figure 2.7d; Table 2.4). For NGSV, catch increased from 2000 while growth decreased (cf. Figure 2.4a and 2.6d). For NSG, high catches from 1984 to 2012 corresponded to declining growth rates. The low catches from then on corresponded to higher growth later (Figure 2.4b, Figure 2.6d). Recruitment improved the model fit for NGSV, NSG and SE (Figure 2.7e). SE and NGSV had significant positive relationships and NSG had a significant negative relationship.

Population-level growth responses to SST were separated into within-individual variation (representing evolutionary-fixed, phenotypically-plastic responses) and among-individual variation (representing facultative environmental responses). There was significant negative among-individual variation for NSG and WC (Figure 2.8). Conversely, NGSV showed substantially higher than average among-individual growth responses. Growth in the SE had moderate positive responses to temperature across the groups, with similar levels of within-individual and amongindividual growth variation (Figure 2.8c). WC had positive phenotypic plasticity to SST but greater negative among-individual responses (Figure 2.8d). Differences in within- and amongindividual temperature slopes were substantial for NGSV (slope difference 0.353, t statistic 1.444), NSG (slope difference -1.048, t statistic -3.517) and WC (slope difference -.512, t statistic -2.56).

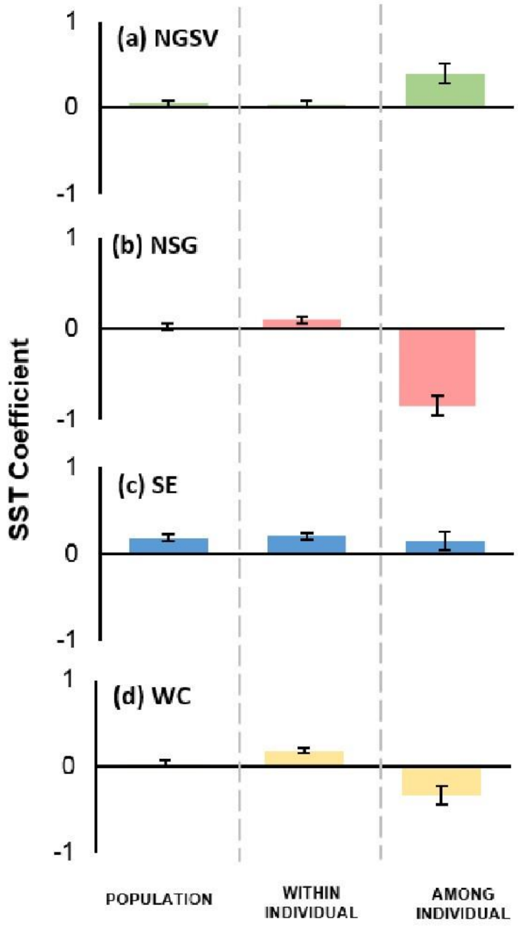

Figure 2.8 - Predicted population-level variation, within-individual (representing evolutionary-fixed, phenotypically-plastic responses) and among-individual variation (representing facultative environmental responses) in SST coefficients (Mean ± SE) for annual snapper growth. Population-level variation reflect the magnitude and direction of SST relationship as represented in Figure 2.6(a). Note different scales on the y-axes.

DISCUSSION

Otolith chronologies reconstructed almost 40 years of fish growth, with strong growth declines occurring in two of the four key fishery regions. Environmental factors were significant predictors of annual and seasonal growth trends, although there was inter-regional variation in magnitude and direction of their effects. Identifying the drivers of snapper growth enabled a better understanding of the present condition of the fishery, which prepares us to anticipate and manage future change.

Intrinsic predictors and growth synchrony

Age was the best predictor of growth, with growth decreasing with age. Significant differences in growth rates at age were evident between NSG and WC, although they share a similar nursery and are likely to be genetically homogenous. Therefore, different environmental climates (particularly differences in SST and Chl-*a*) were likely responsible for the divergent growth signatures.

Temporal growth synchrony varied across regions. Snapper growth in the SE was the most synchronous for both Year and Cohort, while growth for the WC was the least synchronous. High growth synchrony for SE snapper may be driven by the strong climate signal, characterised by a northern boundary current with seasonal upwelling (Middleton and Cirano 2002). In contrast, the WC may be less influenced by broad climatic drivers and more driven by individual microhabitats or smaller-scale population dynamics. Snapper from NGSV and NSG had similar low levels of intra-regional Year growth synchrony, indicating that similar regional climates likely drive growth patterns. The levels of growth synchrony were low and variable, but consistent with other ICC values calculated through mixed-modelling approaches such as for black bream (*Acanthopagrus butcheri*) that ranged from 3% to 13.8% (Doubleday et al. 2015) and tiger flathead (*Platycephalus richardsoni*) ranging from 2% to 21.6% (Morrongiello and Thresher 2015).

Extrinsic predictors

Chl-*a*, an indicator of primary productivity, was the best predictor of growth across all regions. For most regions, higher Chl-*a* related to increased snapper growth, particularly in the seasonal models. Generally, fish physiological functioning correlates with aquatic primary production (Downing et al. 1990), with the expectation that increasing Chl-*a* leads to higher growth and biomass. However, for the WC there was a negative relationship between Chl-*a* and growth. While excessive Chl-*a* can lead to eutrophication (low oxygen) which would affect fish growth, the South Australian levels (generally <4 mg/m^3) fell short of eutrophic classifications (11.03–30.55; Watanabe et al. 2015). Potentially, additional food in WC increased intra-specific or interspecific competition beyond a beneficial threshold and reduced the food potential per individual (Hanson and Leggett 1985, Rahman and Verdegem 2010). The best overall models (indicating best extrinsic predictors) generally included Chl-*a* combined with recruitment or SST. These factors may have acted synergistically on snapper growth. Higher primary productivity may have been associated with greater food availability, facilitating recruitment by allowing a larger number of better-conditioned fish to exist in the populations (Downing et al. 1990). Similarly, higher SST is likely to have increased phytoplankton abundance and thus ocean productivity, leading to greater food availability and thereby an increase in fish growth (Eppley 1972).

SST positively influenced annual growth in all regions. Seasonal SST patterns also match expected ectothermic responses from increasing temperature, whereby growth increased positively with temperature until reaching an optimum apex (pejus temperature), after which growth declined (Neuheimer et al. 2011, Pörtner and Farrell 2008). Hence, where the temperature falls on the performance curve influences the direction and magnitude of the growth-temperature relationship. Growth declined in seasonal SST relationships at 18-20°C, which is the likely pejus temperature for South Australian snapper. This corresponds with optimum growth for juvenile snapper determined from aquaculture experimental work (Fielder et al. 2005). The SE seasonal relationship did not display the same decline. This region has a lower temperature range and more likely represents the steep beginning of a thermal performance curve. Conversely, snapper from NSG experience higher temperatures and range, and the plateau in their seasonal SST pattern indicates they are likely nearing their pejus temperature. Consequently, this demonstrates that otolith sclerochronology may be a useful tool for accurately predicting optimum thermal maxima for hard-to-monitor fish species, such as deep-sea or isolated fish.

Similar levels of positive within-individual variation in SST coefficients in all regions indicate similar positive reaction norms to SST. NSG and WC snapper have negative among-individual variation in SST coefficients, likely as they come from the same nursery area and are genetically homogenous (Donnellan and McGlennon 1996). Yet the significantly more negative amongindividual response from NSG shows that the facultative environmental responses from increasing temperature have a significant negative effect on growth, likely related to the higher temperatures in this region. This is further supported by the differences in growth rates at increasing age between NSG and WC.

As there is a significant difference for NSG between within-individual and among-individual variation in SST coefficients, the results are more complex than a straightforward biological response to higher temperatures. The among-individual differences in NSG plasticity may be due to genetic differences or individual-specific past experiences shaping the early developmental trajectory (Dingemanse and Wolf 2013, Morrongiello and Thresher 2015). NSG may favour slower-growing individuals through long-term adaptation to higher temperatures, selecting for slower growers to cope (genetic). Alternatively, in higher temperatures, there was a reduction of physical condition in larval/juvenile stages, such as reduced food intake due to increased competition, which constrained lifetime growth development (individual-specific past experiences).

The seasonal predictions show slower growth around 20°C that illustrate that at least for the warmer months, most South Australian snapper exist near the upper range of their temperature tolerance. This is noteworthy as sustained increases in water temperature beyond the pejus temperature can have significant ecological consequences by hindering physiological processes and an adaption or shift in organism habitat range (Wang and Overgaard 2007). In the face of increasing ocean temperatures (Harley et al. 2006, IPCC 2014, Resplandy et al. 2018), snapper in NSG is the regional population that will likely be the most affected and growth may further decline or fish may shift to the cooler waters of southern Spencer Gulf.

Snapper growth for NGSV and SE had curvilinear relationships with the SOI where growth decreased at the extremes of the index. SOI is indicative of oceanic-atmospheric climatic shifts between warmer periods (El Niño, <-7) and cooling periods (La Niña, >7) in the Pacific Ocean. We showed that snapper growth decreases during climate extremes in the two eastern regions closest to the South Pacific Ocean (NGSV and SE), but no effects were detected for the two western regions that were further away (WC and NSG). This climatic influence on growth is consistent with observations for other fish species (Gillanders et al. 2012, Ong et al. 2015). SOI may influence growth through influences on upwelling and SST affecting primary productivity. For example, temperature increases during an El Niño event can reduce plankton production by lowering the thermocline, limiting nutrients and by changing trophodynamic relationships (Lehodey et al. 2006).

Region-specific complexity is indicated in the relationship between growth, catch and recruitment. For NSG, there was a positive relationship between growth and catch but a negative relationship with recruitment, while NGSV showed the reverse trend. Of particular note, from 2000 in NGSV catch increased while growth decreased. Conversely, in NSG from 1985 when catch decreased growth also decreased. The differences between NGSV and NSG likely reflect different density-dependent effects. Increased recruitment likely increased intra-specific competition between younger and smaller snapper, whereas increased catch removed biomass of larger and older fish, which likely reduced intra-specific competition between larger and older fish. Snapper growth in NSG is shown to be compensatory density-dependent, with growth negatively correlated to population size. Larger populations in NSG likely increased intra-specific competition, leading to less per capita food availability and reduction in an individual’s feeding rate (Rose et al. 2001). In contrast, NGSV growth is shown to be depensatory density-dependent, with growth positively correlated to population size. This relationship can arise when populations are reduced below a threshold where group dynamics and cooperative interactions can be impaired, limiting mating success, foraging or antipredator strategies (Lewin et al. 2006, Stephens and Sutherland 1999). The different density-dependent effects between NSG and NGSV likely indicate different population dynamics and potentially abundance, with NGSV populations likely to be smaller which benefits individuals, whereas NSG likely has larger populations with high intra-specific competition. While NSG and NGSV have similar climatic environments, these different density-dependent population processes likely contributed to the inter-regional differences in snapper growth responses.

Multi-decadal, size-selective fishing (commercial and recreational) may be a driver of declining snapper growth in NSG and NGSV. Some fish populations respond to long-term, size-selective harvesting by selecting for slower-growing, smaller fish that mature earlier (Ernande et al. 2004, Swain et al. 2007, Olsen et al. 2009). As commercial harvesting directly removes the larger and faster growing fish, this may have skewed snapper populations towards smaller average sizes. The influence of human activities on life-history traits of commercially harvested fish has been determined to be as low as 0.1–0.6% per year on life-history parameters such as size at maturation, consumption and gonad investment (Andersen and Brander 2009); as high as 2.5% per year for growth (Morrongiello and Thresher 2015); and 1–4% per year for size and age at maturity (Audzijonyte et al. 2013). Declining growth can be detrimental as it reduces a population's productivity and interferes with predator-prey relationships (Rose et al. 2001, Lewin et al. 2006). Selection towards smaller, earlier maturing fish can also lead to age-truncation of the fish population wherein the average age of spawning females is lowered. Younger and smaller females generally have a lower maximum reproductive rate (Venturelli et al. 2009), reduced spawning success (Trippel 1998, Hixon et al. 2014), and are less productive than the same weight's worth of large females (Barneche et al. 2018). Snapper populations are particularly reliant on strong cohort years to boost numbers and the decimation of a strong cohort can have long-lasting effects on the biomass (Fowler et al. 2016).

To best anticipate and prepare for the future, external pressures on wild populations must be considered and managed collectively. Climate change will affect fish populations through predicted increases to ocean temperatures of up to 3°C by 2100 and higher frequency of extreme climate events like El Niño or La Niña episodes (Cai et al. 2014, IPCC 2014, Resplandy et al. 2018). Simultaneously, large-scale fishing will continue to exert biological and ecological selective pressures worldwide (Audzijonyte et al. 2013, Swain et al. 2007). Climate change and fishing are predicted to act as cumulative stressors, with the loss of biodiversity and truncation of age and geographic structure due to fishing increasing the sensitivity of fish populations and marine ecosystems to environmental change (Berkeley et al. 2004, Brander 2007, Ottersen et al. 2006). To bolster resilience against these external pressures, it is important to preserve population age structures, which also slows down the selective pressures towards slower-growing fish that mature earlier (Brander 2007). Enacting maximum legal lengths of catch is one approach to protect age structures in fishery species (Berkeley et al. 2004). Establishing and increasing marine protected areas where fishing is prohibited can also be effective. In marine protected areas, relief from fishing pressures allows species to age naturally which increases reproductive rate and productivity, with benefits experienced for protected populations inside and fished populations outside (Hixon et al. 2014, Roberts et al. 2001, Venturelli et al. 2009). Preserving older fish improves resilience in wild populations and should be a key strategy in fishery management to tackle environmental and anthropogenic change.

Conclusions

We used annual and seasonally resolved growth chronologies to investigate drivers of change in an iconic fishery species. Intra-regional differences in growth arose from variation in environmental influences and population dynamics. Few studies have applied fine scale growth profiles (Grammer et al. 2017), despite their value. Here, we developed seasonally-resolved chronologies, which provided nuanced predictions of growth trends which encapsulated and accounted for fluctuations throughout a whole year that may have been otherwise overlooked in broader annual chronologies. Consequently, seasonally-resolved chronologies present significant potential for use on other fish species to determine precise biological and environmental effects.

Hard-calcified structures like otoliths are a valuable tool for retrospectively unearthing long-term ecological datasets that would otherwise be costly and logistically difficult to obtain through direct methods. We illustrated their value in determining long-term trends in populations, and both environmental and anthropogenic drivers. Fisheries provide an important food source for the global population and these techniques can inform sustainable fishery practices which will benefit fish populations, the fishing industry and general community.

Statement of Authorship

Title of Paper	Metabolic effects on carbon isotope biomarkers in fish.	
Publication Status	☑ Published ☐ Submitted for Publication	☐ Accepted for Publication ☐ Unpublished and Unsubmitted w ork w ritten in manuscript style
Publication Details	Martino JC, Doubleday ZA, Gillanders BM (2019) Metabolic effects on carbon isotope biomarkers in fish. Ecological Indicators 97:10-16	

Principal Author

Name of Principal Author (Candidate)	Jasmin Martino		
Contribution to the Paper	Collected, analysed and interpretated data, wrote manuscript and acted as corresponding author.		
Overall percentage (%)	85%		
Certification:	This paper reports on original research I conducted during the period of my Higher Degree by Research candidature and is not subject to any obligations or contractual agreements with a third party that would constrain its inclusion in this thesis. I am the primary author of this paper.		
Signature		Date	

Co-Author Contributions

By signing the Statement of Authorship, each author certifies that:

i. the candidate's statec contribution to the publication is accurate (as detailed above);
ii. permission is granted for the candidate in include the publication in the thesis; and
iii. the sum of all co-author contributions is equal to 100% less the candidate's stated contribution.
iv.

Name of Co-Author	Zöe Doubleday		
Contribution to the Paper	Supervised development of work, helped in data interpretation and manuscript evaluation.		
Signature		Date	24/1/2019.

Name of Co-Author	Bronwyn Gillanders		
Contribution to the Paper	Supervised development of work, helped in data interpretation and manuscript evaluation.		
Signature		Date	24 Jan 2019

CHAPTER THREE

Metabolic effects on carbon isotope biomarkers in fish tissues

This research is published as:

Martino JC, ZA Doubleday, and BM Gillanders (2019) Metabolic effects on carbon isotope biomarkers in fish. Ecological Indicators 97:10-16.

ABSTRACT

Carbon stable isotopes (δ^{13}C) in animal tissues are a powerful tool for tracking biological and environmental change. However, carbon isotope signatures can be altered by both physiological and environmental factors which can cloud interpretation in their use as biomarkers. We investigated metabolic effects (by varying temperatures) on δ^{13}C of three fish tissues (otolith, muscle and liver) and the proportional contributions of environmental water (dissolved inorganic carbon; DIC) and diet (metabolic sources). Juvenile Australasian snapper (*Chrysophrys auratus*) were laboratory-reared at four temperatures for up to two months and then δ^{13}C in otolith, liver and muscle were measured using isotope-ratio mass spectrometry (IRMS). Temperature significantly altered δ^{13}C signatures in all tissues. δ^{13}C in otoliths reflected carbon signatures from diet and water DIC, with values and variation of proportional contributions influenced by temperature. In muscle and liver, we found differences in δ^{13}C between tissues and across temperature treatments with concurrent high diet-to-tissue fractionation. We conclude that metabolic effects influenced carbon incorporation for all tissues, with otolith carbon providing valuable insights into field metabolic rates. However, metabolic effects complicated the use of soft-tissue to track diet. This study deepens our understanding of internal and external drivers of carbon isotopic signatures in fish tissues and enhances their utility as a biomarker in the field. Improved insight into biomarkers facilitates more accurate predictions of ecological and environmental change for better understanding and management of wild populations.

INTRODUCTION

Stable isotopes have been used to reconstruct trophic relationships and food webs (Gronkjaer et al. 2013, Wada et al. 1991), animal movements and migrations (Rubenstein and Hobson 2004), environmental histories (Jones and Campana 2009, Watanabe et al. 2009) and ecosystem fluxes of elements and water (Boecklen et al. 2011, Peterson and Fry 1987). Carbon stable isotope values, denoted as the ratio between primary isotopes ^{12}C and ^{13}C ($\delta^{13}C$), can indicate key dietary and metabolic information through direct isotopic links between consumer tissues and diet. Incorporation of $\delta^{13}C$ into tissues can be altered by geophysical and physiological fractionation processes, creating distinctive signatures which can be retrospectively tracked.

Environmental data from aquatic systems are limited compared to terrestrial systems, largely due to the cost and resources required for direct monitoring (Richardson and Poloczanska 2008), so chemical analysis of tissues provides a cost-effective and efficient method of reconstructing ecological and environmental change. Hard calcified structures, such as bones or shells, have low metabolic activity and slow tissue turn-over, consequently incorporating long-term isotopic signatures. Hard calcified structures also show minimal degradation through time and extensive archives exist in research institutes and museums world-wide. This is particularly true for fish otoliths (ear stones) which are calcium carbonate ($CaCO_3$) structures in teleost fishes that form visible daily and annual increments. Otoliths are acellular and metabolically inert and trace elements are permanently locked into incrementally accreted tissue (Campana and Neilson 1985). These chemical signatures can reflect environmental and physiological conditions, allowing life-long and time resolved biomarkers to be recorded (Campana 1999).

Stable carbon isotopes in otoliths may be a useful tracer of metabolic rates. Metabolic histories are important in understanding and managing fish species, being a fundamental predictor of behaviour, performance, growth, social and lifestyle interactions, and consumption of resources (Chabot et al. 2016, Hulbert and Else 2000). Otolith carbon arises from two sources: dissolved inorganic carbon (DIC) in environmental water uptake via the gill and/or intestinal interfaces and metabolically sourced carbon via cellular respiration of food (Kalish 1991a, McConnaughey et al. 1997, Trueman et al. 2016). Higher respiration and metabolic rates increase the proportion of metabolic carbon, which has a significantly depleted carbon signature (values of $\delta^{13}C$ are more negative) than the DIC proportion. Consequently, changes in $\delta^{13}C$ in otoliths are thought to predominately reflect metabolic shifts. The influence of other carbon sources is considered minimal as seawater DIC typically remains within a narrow range and considerable changes to diet are required to significantly alter values of $\delta^{13}C$ (Shephard et al. 2007, Sherwood and Rose 2003, Trueman et al. 2016). However, further study, particularly controlled experimental work, is necessary to investigate the relationship between $\delta^{13}C$ and metabolic rates.

Carbon signatures in soft-tissues have been used extensively to track diet and uncover trophic and nutrient pathways (Boecklen et al. 2011, Pasquaud et al. 2007, Rau et al. 1983). However, diet-to-tissue carbon fractionation can vary between species, diets and tissues with recorded values from bulk isotope analysis ranging from 1‰ (DeNiro and Epstein 1978) to 5‰

(Bloomfield et al. 2011, Gaston and Suthers 2004). Variation in diet-to-tissue fractionation in soft tissues can be influenced by the physiological and structural characteristics of the tissues. For instance, isotopic composition in tissues can be mediated by growth, whereby existing mass is diluted by newly synthesised mass, and metabolism, which can determine the rate of replacement or conversion of existing tissues (Buchheister and Latour 2010, Hesslein et al. 1993). Metabolically-active tissue, such as the liver, can also have faster tissue turnover but less newly synthesised mass than less metabolically-active tissue, such as muscle, where growth is the primary determinant in isotopic incorporation (Buchheister and Latour 2010, Carleton and Del Rio 2010, Mont'Alverne et al. 2016). Furthermore, lipid content in soft-tissues can also affect carbon signatures, as lipids are typically 6-8‰ depleted in $\delta^{13}C$ compared to tissue protein or carbohydrates (DeNiro and Epstein 1977). Temperature may also affect rates of carbon assimilation and levels of lipids in soft-tissues through metabolic effects. Limited studies have experimentally tested the effect of temperature on the relationship between $\delta^{13}C$ in fish soft tissues and diet, with little work completed on liver tissue (Barnes et al. 2009, Bloomfield et al. 2011). Further work is required to understand species-specific carbon fractionation and to identify factors contributing to variation.

To increase our understanding of the factors controlling carbon isotope values in fish tissues, we performed an experiment on an iconic fishery species, Australasian snapper (*Chrysophrys auratus*). Temperature is known to directly influence metabolic rates of fish (Clarke and Johnston 1999, Gillooly et al. 2001), therefore juvenile snapper were reared at four temperatures in controlled laboratory conditions. Values of $\delta^{13}C$ in carbon sources (DIC and diet) and fish tissues (otolith, liver and muscle) were then analysed. Our objectives were to 1) investigate the relationships between $\delta^{13}C$ in carbon sources and fish tissues and 2) assess the influence of metabolic effects on $\delta^{13}C$.

METHODS

The study species, Australasian snapper (*Chrysophrys auratus*), is an iconic long-lived demersal species that supports important commercial and recreational fisheries in the Australasia and Indo-Pacific regions. Snapper culture is typically carried out in water temperatures of 13 – 28˚C, with optimum growth rate between 20 and 28˚C (Pecl et al. 2011).

Snapper eggs were collected from Cockburn Sound, Western Australia and reared at 25°C and 35 psu at the Challenger Institute of Technology in Fremantle. Two-month old juvenile fish (approximately 40mm, 1g) were transported to the University of Adelaide, South Australia. To acclimatise to experimental conditions in the laboratory, fingerlings were kept in a 200 L holding tank at 25°C. After this period the fingerlings were batch marked via immersion in an alizarin complexone ($C_{19}H_{15}NO_8$) solution (40 mg/L of tank water) for 24 hr. Alizarin marks otoliths allowing pre-experimental and experimental otolith growth to be distinguished (van der Walt and Faragher 2003). Acclimation period totalled 2 weeks. Fingerlings were then separated into 16 tanks with 5 fish stocked in each. Each tank contained 40 L of seawater (salinity: 35 psu), as well as a submerged filter and aerator. Seawater was locally sourced from coastal waters (Gulf St Vincent, South Australia). Light was administered under a 12 h light:12 h dark cycle from fluorescent tubes. For both acclimation and experimental periods, fingerlings were fed twice daily to satiation with commercial fish food (Skretting Protec FF) that was 50% protein, 17% lipid and made from a range of animal and plant protein. Fish were gradually acclimatised to experimental temperatures by increasing temperature at a rate of 1.5°C per day. Tank temperatures were set at four levels (20°C, 24°C, 28°C, 32°C) with 4 replicates of each temperature controlled by external heating units (Teco Seachill) in surrounding water baths. Water temperature was measured daily throughout the experiment with a handheld probe (Hanna Instruments HI-98127). Salinity was tested twice weekly using a refractometer (Vertex RF-1) and maintained at 40 psu via the addition of aged bore water. To maintain water quality, 50% water changes occurred weekly and water was regularly tested for ammonia through commercial testing kits (API). Fish were exposed to experimental conditions for up to 2 months and then euthanised in an ice slurry. Weights and lengths of euthanised fish were measured. Sagittal otoliths were dissected, cleaned of adhering tissue and air-dried. Liver and muscle tissue (dorsal flank) were extracted and frozen.

Experimental otolith material, distinguished by a purple (alizarin) band, was chipped off into filter paper and placed in acid-sterilised 4.5ml vials. Vials were purged for 2.5 minutes with nitrogen gas and injected with 100µl - 120µl of 103 – 104% phosphoric acid. Carbon isotopes in otolith samples were analysed using a GasPrep headspace analyser connected to Nu Horizon (Nu instruments) isotope-ratio mass spectrometer (IRMS). Powder standards (ANU-P3, UAC $CaCO_3$ UniA, IAEA-CO-8) were analysed to assess instrument drift and calculate precision. Analytical errors averaged 0·19‰ for $\delta^{13}C$ otolith values.

Liver and muscle tissue were freeze-dried (Dynavac, model FD-5) for 48 hours and then 2 mg weighed into tin capsules. To analyse for $\delta^{13}C$, soft-tissue samples were then loaded into an EUROEA300 elemental analyser (Eurovector) connected to Nu Horizon (Nu instruments) IRMS. Powder standards (Glutamic acid, Glycin, TPA) and replicate tissue were analysed every 9th sample to assess instrument drift and calculate precision. Analytical errors averaged 0.10‰ for liver and 0.07‰ for muscle.

The influence of lipids on $\delta^{13}C$ in soft-tissue samples was mathematically accounted for, as lipids are typically 6-8‰ depleted compared to protein or carbohydrates (DeNiro and Epstein 1977). To account for lipids in muscle, the optimum lipid-normalisation method for muscle was used (Post et al. 2007):

$$\Delta\delta^{13}\mathrm{C} = -3.32 + 0.99 \text{ x } C{:}N \qquad \text{(Equation 1)}$$

where C:N is the proportion of carbon to nitrogen in the sample. Subsequently, an estimate of normalised $\delta^{13}C$ was derived:

$$\delta^{13}\mathrm{C}_{\mathrm{normalised}} = \delta^{13}\mathrm{C}_{\mathrm{untreated}} + \Delta\delta^{13}\mathrm{C} \qquad \text{(Equation 2)}$$

There is an alternative optimum method to account for lipids in liver (Skinner et al. 2016). A percent lipid calculation was first used (Post et al. 2007):

$$\%\ \mathrm{lipid} = -20.54 + 7.24\ x\ C{:}N \qquad \text{(Equation 3)}$$

where % lipid is the lipid in the soft tissue. Secondly a mathematical lipid-normalisation model as used (Kiljunen et al. 2006):

$$\delta^{13}\mathrm{C}_{\mathrm{normalised}} = \delta^{13}\mathrm{C} + \mathrm{D\ x}\left(\mathrm{I} + \frac{3.9}{1+287/\%\ \mathrm{lipid}}\right) \qquad \text{(Equation 4)}$$

where D is 7.018 and represents the carbon isotopic difference between protein and lipid, while *I* is a constant at 0.048. The lipids in diet were not accounted for as fish consume and metabolise the entire feed (Bloomfield et al. 2011).

Water samples (50ml) were taken at the beginning and end of the experiment, filtered through a 0.21 μm filter and refrigerated. DIC was measured using a GasBench II coupled with a Delta XL Mass Spectrometer in continuous flow mode (Thermo-Fisher Scientific; West Australian

Biogeochemistry Centre). Fish food samples (*n*=3) were collected, ground to a fine powder using a mortar and pestle and analysed using a continuous flow system consisting of a Delta V Plus mass spectrometer connected with a Thermo Flush 1112 via Conflo IV (Thermo-Finnigan/Germany; West Australian Biogeochemistry Centre).

Carbon isotope values were reported relative to Vienna Pee Dee Belemnite (VPDB) and expressed in standard delta (δ) notation as parts per thousand (‰):

$$\delta = \left(\frac{R_{sample} - R_{standard}}{R_{standard}}\right) x\ 1000\ (‰) \qquad \text{(Equation 5)}$$

where R is the ratio of ^{13}C:^{12}C.

To calculate the proportional contribution from carbon sources to otoliths, the following isotopic mixing model was used (Jamieson et al. 2004):

$$\delta^{13}C_{oto} = M\delta^{13}C_{diet} + (1 - M)\delta^{13}C_{DIC\text{-}SW} + \Delta_{arag\text{-}HCO_3} \qquad \text{(Equation 6)}$$

where M is the fraction of carbon from metabolic sources; $\delta^{13}C_{oto}$ is the $\delta^{13}C$ of otolith; $\delta^{13}C_{diet}$ is the $\delta^{13}C$ of fish diet (metabolically sourced carbon); $\delta^{13}C_{DIC\text{-}SW}$ is the value of dissolved inorganic carbon (DIC) in ambient water; and $\Delta_{arag\text{-}HCO_3}$ is the isotopic fractionation between aragonite and bicarbonate, taken as ~2.7‰ (Romanek et al. 1992).

Two-factor permutational univariate analysis of variance (ANOVA) was used to determine differences in $\delta^{13}C$ ratios in all tissues, between whole and lipid-normalised soft-tissues and dietto-soft tissue fractionation among temperature treatments (*PRIMER* v6.0/*Permanova*). Permanova is a non-parametric and non-sensitive to heteroscedasticity. Temperature was considered a fixed factor, while replicate tanks were treated as a random factor (nested in temperature) to test for tank effects. One 32.0°C replicate tank was lost due to mortalities. Nontransformed data were converted to Euclidean distance matrices with analyses performed using unrestricted permutations of the data. Where significant differences were detected, post-hoc pairwise *t*-tests were performed. Variation in *M* within temperature treatments was assessed in SPSS (v22). Assumptions of normal distribution were first established by the Shapiro-Wilk test and then differences in variance between treatments were assessed by Levene's test (Gastwirth et al. 2009). To assess the influence of other biological variables, correlation tests (Pearson's product-moment correlation) were performed in R (v3.2.0) to determine if fish size (weight, length, height, girth) and fish age correlated with *M* or otolith $\delta^{13}C$. An analysis of covariance (ANCOVA) in R was used where fish age at sampling was the covariate to account for the significant influence of age on fish size variables (weight, length, height, girth). Covariate-adjusted means were derived using the effects package.

RESULTS

Rearing conditions remained stable throughout the experimental period, with desired temperature levels maintained for each treatment ($p<0.05$; Table 3.1). Tank DIC did not vary among temperatures treatments (ANOVA: $F_{3,11} = 0.83$, p = 0.5; Table S1).

Lipid normalisation increased values of $\delta^{13}C$ in muscle and liver tissues, with larger differences seen in liver ($\Delta\delta^{13}C_{mean} = 5.88‰ \pm 0.4$) than muscle ($\Delta\delta^{13}C_{mean} = 0.78‰ \pm 0.04$; Figure 3.1). Values of $\delta^{13}C$ in $\text{muscle}_{\text{normalised}}$ were significantly different between the highest three temperatures and increased (became less negative) with higher temperatures (Figure 3.2). Conversely, $\delta^{13}C$ in $\text{Liver}_{\text{normalised}}$ increased (became less negative) through the lowest three temperature treatments but decreased at the highest temperature treatment (Figure 3.2). Diet-to-tissue fractionation (enrichment) was larger for liver ($\Delta\delta^{13}C_{mean} = 8.32‰ \pm 0.82$) than muscle ($\Delta\delta^{13}C_{mean} = 6.00‰ \pm 0.05$; (ANOVA: $F_{1,76} = 125.36$, p = 0.001).

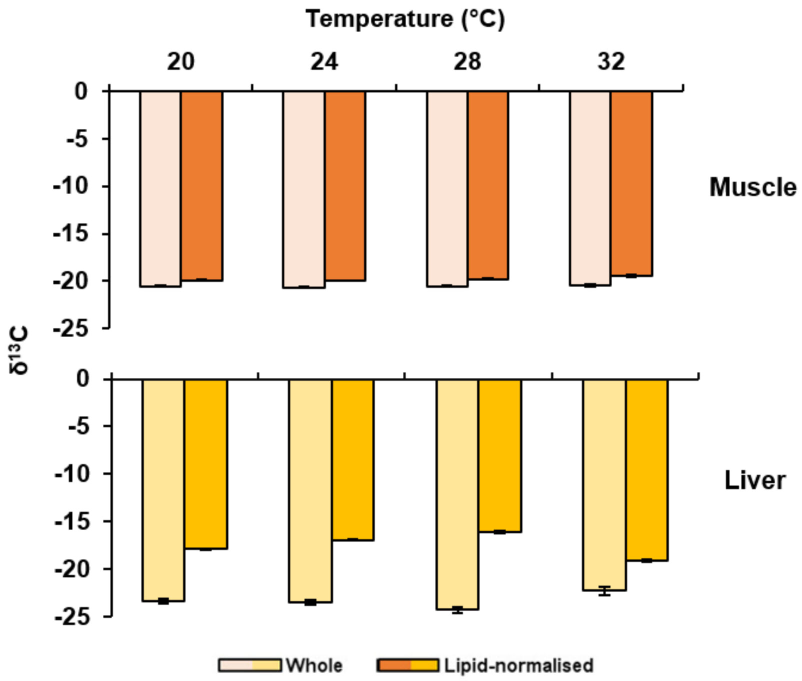

Figure 3.1 - Mean (± SE) $\delta^{13}C$ in whole and lipid-normalised muscle and liver tissue in juvenile snapper reared in different temperatures. Significant differences (p<0.05) between temperatures are as indicated in Figure 3.2.

Values of $\delta^{13}C$ in otoliths decreased (became more negative) with the lowest three temperature treatments, before increasing at the highest temperature (Figure 3.2). There was no statistically significant effect of temperature on the proportional contribution of metabolic carbon (M) to otolith carbon when tank effects were included in the design. We also re-ran the analysis without tank in the design to increase sample size. The treatment level effect on M showed significant temperature effects. There was significant difference in variation in M across temperature treatments (Levene's test: $F_{14,40} = 2.195$, $p = 0.026$; Figure 3.3). This difference in variation was also shown with average standard deviations for M decreasing with increasing temperature (20°C = 9.21; 24°C = 6.07; 28°C = 5.29; 32°C = 4.50). Fractionation between DIC and otoliths was not significant when tank effects were included, but when tanks were pooled and only temperatures investigated the fractionation difference significantly increased with increasing temperature (20°C = 1.14‰; 24°C = 1.47‰; 28°C = 1.86‰; 32°C = 3.00‰).

Table 3.1 - Mean (±SE) carbon isotope composition in fish tissues (otolith, liver and muscle); diet and tank water DIC; average tank temperature and salinity; and metabolic carbon contribution (*M*) across temperature treatments.

Treatment (°C)	Otolith $\delta^{13}C$ (‰ VPDB) (n=56)	Liver $\delta^{13}C$ (‰ VPDB) (n=56)	Muscle $\delta^{13}C$ (‰ VPDB) (n=56)	Water DIC (‰ VPDB) (n=30)	Diet $\delta^{13}C$ (‰ VPDB) (n=3)	Temperature (°C) (n=15)	Salinity (ppm) (n=15)	*M* (%) (n=56)	Length (mm) (n=56)
20	-8.18 ±0.11	-23.36 ±0.27	-20.55 ±0.07	-6.68 ±0.9	-25.35 ±0.16	19.77 ±0.06	35.45 ±0.3	21.1 ±2.3	77.49 ±3.8
24	-8.91 ±0.14	-23.55 ±0.24	-20.66 ±0.06	-7.43 ±0.6	-25.35 ±0.16	23.94 ±0.07	35.69 ±0.3	23.0 ±1.5	73.91 ±2.85
28	-9.75 ±0.19	-24.35 ±0.14	-20.61 ±0.06	-7.81 ±0.6	-25.35 ±0.16	27.98 ±0.03	35.14 ±0.4	25.9 ±1.3	64.5 ±2.5
32	-8.12 ±0.37	-22.47 ±0.42	-20.39 ±0.13	-6.26 ±0.9	-25.35 ±0.16	32.07 ±0.09	35.90 ±0.4	28.2 ±1.6	56.1 ±2.8

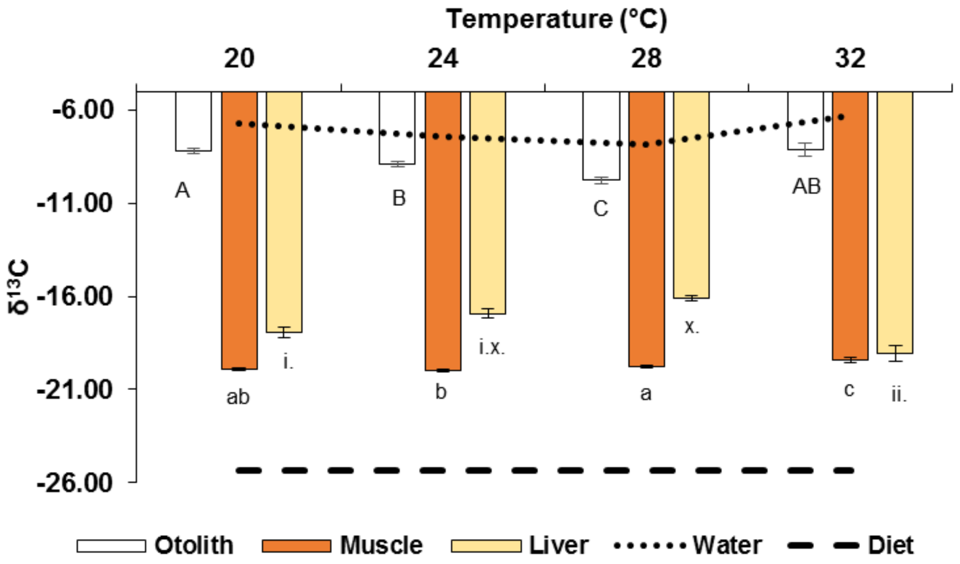

Figure 3.2 - Mean (± SE) $\delta^{13}C$ in otolith and lipid-normalised liver and muscle tissues for juvenile snapper reared in different temperatures. Different letters represent significant differences ($p<0.05$) between individual treatments with different types of letters used for each tissue.

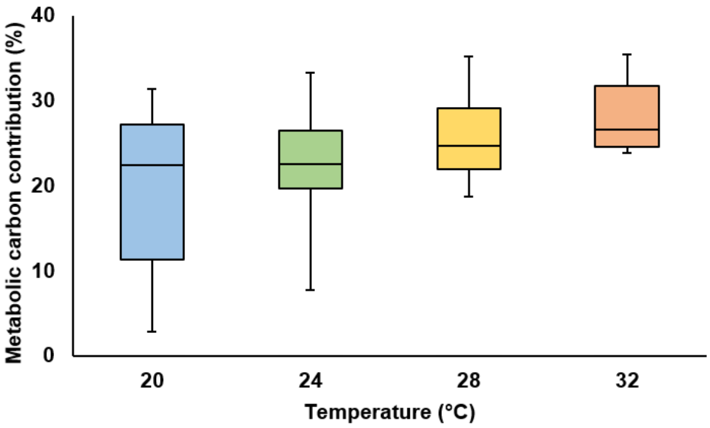

Figure 3.3 - Boxplots of proportional contributions of metabolic carbon (M) to otolith δ^{13}C in juvenile snapper reared in different temperatures. For each boxplot, the box and whisker components individually represent 50% of the data, with the horizontal line representing the median.

Other biological variables were found to have minimal effects. One-way ANCOVA found no significant effect of temperature on fish size (weight, length, height, girth) after controlling for fish age. Additionally, there was no significant correlation between fish size (weight, length, height, girth) and *M* or δ^{13}C in otoliths or liver. However, significant correlations were found between fish size and δ^{13}C in muscle (Figure 3.4).

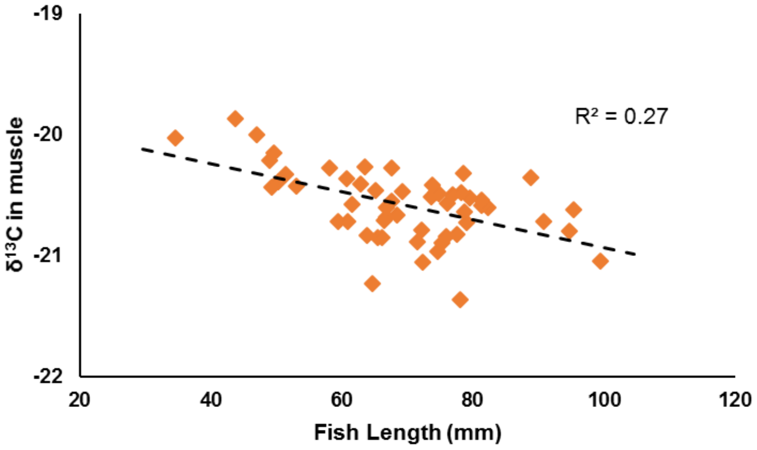

Figure 3.4 - Relationship between δ^{13}C in muscle tissue and length (mm) in juvenile snapper.

DISCUSSION

Our results reveal how metabolic rate can affect carbon isotope signatures in fish tissues. We found that δ^{13}C in otoliths reflected carbon signatures from diet and environmental DIC, with proportional contributions influenced by temperature. As temperature increased, values of M also increased but variation in M between individuals decreased. Temperature also had significant effects on δ^{13}C values in muscle and liver tissues. High levels of diet-to-tissue fractionation were found for soft-tissues, with the highest values recorded in liver. These findings suggest δ^{13}C provides valuable insights into the biological histories of fish, particularly metabolic rates and diet composition, but can also be influenced by the environment.

Carbon stable isotopes in otoliths

Values of δ^{13}C in otoliths increased with temperature, then decreased at the highest temperature. While these patterns roughly reflected water DIC trends (Figure 3.2), there was a significant difference between temperature treatments for δ^{13}C in otoliths but not DIC. Consequently, temperature also influenced carbon uptake into otoliths and this is supported by increased M values and water DIC-to-otolith fractionation in higher temperatures. Other experimental studies investigating temperature effects on otoliths found depletion of δ^{13}C with temperature (Radtke et al. 1996, Thorrold et al. 1997) or no change in δ^{13}C at higher temperatures (Kalish 1991b, Radtke et al. 1996). After considering water DIC values, our study aligns with research suggesting otolith δ^{13}C declines with temperature due to higher levels of metabolic carbon incorporated into the otolith.

Metabolic contribution to otolith δ^{13}C ranged from 21-28%. This value is slightly lower than other experimental marine studies (~30%) (Høie et al. 2003, Kalish 1991b), but still within the published range (Weidman and Millner 2000). Our lower M value may be due to high tank DIC (6.9 ‰), which many studies assume to be ~0‰ - 2‰ (Elsdon et al. 2010, Kalish 1991b), but is consistent with local marine waters (Inoue and Sugimura 1986). Additionally, there has been variation in methods used to experimentally derive M. For example, a range of different isotopic mixing models have been used (Jamieson et al. 2004, Kalish 1991b, Solomon et al. 2006) and variation in values of carbon sources in calculations, with many studies using assumed rather than measured data (i.e. for DIC). Furthermore, environmental differences in experimentally determined M have been found with freshwater fish possessing significantly lower proportions of metabolic carbon (~17%) in otoliths than marine fish (Solomon et al. 2006, Tohse et al. 2004).

M did not significantly increase with higher temperatures when tank was included in the statistical analyses. However, when the treatment level samples were pooled (increasing sample size) then M significantly increased with temperature. Previous studies showed no or weak relationships between M and temperature (Høie et al. 2003, Kalish 1991b). Changes to M and $\delta^{13}C$ in otoliths likely arose from raised temperatures accelerating physiological processes (Schulte et al. 2011). Higher metabolic demands likely increased respiration and food consumption, thus producing more metabolic CO_2 in the blood that was incorporated in the endolymphatic fluid and otolith carbonate (Trueman et al. 2016). As the rates of diffusion of water DIC are constrained and constant, $\delta^{13}C$ in otoliths more likely reflects metabolically sourced carbon (Trueman et al. 2016).

As temperature increased, there was reduced variation of M between individual fish. Concurrently, there was a lower survival rate at the higher temperatures. These combined results suggest that the fish that were able to survive at higher temperatures possessed similar physiological traits with decreased metabolic variability. These fish may have possessed better adaptive ability for physiological performance and fitness at higher temperatures, potentially through a higher capacity for concentration and stability of enzymes and increased intracellular stabilisers (Angilletta et al. 2003). However, these specialised traits may come at a cost and adaptive traits often balance trade-offs between generalist versus specialist forms. For example, with thermal reaction norms, there can be a preference between survival and performance being moderate at a wide range of temperatures (generalist) or survival and performance being higher at niche temperatures but reduced over a wider range of temperatures (specialist) (Angilletta et al. 2003, Rungruangsak-Torrissen et al. 1998). Shifts to more specialist thermal reaction norms could lead to reduced capacity in populations to cope with a broader range of environmental temperatures. Furthermore, loss of genetic and metabolic diversity in natural conditions would be inherited by subsequent generations. This could reduce the range of possible biological and adaptive responses as a buffer against changing environmental conditions (Laikre et al. 2010, McGinnity et al. 2009), with significant adverse effects on population biomass and survival (Smith et al. 1991).

Metabolic rate is the "energetic cost of living" and a fundamental biological and ecological trait (Hulbert and Else 2000). Retrospectively tracing metabolic histories can provide information on important lifestyle attributes, e.g. performance, growth, lifestyle and diet variability, environmental tolerance and population productivity. Our study is an important precursor to using otolith $\delta^{13}C$ as a metabolic tracer. Thus far most of the work has been either theoretical in developing this tracer or in the field (Kalish 1991a, Shephard et al. 2007, Tohse et al. 2004, Trueman et al. 2016). For example, the relationship between caudal fin area (proxy of aerobic swimming activity and MR) and otolith $\delta^{13}C$ has been explored (Sherwood and Rose 2003). Our study indicates the potential of carbon isotopes in otoliths as metabolic biomarkers, once carbon sources and environmental variables have been carefully considered in field studies. Future research quantifying the relationship between measured metabolic rates and carbon isotopes will strengthen the potential of otoliths as metabolic biomarkers.

Carbon stable isotopes in soft-tissues

Our study demonstrates that temperature can alter carbon incorporation into soft-tissues, with increased values of $\delta^{13}C$ in muscle and liver with higher temperatures. These changes occurred at different temperature ranges for muscle and liver, with increased $\delta^{13}C$ values at the three highest temperature treatments in muscle and the three lowest temperatures for liver. The variation in $\delta^{13}C$ may be explained by differences in isotopic incorporation and routing because of structural and physiological differences between muscle and liver, in addition to the influence of temperatures on tissue metabolic rates. For example, visceral organs such as liver have higher metabolic rates and lower growth than supportive tissue like muscle (Dalerum and Angerbjörn 2005). In this study, muscle, but not liver, was significantly correlated with fish size, suggesting a strong growth influence. Therefore, the isotopic composition in muscle was likely driven by the synthesis of new tissue, whereas liver composition was likely driven by high metabolic rates replacing or converting existing tissues (Buchheister and Latour 2010, Carleton and Del Rio 2010, Mont'Alverne et al. 2016). Changing temperatures may have also affected the balance between metabolic and growth influences on isotopic incorporation (Carleton and Del Rio 2010, Sweeting et al. 2007). For example, carbon isotope incorporation can be primarily linked to growth in optimum growth conditions (such as favourable temperature conditions) but strongly related to metabolic rate under sub-optimal growth conditions (Weidel et al. 2011). Consequently, physiological differences between the soft-tissues and the effect of temperature on physiology likely influenced isotopic incorporation.

Carbon isotope fractionation between diet and tissue was traditionally considered to be at 1‰ per trophic level (DeNiro and Epstein 1978), although other studies have seen differences of up to 5‰ (Bloomfield et al. 2011, Gaston and Suthers 2004). Our levels of enrichment were higher at an average 6‰ for muscle and 8.3‰ for liver. Our fish were fed the same diet for 10 weeks (including acclimation and experimental period) and isotope half-lives in fish range from 2–8 weeks in muscle and 1–7 weeks in liver tissue (Boecklen et al. 2011). The soft-tissue therefore most likely consisted of the analysed diet and old diet signatures were unlikely to be the main contributor of the fractionation difference. The high protein diet (approximately 50% mass) used in this study may have contributed to widening the fractionation gap. At low protein levels, the bulk muscle tissue is statistically indistinguishable from that of bulk diet (Newsome et al. 2011), whereas higher protein diets can induce higher diet-tissue fractionation (Elsdon et al. 2010) and significant isotopic routing (Kelly and del Rio 2010). Increased metabolic rates may have driven increased routing of specific dietary components, altering the bulk tissue carbon signatures. As $\delta^{13}C$ increased with temperature, there may have been increased routing from more positive components such as proteins or carbohydrates. Furthermore, isotopic routing may be responsible for the fractionation differences between lipid-normalised liver and muscle, with liver being further from the diet signature. Potentially, more lipid $\delta^{13}C$ was routed to lipid-heavy liver, but these signatures may have been concealed with lipid-normalisation.

The fractionation trends may also have been driven by underlying amino acid signatures, with fractionation between bulk diet and tissue in part reflecting amino acid composition (Gannes et al. 1998). Amino acids can be separated into essential amino acids that must be assimilated from diet and non-essential amino acids, that can be assimilated or de-novo synthesised through either glycosis or the Krebs cycle (Boecklen et al. 2011). Assimilated molecules will generally reflect bulk diet carbon signatures while de-novo synthesised molecules can vary, with the balance between these processes triggering carbon signatures of non-essential amino acids to differ from bulk diet by up to 20% (McMahon et al. 2010). Non-essential amino acids can have a significant effect on bulk carbon values as they can make up a large proportion of amino acid composition, for example glutamic acid and arginine can account for up to 18% of amino acid composition in fish muscle (McMahon et al. 2010). Differences in carbon values among temperature treatments could have arisen from varying metabolic rates stimulating variable food demands and amino acid requirements that consequently led to changing balances between non-essential amino acid assimilation vs de-novo synthesis. In this study, we used IRMS to determine bulk soft-tissue $\delta^{13}C$. Compound specific isotope ratio mass spectrometry is a valuable alternative that provides values of $\delta^{13}C$ in amino acids in both diet and tissue (e.g. Blanke et al. 2017, Bloomfield et al. 2011). This method may be able to further explain differences in diet-tissue fractionation by directly tracking the integration routes of amino acids.

Conclusions

This study reveals metabolic effects on carbon incorporation in fish tissues, with otolith carbon shown to uncover valuable insights into metabolic rates and soft-tissues incorporating diet signatures that are altered by changing environments. Our ability to use these tools as field biomarkers of metabolic rate and diet hinges on understanding the factors controlling isotopic uptake in fish tissues. Biological histories provide insights into the drivers of past ecological trends and enable us to better manage our natural resources into the future.

Statement of Authorship

Title of Paper	Biominerals track metabolic rates in fish	
Publication Status	☐ Published ☑ Submitted for Publication	☐ Accepted for Publication ☐ Unpublished and Unsubmitted work written in manuscript style
Publication Details	Submitted to Proceedings of the Royal Society B: Biological Sciences on 17 Jan 2019	

Principal Author

Name of Principal Author (Candidate)	Jasmin Martino		
Contribution to the Paper	Collected, analysed and interpretated data, wrote manuscript and acted as corresponding author.		
Overall percentage (%)	85%		
Certification:	This paper reports on original research I conducted during the period of my Higher Degree by Research candidature and is not subject to any obligations or contractual agreements with a third party that would constrain its inclusion in this thesis. I am the primary author of this paper.		
Signature		Date	

Co-Author Contributions

By signing the Statement of Authorship, each author certifies that:

i. the candidate's stated contribution to the publication is accurate (as detailed above);
ii. permission is granted for the candidate in include the publication in the thesis; and
iii. the sum of all co-author contributions is equal to 100% less the candidate's stated contribution.
iv.

Name of Co-Author	Zöe Doubleday		
Contribution to the Paper	Supervised development of work, helped in data interpretation and manuscript evaluation.		
Signature		Date	24/1/2019.

Name of Co-Author	Bronwyn Gillanders		
Contribution to the Paper	Supervised development of work, helped in data interpretation and manuscript evaluation.		
Signature		Date	24/1/2019

CHAPTER FOUR

Biominerals track metabolic rates in fish

ABSTRACT

Metabolic rate underpins our understanding of how species survive, reproduce and interact with their environment. An intrinsic proxy of metabolic rate could be an inexpensive and effective approach to reconstruct lifetime metabolic histories. We investigated the relationship between metabolic rate and carbon isotopes ($\delta^{13}C$) in fish ear stones (otoliths) to test their potential as a metabolic biomarker. Juvenile snapper (*Chrysophrys auratus*), an iconic and valuable fishery species, were reared at different temperatures and intermittent-flow respirometry was used to calculate standard metabolic rate, maximum metabolic rate and absolute aerobic scope. Carbon and oxygen ($\delta^{18}O$) isotopes in otoliths were then analysed using isotope ratio mass spectrometry. A significant negative linear relationship was found between carbon isotopes and metabolic rates. However, with increasing stress (heat and exertion), this negative relationship switched to an increasingly positive relationship. Our study validates the use of carbon isotopes in otoliths as a metabolic biomarker in temperate/sub-tropical fish but indicates that physiological stress is a key consideration. We demonstrate the potential of chemical biomarkers for reconstructing metabolic histories, information that can assist in better understanding and management of wild populations.

INTRODUCTION

Metabolic rates reflect available energy for fuelling biological processes and is widely used to study physiological potential and interactions between organisms in natural environments (Gillooly et al. 2001, Nagy 2005). Metabolic rates provide understanding of biology at an individual (performance, growth, reproduction, and excretion), population (population dynamics and interactions) and ecosystem (trophic dynamics and food availability) level (Brown et al. 2004, Chabot et al. 2016b). Individuals that obtain and process energy with the most efficiency will often have ecological advantages and greater genetic fitness (Tolkamp et al. 2002, Butler et al. 2004). As such, metabolic measures can be used to address a wide range of ecological questions and are important in understanding and managing wild fish populations.

Field metabolic rates can be difficult to measure in fish. The doubly labelled water method, which involves measuring the elimination of an introduced oxygen isotope signature, is used for most air-breathing animals but is unsuitable for fish. Metabolic rates have therefore been measured using electromyogram telemetry (Cooke et al. 2004, Quintella et al. 2009), heart rate monitoring (Thorarensen et al. 1996, Clark et al. 2005) or accelerometry (Metcalfe et al. 2016). However, these approaches can be expensive, logistically difficult and only offer short-term 'snapshots' of metabolic rates. Records conserved in biominerals offer a valuable alternative to uncovering long-term biological histories. Otoliths (ear stones) are calcium carbonate ($CaCO_3$) structures in teleost fishes which permanently retain life-time environmental and physiological signatures (Campana 1999). Alternating translucent and opaque bands are formed annually and provide age estimates, allowing chemical signatures to be matched to specific age and calendar years (Campana & Thorrold 2001). Otoliths are widely accessible as long-term collections are stored in research institutes and museums worldwide. Furthermore, analysis is both cost-effective and efficient. Otoliths are a valuable tool for reconstructing environmental histories of fish (Elsdon et al. 2008, Izzo et al. 2018), but further investigation will enhance their potential as physiological biomarkers.

Stable carbon isotopes in otoliths may reflect metabolic rates in fish. Otolith carbon arises from two sources: (1) dissolved inorganic carbon in environmental water incorporated via the gill and/or intestinal interfaces and (2) metabolically-sourced carbon via cellular respiration of food (Kalish 1991, McConnaughey et al. 1997, Trueman et al. 2016). As metabolic demand increases, there is a concurrent increase in respiration and metabolic CO_2 which increases the proportion of the metabolic carbon in the blood and endolymph, which is subsequently deposited onto the otolith (Trueman et al. 2016). Metabolic carbon has a significantly depleted carbon signature (values are more negative) compared to water so changes to carbon signatures are thought to be driven by metabolic shifts. Additionally, as the proportion of metabolic carbon is low, significantly large differences in diet is required to significantly alter end carbon values in otoliths, making diet influences minimal (Chung et al. 2019a). Previous research established that carbon isotopes negatively correlated with estimates of standard metabolic rate predicted by metabolic theory in Arctic fish (Chung et al. 2019b). Further experimental work is needed to validate this relationship in other species, particularly in temperate or tropical fish and different temperature ranges.

We investigated the relationship between biominerals and metabolic rates in an iconic fishery species. We experimentally manipulated temperature to establish a range of metabolic conditions. Our objectives were to individually measure and investigate the relationship between isotopes in otoliths (carbon and oxygen) and metabolic parameters (standard metabolic rate, maximum metabolic rate and absolute aerobic scope). A significant relationship will indicate the potential of carbon isotopes as a metabolic proxy in temperate/sub-tropical fish.

METHODS

Experimental design

Australasian snapper (*Chrysophrys auratus*) is an iconic long-lived demersal species that supports important commercial and recreational fisheries in the Australasia and Indo-Pacific region (Fowler et al. 2016). Wild snapper eggs were collected in Cockburn Sound, Western Australia, reared at Challenger TAFE (Western Australia) for two months and then transported to the University of Adelaide, South Australia, for experiments. Fish were batch marked via immersion in an alizarin complexone ($C_{19}H_{15}NO_8$) solution (40 mg/L of tank water) for 24 hr (van der Walt & Faragher 2003). Fingerlings were separated into 16 tanks (4 treatments x 4 replicate tanks) which contained 40 L of locally sourced coastal seawater (salinity: 40 psu) as well as a submerged filter and aerator. After acclimating to local conditions for 7 days, temperature was adjusted by 1.5°C per day until experimental temperatures (20°C, 24°C, 28°C, 32°C) were reached. Water temperature was measured daily throughout the experiment with a handheld probe (Hanna Instruments HI-98127). Salinity was tested twice weekly using a refractometer (Vertex RF-1) and maintained at 35 psu via the addition of aged bore water. To maintain water quality, 50% water changes occurred weekly and water was regularly tested for ammonia through commercial testing kits (API). Fingerlings were fed to satiation twice daily with commercial fish food (Skretting Protec). Fish (n=31) were exposed to experimental conditions for up to 2 months (Table 4.1).

Intermittent-flow respirometry

Intermittent-flow respirometry was used to measure fish oxygen consumption (mg/L [ppm]). Fish were fasted for 24 hours prior as digestion can increase oxygen consumption (Chabot et al. 2016b). The respirometry system consisted of four chambers with a maximum of three chambers at a time used to measure fish oxygen consumption (mg/L [ppm]) and the fourth used to measure background respiration (Figure S4.1). Each chamber was a closed system attached to a pump (approximately 250 ml/s), to recirculate water through the system loop, and a FireSting O_2 Optical Oxygen Meter (Pyroscience), which was used to measure oxygen levels (Figure S4.1). Logging software (Pyro Oxygen Logger v 3.1) was used to record oxygen and time data. The oxygen sensor system was calibrated prior to each run. To measure maximum metabolic rate

(MMR), fish were exerted through a combined exhaustive chase and air exposure procedure (Roche et al. 2013, Gilmore et al. 2018). Fish were then left in the respirometry chamber for 24 hours to reach a resting state. Each respirometry cycle consisted of three stages: a 3-min flush stage where the pump pushed oxygenated water through each system; a 30-sec wait stage where the system is closed awaiting oxygen measurement; and a 12-min measuring period where the pump was off, the loop was closed, and oxygen was measured.

The effective respirometer volume was calculated:

$$V_{RE} = V_{RT} - W_o \qquad \text{(Equation 1)}$$

where V_{RE} is the effective respirometer volume (L), V_{RT} is the total respirometer volume of the empty respirometer including the recirculation loop, and W_0 is the mass of the organism (kg) (Svendsen et al. 2016). As fish were assumed to be neutrally buoyant; the density of the organism was not used in the above equation (Svendsen et al. 2016). Rate of oxygen decline was determined using the slope of each measurement period, converted into hours and then mass-specific oxygen consumption ($M\mathrm{O}_2$; $\mathrm{mgO_2kg^{-1}h^{-1}}$) was calculated:

$$M\mathrm{O}_2 = V_{\mathrm{RE}} \mathrm{W}_o^{-1} \frac{\delta C\mathrm{O}_2}{\delta t} \qquad \text{(Equation 2)}$$

where $\frac{\delta C\mathrm{O}_2}{\delta t}$ is the slope of the linear decrease in oxygen content over the measurement period (Steffensen 1989, Svendsen et al. 2016). Mass-specific background respiration was accounted for by subtracting it from the whole animal consumption rate using the following equation:

$$M\mathrm{O}_{2\mathrm{corr}} = M\mathrm{O}_2 - M\mathrm{O}_{2\mathrm{B}} \mathrm{V}_{R\mathrm{T}} \mathrm{V}_{\mathrm{RE}}^{-1} \qquad \text{(Equation 3)}$$

where $M\mathrm{O}_{2\mathrm{corr}}$ is the corrected oxygen consumption and $M\mathrm{O}_{2\mathrm{B}}$ ($\mathrm{mgO_2kg^{-1}h^{-1}}$) is the mass-specific background respiration calculated as if the organism was present in the chamber (Svendsen et al. 2016).

Standard metabolic rate (SMR) is a key physiological trait representing the minimum amount of energy needed to sustain life and has important implications for maximum performance, growth rate, lifestyle, and social interactions (Chabot et al. 2016b). Standard metabolic rate was estimated as the lowest 20th percentile ($q_{0.20}$) of the recorded $M\mathrm{O}_2$ values (Chabot et al. 2016b). Maximum metabolic rate (MMR) indicates the upper limit of metabolic capacity and highlights the potential energy usage (Norin & Clark 2016, Treberg et al. 2016). Maximum metabolic rate was calculated from the $M\mathrm{O}_2$ measured after exertion, with the first two respirometry cycles excluded to allow stabilisation, and then an average taken of the next 5 respirometry cycles.

Absolute aerobic scope (AAS), illustrates energy niches and fitness/performance windows (Clark et al. 2013). Absolute aerobic scope was calculated as the difference between maximum and standard metabolic rates (Clark et al. 2013):

$$AAS = MMR - SMR \qquad \text{(Equation 4)}$$

After intermittent-flow respirometry, fish were euthanised in an ice slurry and immediately frozen. Each fish was measured for length (mm, FL) and weight (g). Fulton's condition factor (K), representing somatic condition was calculated (Bolger & Connolly 1989):

$$K = 10^5 M_W L_s^{-3} \qquad \text{(Equation 5)}$$

where M_w is weight (g) and L_s is fork length (mm) of fish. Both sagittal otoliths were dissected from each fish, cleaned of adhering tissue and air-dried. Experimental otolith material, distinguished by a purple alizarin complexone band, was chipped off onto filter paper and placed in acid-sterilised 4.5 ml vials.

Isotope analysis

Vials containing otolith material were purged for 2.5 minutes with nitrogen gas and injected with 100µl - 120µl of 103 – 104% phosphoric acid. Otolith samples were analysed for carbon and oxygen isotopes using a GasPrep headspace analyser connected to a Nu Horizon (Nu instruments) isotope-ratio mass spectrometer (IRMS). Powder standards (ANU-P3, UAC CaCO3 UniA, IAEA-CO8) were analysed to assess instrument drift and calculate precision. Isotope values were reported relative to Vienna Pee Dee Belemnite (VPDB) and expressed in standard delta (δ) parts per thousand (‰):

$$\delta = \left(\frac{R_{sample} - R_{standard}}{R_{standard}}\right) x\ 1000\ (‰) \qquad \text{(Equation 6)}$$

where R is the ratio of ^{13}C:^{12}C or ^{18}O:^{16}O. Analytical errors were <0·18‰ for $\delta^{13}C$ and <0·33‰ for $\delta^{18}O$ values in otoliths. Water samples (50 ml) were collected at the beginning and end of the experiment and filtered through a 0.21 µm filter and refrigerated. Dissolved inorganic carbon in water samples were measured using a GasBench II coupled with a Delta XL Mass Spectrometer in continuous flow mode (Thermo-Fisher Scientific). Fish food samples (*n*=3) were collected, ground to a fine powder using a mortar and pestle and were analysed for carbon isotopes using a continuous flow system consisting of a Delta V Plus mass spectrometer connected with a Thermo Flush 1112 via Conflo IV (Thermo-Finnigan/Germany). Water and diet samples were both analysed at the West Australian Biogeochemistry Centre. The proportional contribution from carbon sources to snapper otoliths was taken from previously calculated isotopic mixing models (Martino et al. 2019a).

Statistical analyses

Two-factor permutational univariate analysis of variance (ANOVA) was used to determine differences in metabolic rates and carbon isotope ratios between temperature treatments (*PRIMER* v6.0/*Permanova*). Non-transformed data were used to calculate resemblances matrices based on Euclidean distance non-similarity and analysed by unrestricted permutations of the data for all tests. Within the two-factor design, temperature was a fixed factor and nested replicate tanks a random factor. When tank effects were absent, ANOVAs were repeated with temperature as a single factor. When significant differences were detected, post-hoc pair-wise comparisons were used to identify the source of differences in metabolic rates and isotopic ratios between temperature treatments. Linear regressions and correlation tests (Pearson’s product moment correlation) were used to assess the strength and significance of the relationships between biological variables (R Studio v3.2.0; Wright 2012, Team 2014).

RESULTS

Rearing conditions remained stable throughout the experimental period, with desired temperature levels maintained for each treatment (Table 4.1). Mortality rate increased sharply at 32°C and no fish survived at this temperature, and were therefore not included in the respirometry experiments. Dissolved inorganic carbon in tank water, fish size (weight and length) and Fulton's k representing condition did not vary among temperatures (Table S4.2). There were no significant differences between temperature treatments for standard metabolic rate, maximum metabolic rate and absolute aerobic scope when tank effects were included in the design (Table S2). As there were no significant tank effects for SMR, analyses were rerun with temperature as the sole factor.

Table 4.1 - Summary of water and fish parameters in experimental study. Values are mean (± standard error) of measured temperature (°C) and dissolved inorganic carbon (DIC) in tank water; carbon isotopes ($\delta^{13}C$) in diet; and sample sizes and lengths (mm) of experimental fish, and the fraction of metabolically-sourced carbon (*M*) in otoliths.

Treatment (°C)	Temperature (°C)	Water DIC (‰ VPDB)	Diet $\delta^{13}C$ (‰ VPDB)	Sample size (n)	Length (mm)	*M* (%)
20	19.8±0.06	-6.7±0.9	-25.4±0.2	12	80.6±2.9	19.1±2.6
24	23.9±0.07	-7.4±0.6	-25.4±0.2	14	78.0±1.9	23.6±1.13
28	28.0±0.03	-7.8±0.6	-25.4±0.2	5	69.8±2.9	27.7±2.9

Significant temperature effects were found for SMR (Figure 4.1; Table S2), with the differences occurring between the 20°C and 24°C temperature treatments and the 28°C temperature treatment. Carbon and oxygen isotopes in otoliths significantly decreased with increasing temperature (Figure 4.2; Table S2).

Figure 4.1 - Mean (± SE) standard metabolic rate (SMR), maximum metabolic rate (MMR) and absolute aerobic scope (AAS) measured by intermittent-flow respirometry in snapper reared at different temperatures. Significant differences ($p<0.05$) in SMR were found between temperatures and are represented by different letters.

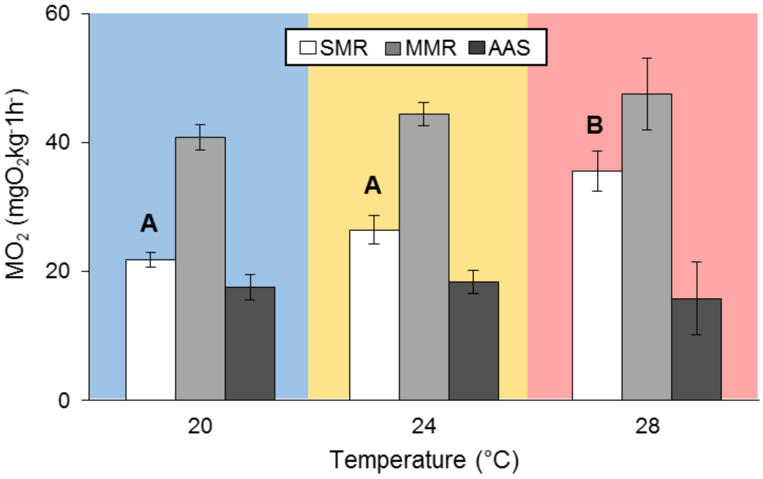

Figure 4.2 - Mean (± standard error) carbon ($\delta^{13}C$) and oxygen ($\delta^{18}O$) isotopes in snapper otoliths reared at different temperature treatments. Significant differences ($p<0.05$) between temperatures for both isotopes are represented by different letters. Separate axes are used for each isotope.

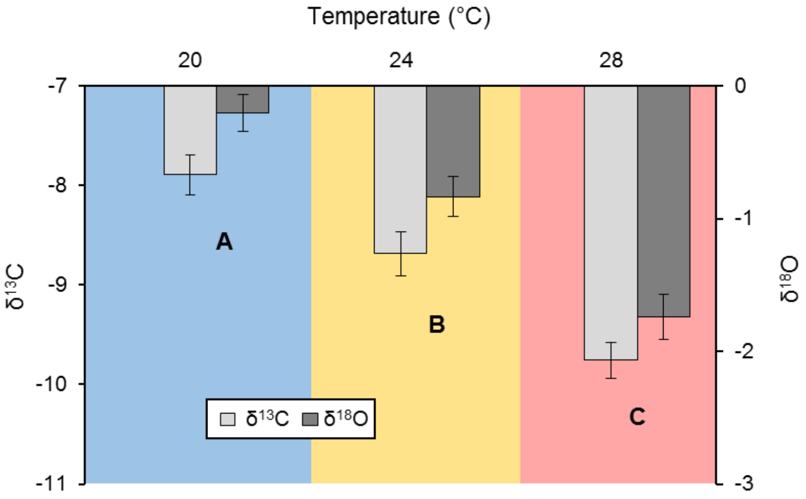

Carbon isotopes had an overall negative relationship with standard metabolic rates (Figure 4.3a; R^2 = 0.45 $p<0.05$) and maximum metabolic rates (Figure 4.3b; R^2 = 0.42 $p<0.05$). However, temperature significantly influenced the relationship. The relationship between carbon isotopes and metabolic rate was negative at the lowest temperature but with higher temperatures, the relationship became increasingly more positive (Figure 4.3c, Figure 4.3d). The change was stronger for maximum metabolic rate than standard metabolic rate.

Figure 4.3 - Relationships between carbon isotopes in snapper otoliths and standard metabolic rate (SMR) (a, c) and maximum metabolic rate (MMR) (b, d); also shown are regression lines. Overall relationship is displayed (a, b) and trends separated into individual 20°C, 24°C and 28°C temperature treatments (b, d).

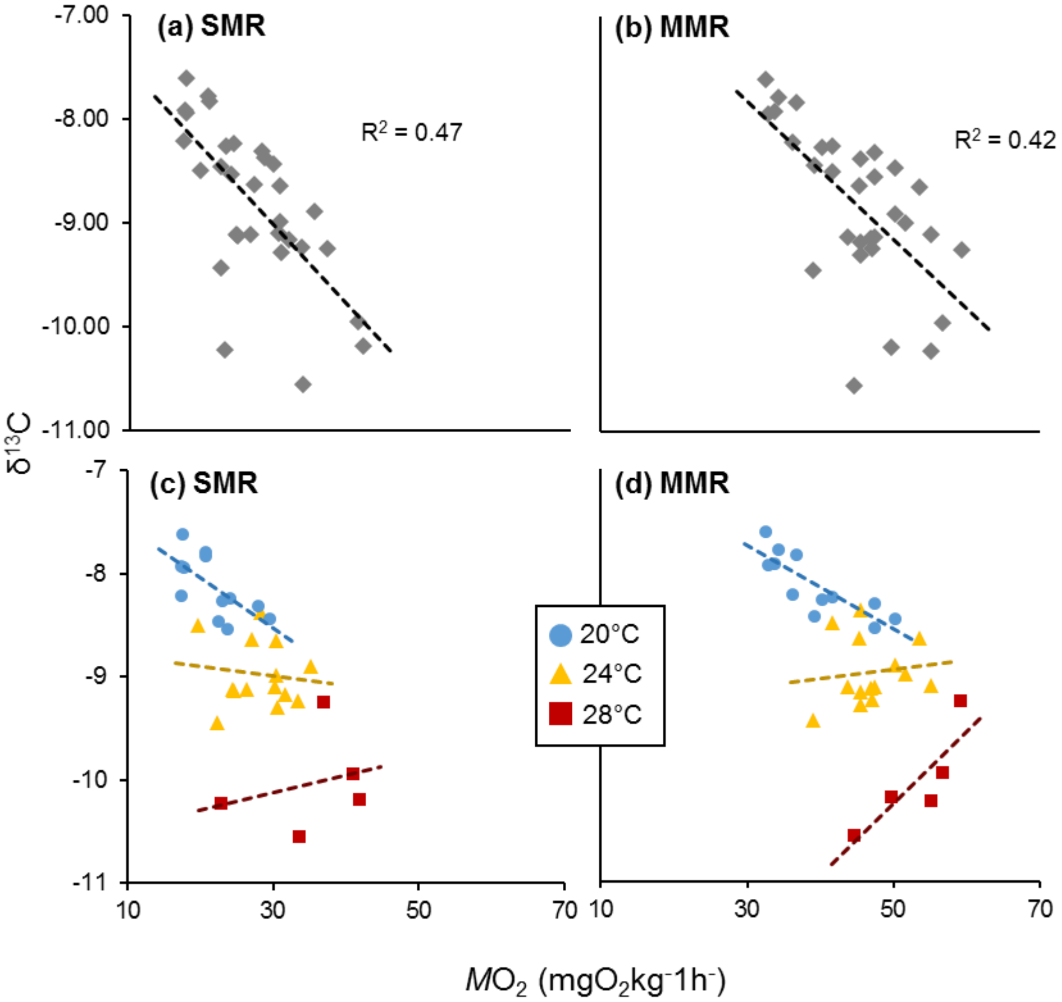

DISCUSSION

Tracking metabolic rates in marine animals provides understanding into behaviour, resource-use and interactions within ecosystems and environments. We experimentally tested the extent to which carbon isotopes in otoliths act as a metabolic proxy. We found significant negative linear relationships between carbon isotopes in otoliths and standard and maximum metabolic rates. However, at higher levels of stress (heat and exertion) the relationship was reversed. This study is an important precursor for using carbon isotopes to track metabolic rates in the wild.

Our results experimentally validated carbon isotopes as a proxy of metabolic rates. Otolith carbon arises from two sources: (1) dissolved inorganic carbon in environmental water and (2) metabolically-sourced carbon from diet (Kalish 1991, Solomon et al. 2006, Tohse and Mugiya 2008). We show that shifts in carbon isotopes do not primarily reflect the trends in diet or water as these factors remained constant across treatments, but values in otoliths were significantly altered. As average metabolic rates increased, likely higher respiration and food consumption increased the proportion of more depleted metabolic carbon (more negative values of carbon isotopes) into the otoliths (Chung et al. 2019a). Our results suggest metabolic effects are a dominant influence of carbon isotope signatures in otoliths. Significant relationships have been previously seen between carbon isotopes with predicted swimming capacity (Sherwood and Rose 2003) and estimates of standard metabolic rate predicted by metabolic theory (Chung et al. 2019b). In Chung et al. (2019b), carbon isotopes were correlated with predicted standard metabolic rates under 4 - 14°C in Atlantic cod (*Gadus morhua*). This study confirms that a relationship between carbon isotopes and metabolic rate exists for temperate/sub-tropical fish reared at significantly higher temperature levels (20 - 28°C). Consequently, metabolic proxies in otoliths are shown to be applicable in fish across a range of environmental niches.

While the overall relationship between carbon isotopes in otoliths and metabolic rates was a linear negative relationship, we found the relationship was altered by physiological stress. As fish were exposed to increasing temperatures and greater physical exertion, the relationship between carbon isotopes and metabolic rates switched from negative to neutral or positive. This suggests an increased proportion of carbon from water or decreased proportion of metabolically sourced carbon at high metabolic rates. Stress responses, such as the release of cortisol, can affect uptake of ions such as increasing the permeability of the surface epithelia of the gills to water and ions (Bonga 1997). Stress can also induce rapid breathing, which can cause fish to exchange more of their internal respired CO_2 for ambient water CO_2 (McConnaughey & Gillikin 2008). Alternatively, temperature effects could be the principle influence behind the changing relationship. Temperature affects gas solubility, which could be potentially increasing the passive influx of ambient water CO_2 and diluting the internal carbon pool (McConnaughey et al. 1997). Consequently, care should be taken in using carbon isotopes in otoliths as a metabolic biomarker when fish are predicted to experience sustained periods of physiological stress, such as beyond their optimal temperature thresholds. Tolerances could be determined from reconstructions of temperature environments from oxygen isotope signatures in otoliths (Høie et al. 2004, Darnaude et al. 2014, Shirai et al. 2018), which can be matched with experimentally-determined optimum thermal limits for individual species. This study highlights the impact of physiological condition on biomineral incorporation and illustrates it should be an important consideration in chemical reconstructions.

Intrinsic biomarkers offer an advantageous approach for recording metabolic rates in the wild. Otoliths can reconstruct lifetime profiles and analytical costs are comparatively low compared with most field sampling and *in situ* experiments, which allows for larger sample sizes. Otolith archives are also kept in research institutes and museums worldwide, providing easy access to a wide range of species, locations and year classes. Biogeochemical techniques can also reconstruct histories when direct measures are not possible, such as historical or extinct species using archaeological samples (Wurster & Patterson. 2003, Disspain et al. 2016); or inaccessible species, such as deep-sea fish (Shephard et al. 2007, Trueman et al. 2013). Although chemical proxies may be less accurate than direct measurements via electromyogram telemetry, accelerometry or heart rate measures (Metcalfe et al. 2016), these direct approaches can have limited application due to high costs and logistics from expensive equipment and field time required. These direct measures also typically capture only a short-term ‘snapshot’, spanning hours to a maximum of one or two years (Butler et al. 2004). Direct measures also generally involve locating the study species in the wild and then either implanting or attaching a device. Some of these devices require recapture and are unable to be used on small individuals, which limits measurements of immature fish, or soft-bodied organisms such as cephalopods (Butler et al. 2004). Overall, intrinsic biomarkers can be a comparatively useful, efficient and cost-effective alternative for investigating metabolic histories. However, direct measures and intrinsic biomarkers both offer valuable insights into field metabolic rates. Combining direct measures in the wild with chemical proxies may be the next step to enhancing this tool and could improve the accuracy of metabolic biomarkers for long-term reconstructions.

This study opens opportunity to explore new perspectives of biominerals by providing metabolic insights into other aquatic animals. Hard-parts in molluscs could potentially be used in a similar manner. Carbon isotopes in bivalve shells can have a metabolic/respired carbon component and may provide insights into metabolic activity and the physio-chemical environment of ambient water (Schöne et al. 2011, Henderson & Price 2012, Immenhauser et al. 2016). Additionally, carbon isotopes in cephalopod hard-parts such as statoliths (cephalopod equivalent to otoliths), cuttlebones or beaks may be controlled by vital effects, such as ontogeny and maturation, and metabolic or diet influences (Bettencourt & Guerra 1999, Price et al. 2009, Rexfort & Mutterlose 2009). However, experimental work on cephalopods is limited and the incorporation of carbon into hard-parts is poorly understood. A metabolic tracer would be a valuable tool for understanding physiological responses and ecological interactions of molluscs in the wild, so further experimental research is needed.

We show that carbon isotopes in otoliths can act as a metabolic proxy for fish within optimal physiological limits. Assessing optimal limits, such as through temperature reconstructions using oxygen isotopes, is suggested to be an important step when using this tool. We highlight that biogeochemical reconstructions using hard calcified structures like otoliths offer an inexpensive approach to develop long-term thermal and metabolic histories. Metabolic biomarkers could provide understanding into physiological responses to environments and trophic interactions. This information will enable ecologists and fishery managers to identify physiological stressors and when necessary, to develop effective countermeasures (Wikelski and Cooke 2006). Consequently, metabolic biomarkers possess high value as a powerful conservation and management tool.

Statement of Authorship

Title of Paper	Linking chemical chronologies and physiology in a wild fish
Publication Status	☐ Published ☐ Accepted for Publication ☐ Submitted for Publication ☑ Unpublished and Unsubmitted work written in manuscript style
Publication Details	

Principal Author

Name of Principal Author (Candidate)	Jasmin Martino		
Contribution to the Paper	Collected, analysed and interpretated data, wrote manuscript and acted as corresponding author.		
Overall percentage (%)	85%		
Certification:	This paper reports on original research I conducted during the period of my Higher Degree by Research candidature and is not subject to any obligations or contractual agreements with a third party that would constrain its inclusion in this thesis. I am the primary author of this paper.		
Signature		Date	

Co-Author Contributions

By signing the Statement of Authorship, each author certifies that:

i. the candidate's stated contribution to the publication is accurate (as detailed above);

ii. permission is granted for the candidate in include the publication in the thesis; and

iii. the sum of all co-author contributions is equal to 100% less the candidate's stated contribution.

Name of Co-Author	Anthony Fowler		
Contribution to the Paper	Supervised development of work, helped in data interpretation and manuscript evaluation.		
Signature		Date	25/1/19

Name of Co-Author	Zöe Doubleday		
Contribution to the Paper	Supervised development of work, helped in data interpretation and manuscript evaluation.		
Signature		Date	24/1/2019.

Name of Co-Author	Bronwyn Gillanders		
Contribution to the Paper	Supervised development of work, helped in data interpretation and manuscript evaluation.		
Signature	[redacted]	Date	25 Jan 2019

CHAPTER FIVE

Disentangling intrinsic and extrinsic drivers of otolith chemistry in a coastal marine fish

ABSTRACT

Otolith chemistry is a valuable tool for reconstructing environmental histories of fish. However, incorporation of chemical signatures can be moderated by physiological processes, which potentially confounds environmental and biological applications. As such, we investigated the relationship between otolith chemistry, intrinsic (physiological) properties, and extrinsic (environmental) factors to 1) further our understanding of the magnitude and direction of influences on otolith chemistry and 2) assess the potential of chemical markers in otoliths to track physiological processes. Using otoliths of an iconic and valuable fishery species, Australasian snapper (*Chrysophrys auratus*), we analysed lifetime profiles of stable carbon ($\delta^{13}C$) and oxygen ($\delta^{18}O$) isotopes, and elemental concentrations of magnesium (Mg:Ca), strontium (Sr:Ca), barium (Ba:Ca), manganese (Mn:Ca) and lithium (Li:Ca). Otoliths were taken from fish across two oceanographically diverse regions (northern Spencer Gulf and the South-East in South Australia) and three cohorts (1979, 1991, 2006) to examine regional and temporal variation. Mixed-effects modelling was used to investigate the influence of intrinsic properties (age, otolith growth, fish size, sex) and environmental factors (sea surface temperature and chlorophyll-*a*) on chemical markers. Lifetime change in chemical trends were revealed, indicating ontogenetic influences on chemical incorporation or changes in composition of environmental water across lifetimes. Further, we revealed carbon isotopes, magnesium and, to a lesser extent, strontium strongly reflect physiological characteristics. In contrast, barium, oxygen and lithium reflect past environmental conditions. Chemical signatures were then applied to improve our understanding of wild snapper populations in southern Australia. Our results highlight that intrinsic properties such as age, cohort, sex and growth can affect chemical incorporation into otoliths, highlighting the need for consistency in sampling designs. This study furthers our understanding of the sources and influences on otolith chemistry, reinforcing confidence in their applicability for retrospective reconstructions of both the physiological and environment histories of wild fish.

INTRODUCTION

Otolith chemistry is a powerful tool for addressing a wide-range of biological and ecological questions. Otoliths (ear stones) of teleost fish are calcium carbonate ($CaCO_3$) structures which are acellular and metabolically inert, creating lifetime chemical profiles that are permanently locked into the structure (Campana 1999). Many applications of otolith chemistry are based on the premise that chemical signatures in otoliths reflect the water composition of local environmental conditions and can be used to track movement and environmental patterns. However, physiological processes in fish can affect otolith chemistry, suggesting that otoliths can also be used to track physiological trends. Generally the pathway of chemical incorporation into otoliths involves ions being taken up from the surrounding water via the gills or intestines into the blood plasma, then into the endolymphatic fluid before being accreted onto the surface of the otolith (Campana 1999). Chemical discrimination can occur at each physiological barrier along this pathway with varying degrees of discrimination among elements (Campana 1999). Chemical signatures with high physiological regulation may reflect physiological processes and individual genetic makeup in fish (Gronkjaer 2016), whereas chemical signatures with little physiological discrimination are more likely to reflect environmental conditions (Thomas et al. 2017, Izzo et al. 2018).

Identifying the relationships between otolith chemistry and physiological processes is an important first step in using otoliths to track physiological histories (Kalish 1991, Sturrock et al. 2014, Gronkjaer 2016, Chung et al. 2019a). Physiological histories uncover energy dynamics and interactions in ecosystems, which can address a wide-range of biological and ecological questions. For example, stable carbon isotopes ($\delta^{13}C$) are a likely proxy of metabolic rates in fish (Chung et al. 2019b, Martino unpublished). Otolith carbon arises from two sources: (1) dissolved inorganic carbon in surrounding water and (2) metabolically-sourced carbon via cellular respiration of food (Kalish 1991, McConnaughey et al. 1997, Trueman et al. 2016). Higher respiration and metabolic rates increase the proportion of metabolic carbon, which has a significantly depleted carbon signature compared to that of water, and cause detectable shifts in otolith carbon isotopes. Consequently, changes in carbon isotopes in otoliths are thought to predominantly reflect metabolic shifts. The influence of other carbon sources is considered minimal as carbon signatures typically remain within a narrow range in marine waters, whilst considerable changes to diet are required to significantly alter values of otolith carbon (Kroopnick 1985, Sherwood & Rose 2003, Shephard et al. 2007, Schmittner et al. 2013, Trueman et al. 2016, Chung et al. 2019a). Magnesium concentrations (Mg:Ca) in otoliths may also track physiological trends in fish. No relationship has been found between magnesium and environmental composition such as water or diet, whilst there are suggestions that magnesium is taken up in proportion to metabolic activity (Woodcock et al. 2012, Limburg et al. 2018). Furthermore, strontium concentrations (Sr:Ca) have been related to both environmental influences and physiology. While water sources contribute 59 - 83% of strontium in marine fish (Walther & Thorrold 2006, Webb et al. 2012, Doubleday et al. 2013), it has also been shown to be controlled by physiological processes (Sturrock et al. 2015, Izzo et al. 2016, Grammer et al. 2017).

Environmental parameters can affect chemical signatures in otoliths, either by altering the chemical composition of ambient water or by mediating the incorporation of chemical signatures through influences on physiological processes. For example, temperature can alter the chemical composition of ocean waters, such as ratios of oxygen isotopes and strontium concentrations (Webb et al. 2012, Adkins et al. 2002). Temperature can also accelerate physiological processes, as fish are ectothermic and available somatic energy reflects water temperatures (Martino et al. 2019b, Barrow et al. 2017, Smoliński and Mirny 2017). Chlorophyll-*a*, a representation of primary productivity in the ocean, may also affect chemical signatures. Chlorophyll-*a* can relate to chemical composition with relationships to nutrient loadings through upwelling (Brodie et al. 2007, Woodson et al. 2013) or increased food availabilities increasing energy input into physiological processes (Martino et al. 2019b, Downing et al. 1990)

Here, we aim to improve our understanding of the relationship between otolith chemistry, intrinsic properties and environmental parameters in a coastal marine fish. We investigated an iconic and valuable fishery species, snapper (*Chrysophrys auratus*), across two oceanographically diverse regions (Northern Spencer Gulf and the South-East in South Australia) and three cohorts (1979, 1991, 2006) to examine regional and temporal variation. In recent years, there have been significant changes to the catches and spatial structure of regional snapper fisheries in South Australia, raising management concerns about its long-term sustainability (Fowler et al. 2017). Chemical chronologies may uncover past activity, ontogenetic trends and environmental habitats in snapper and contribute to understanding of long-term changes in the fishery. The key objectives of this study were to 1) investigate intrinsic (age, fish length, otolith growth and sex) and extrinsic (sea surface temperature and chlorophyll-*a*) influences on otolith chemistry in snapper, 2) assess the potential of carbon isotopes, magnesium or strontium as metabolic proxies, 3) use chemical chronologies to reconstruct temporal and spatial patterns of wild snapper.

METHODS

Study species

Snapper is a long-lived (up to 40 years) demersal finfish species that is broadly distributed in the Australasia and Indo-Pacific regions (Kailola et al. 1993, Norriss & Crisafulli 2010, Fowler et al. 2016). Australian snapper are slow growing, but can reach 1.3 m and 20 kg (Gomon et al. 2008).

Each mainland Australian state supports commercial and recreational fisheries, making it one of Australia's most important and iconic fishery resources (Fowler et al. 2017). Record snapper catches in South Australia (SA) were recorded from 2007 to 2012 followed by a considerable downturn. Management concerns were raised about long-term sustainability and changes to the spatial structure of the fishery (Fowler et al. 2017). Chemical histories may enhance our understanding of the regional differences between snapper and provide insights into the processes that drive the population and fishery dynamics.

Sample collection and processing

Snapper otoliths were chosen from two oceanographically-diverse regions in South Australia (Figure 5.1). Northern Spencer Gulf (NSG) is a semi-enclosed reverse-estuary which experiences warm semi-arid/Mediterranean climates (Edyvane 1999). This region is hypersaline and displays high variation in temperatures between summer and winter months (Figure 5.2). In contrast, the South East (SE) is an open ocean ecosystem which experiences low oceanic temperatures with a cool, temperate, meso-thermal climate which is influenced by seasonal cold-water, coastal upwellings (Bonney Upwelling) that bring nutrients to surface waters (Edyvane 1999).

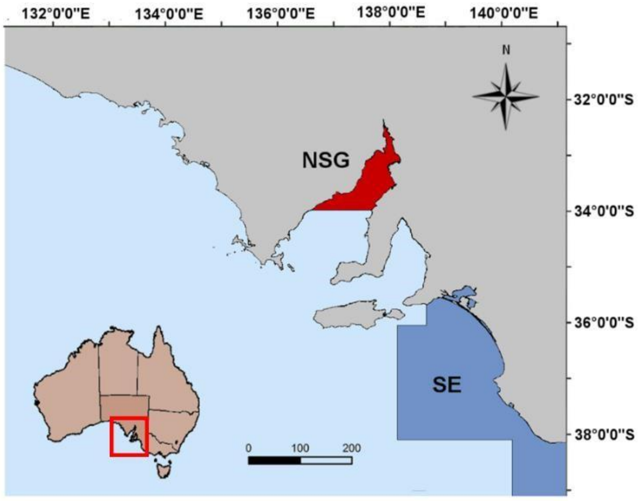

Figure 5.1 - Map of South Australian coast showing study regions Northern Spencer Gulf (NSG) and the South East (SE).

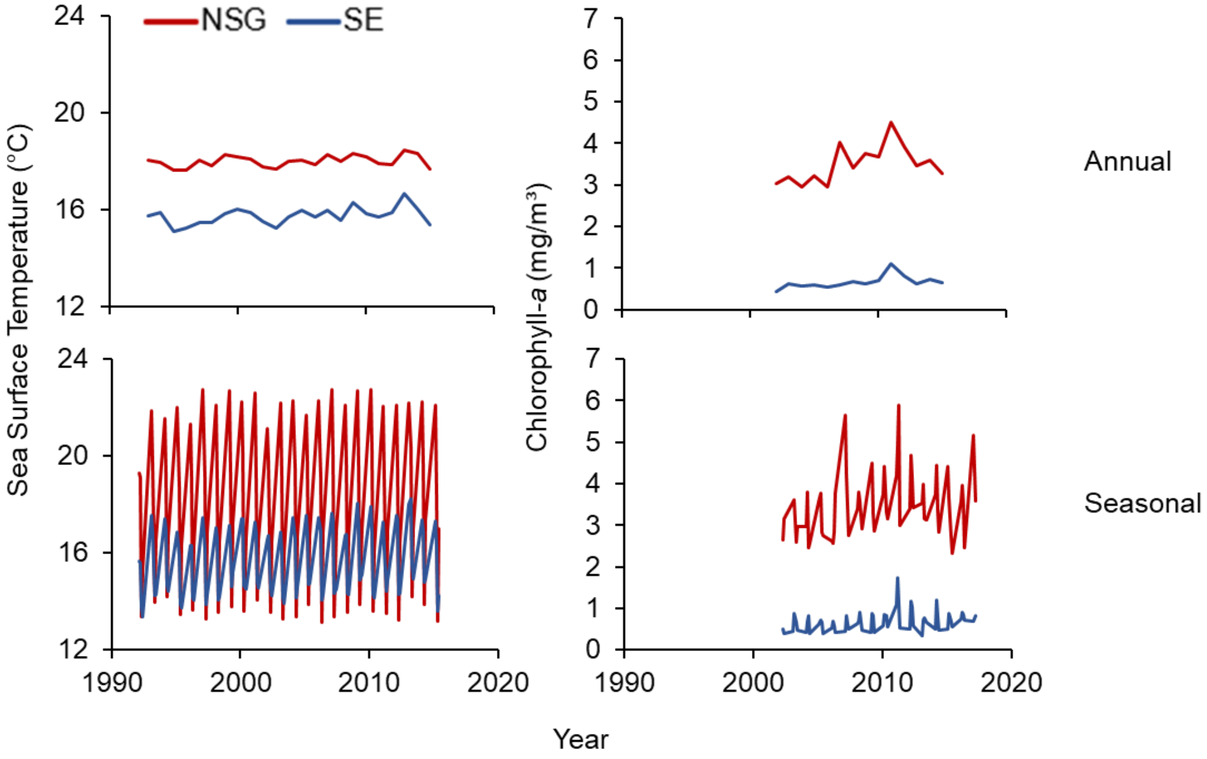

Figure 5.2 - Mean annual and seasonal values of Sea Surface Temperature and Chlorophyll-*a* in Northern Spencer Gulf (NSG) and the South East (SE) regions. Data were sourced via the IMOS AODN and provided as a 72-hour, night-time composite from polar-orbiting satellites (IMOS 2017).

Snapper otoliths in an archived collection at the South Australian Research and Development Institute (SARDI) were chosen from older (Cohort: 1991) and recent (Cohort: 2006) cohorts using 8 and 9-year-old fish from both regions (Table 5.1). Several otoliths from 21-year-old fish from NSG (Cohort: 1979) were also selected, although similar-aged fish were not available from the SE. All archived otoliths were collected by market sampling of the commercial catch at Adelaide's wholesale fish market. Caudal fork length (CFL) was measured and both sagittal otoliths were removed, cleaned and stored until processing. One otolith from each fish was embedded in clear setting epoxy resin (Struers Epofix) spiked with indium (40 mg l^{-1}). Embedded otoliths were sectioned (~400 μm) to expose the core and then polished using progressively finer grades of lapping film lubricated with ultrapure (Milli-Q) water. Polished sections were sonicated for 5 min in Milli-Q water, liberally rinsed with Milli-Q water, dried in a laminar flow cabinet and then mounted onto a microscope slide using indium-spiked thermoplastic glue (CrystalBond™ 509). Transverse otolith sections were viewed with a stereo microscope (Olympus SZX7) and photographed using an attached digital camera (Olympus DP72). Annual increment widths were marked and measured (mm) using the imaging software Stream Basic (v1.9.1) along the dorsal antisulcus axis from core to marginal increment (Figure 5.3). For snapper, otolith width strongly correlates with somatic length (Martino et al. 2019b), allowing increment measurements to act as a proxy of fish growth (Campana & Thorrold 2001). Increments were assigned a year, back calculated from date-of-capture and taking into consideration the marginal increment.

Table 5.1 - Characteristics of snapper and otolith samples used in isotope and element analysis separated into three cohorts and two regions. In-text identifiers (ID) for each region and cohort sample group are included. Sample ratio between male (M), female (F) or unknown sex (U) is indicated. Mean (+ standard error) of caudal fork length (CFL) is indicated. Average length of axis 2 in sample otoliths in otoliths is also indicated (Figure 5.3).

Region	Cohort	ID	*n*	Sampling Year	Age	Sex ratio (M:F:U)	Mean CFL ± SE (mm)	Mean length of axis 2 ± SE (μm)
Northern Spencer Gulf (NSG)	2006	NSG-2006	1	2014	8	1:0:0	370	3603
			3	2015	9	2:1:0	746 ± 20	4465 ± 326
	1991	NSG-1991	5	2000	9	3:2:0	669 ± 15	4721 ± 217
	1979	NSG-1979	5	2000	21	3:1:1	931 ± 10	6136 ± 283
South East (SE)	2006	SE-2006	3	2014	8	0:3:0	546 ± 9	3952 ± 139
			2	2015	9	1:0:1	512 ± 73	3476 ± 253
	1991	SE-1991	5	2000	9	0:0:5	572 ± 12	3821 ± 269

To remove material for isotopic analyses, sectioned otoliths were placed on a moveable microscope stage fitted with a digital camera and positioned using a computer-controlled micromilling machine (ESI New Wave Research, USA) with a 300 μm carbide cutter (Brasseler, USA). Images were viewed in software MicroMill System (v1.4.1.0) where spots corresponding to annual otolith increments were marked. Digital spots were defined and digitised as two-dimensional coordinates using MicroMill System and set in the translucent zone adjacent to the start of the opaque zone (Figure 5.3). Paths for spots were marked for the whole otolith including the core and each annual increment before milling. Some spots were not milled if they were too close to adjacent spots such that the integrity of the sample would be compromised by cracking of the otolith surface. The minimum amount of carbonate powder aimed to be removed per spot was 30 μg. Otoliths were micromilled at an approximate depth of 50 μm. Otolith material was mopped up with precombusted 3mm glass microfiber filter paper (Wattmans) dipped in ultrapure (Milli-Q) water, which is unlikely to affect carbon and oxygen isotope signatures (Schöne et al. 2017). Otolith material and filter paper were then placed in acid-sterilised 4.5ml vials awaiting isotopic analysis. An average of 10 spots made up each ‘transect’ across the life history of the fish, with the range spanning 7 – 13 spots. Otolith slides were then rinsed with MiliQ water and air-dried before reuse in elemental analyses.

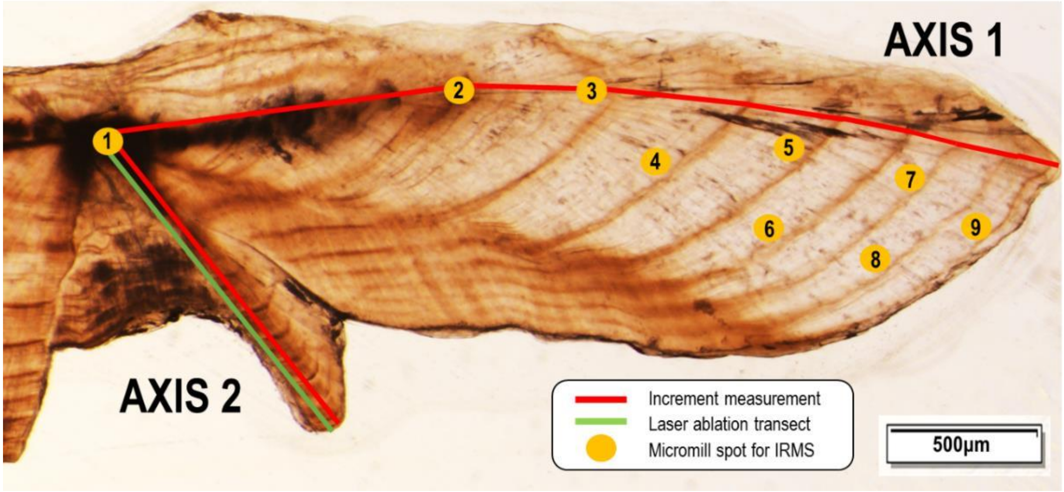

Figure 5.3 - Transverse section of snapper otolith indicating the axes used for chemical and growth analysis. Otolith increments were measured along axis 1 and then spots were micro-milled immediately adjacent to the opaque zone for isotope-ratio mass spectrometer (IRMS) analysis of carbon and oxygen isotopes. A transect along axis 2 was then analysed by laser ablation Inductively Coupled Plasma-Mass Spectrometer (ICP-MS) for elemental analysis. Increment widths alongside the laser ablation transect were then measured.

Chemical analysis

Carbon and oxygen isotopes in otolith samples were analysed using a GasPrep headspace analyser connected to Nu Horizon (Nu instruments) isotope-ratio mass spectrometer (IRMS). Vials containing otolith samples were placed in a random order, purged for 2.5 minutes with nitrogen gas and injected with 100µl - 120µl of 103 – 104% phosphoric acid. Powder standards (ANU-P3, UAC $CaCO_3$ UniA, IAEA-CO-8) were analysed to assess and correct for instrument drift and precision. Analytical errors averaged 0·19‰ for carbon isotope values and 0.41‰ for oxygen isotope values. Reported errors are based on the standard deviation of the repeated measurements (*n*=4) for each sample after correcting for the effects of peak size and drift. Isotope values were reported relative to Vienna Pee Dee Belemnite (VPDB) and expressed in standard delta (δ) notation as parts per thousand (‰) where R is the ratio of ^{13}C:^{12}C for carbon and ^{18}O:^{16}O for oxygen:

$$\delta = \left(\frac{R_{sample} - R_{standard}}{R_{standard}}\right) x\ 1000\ (‰) \qquad \text{(Equation 1)}$$

The same transverse sections of otoliths were analysed for elemental concentrations using a New Wave NRW213 Laser Ablation System connected to an Inductively Coupled PlasmaMass

Spectrometer (ICP-MS; Agilent 7900x). Transects 30 µm wide from core to edge of the otolith were analysed along Axis 2 (Figure 5.3). All samples were analysed for magnesium (^{25}Mg), strontium (^{88}Sr), barium (^{138}Ba), manganese (^{55}Mn) and lithium (^{7}Li). Sampling was done at energy 55%, fluence 9.5 J/cm^{2} and scan speed 5 µm s^{-1}. Each transect path was pre-ablated as a final surface cleaning step. To calculate element:Ca ratios, ^{43}Ca was also analysed. Additionally, ^{115}In was included as an indicator of when the laser ablated epoxy or glue rather than otolith material. After every 10 samples, an aluminosilicate glass reference standard (NIST612) was analysed and used to correct for mass bias and instrument drift. At the beginning and conclusion of a run, an internal calcium carbonate standard (MACS-3: United States Geological Survey) was analysed as a measure of precision, with coefficient of variation (CVs) of focus elements being < 5% (n = 20). Mean recovery for the NIST 612 averaged 106.7%. Mean relative standard deviation (RSD) for the NIST 612 was 1.7% (Mg), 0.44% (Sr), 0.4% (Ba), 0.2% (Mn), 1.15 (Li). Data processing was done with software Iolite (v2.5; Hellstrom et al. 2008, Paton et al. 2011) using the Trace Elements internal standard (IS) data reduction routine.

After laser ablation ICP-MS, otoliths were viewed again by stereo microscope and annual increment widths were marked and measured along the trench left by the ablation path. Using the measured distances, the elemental transects were then divided into annual means (Fowler et al. 2005, Fowler et al. 2017). Each isotope, elemental and annual increment width was matched with calendar year and fish age allowing for direct comparisons. Elemental transects were further divided into seasonal means based on percentages from a marginal increment analysis [average values taken from Fowler et al. (2004)], such that there were four estimates of each element:Ca ratio corresponding to each season per increment.

Statistical analysis

A series of hierarchical mixed-effects models were used to investigate factors influencing isotopic and elemental variation in wild snapper otoliths. Increasingly complex combinations of intrinsic (physiological) and extrinsic (environmental) predictors were added to establish optimal models. Generalised linear mixed effects modelling was performed in R using packages lme4 (Bates et al. 2015), AICcmodavg (Mazerolle 2015) and effects (Fox 2003). Isotopes were analysed on an annual scale while elemental markers were analysed on a seasonal scale. The first increment (core to first opaque zone) and marginal increment were removed from analysis, as they did not represent a complete year of the fish’s life. Chemical signatures and age were log-transformed when appropriate to meet model assumptions. All intrinsic and extrinsic variables were meancentred to assist model convergence and random slope interpretation (Morrongiello et al. 2014, Morrongiello & Thresher 2015). Random intercepts were investigated for unique fish identifiers (FishID), Year/Season, Cohort and Region to allow for correlations among chemical profiles within individual fish, calendar year, year class, and region. Random intercepts allowed for higher or lower signatures within each variable relative to the model average (intercept). Random age slopes were also investigated for both FishID and Year to facilitate detrending the age-related influences.

Intrinsic models were developed by analysing all intrinsic fixed effects (Age, Sex, Otolith Growth [represented by increment widths] and Fish Length) with a series of increasingly complex random effect structures (combinations of random slope and/or intercepts of fishID, age, year, cohort and region). Assumptions of normality, homoscedasticity and independence were tested for all models and Durbin-Watson tests were used to check for autocorrelation of residuals. Models were ranked using Akaike's Information Criterion (AIC) corrected for small sample sizes ($AICc$; Burnham and Anderson 2004). Models with the best ranked random effect structure were then reanalysed with a series of intrinsic fixed effects to determine best intrinsic models. Best ranked models were fitted using restricted maximum likelihood estimation to produced unbiased parameter estimates where appropriate (REML; Zuur et al. 2009). The variance of models was assessed by calculating two R^2 metrics: marginal R^2 which describes the proportion of variance of fixed effects, and conditional R^2 which describes the variance explained by both fixed and random effects (Morrongiello and Thresher 2015).

To assess environmental influences on otolith chemistry, linear and quadratic terms of sea surface temperature and chlorophyll-*a* were added to and compared against the best intrinsic models. Estimates were accessed via the IMOS AODN (IMOS 2017) and derived for each study region by defining boundary coordinates in AODN. Sea surface temperature data were provided as a 72-hour, night-time composite from polar-orbiting satellites and were available for 24 years (1992 – 2015). Chlorophyll-*a* data, a representation of ocean productivity including phytoplankton biomass and abundance, were recorded from satellite daily images computed through OC3M algorithm and were available for 14 years (2002 – 2015). Additionally, sea surface temperature and chlorophyll-*a* estimates were grouped in regional-specific annual averages for annual isotope models and 3-month averages for seasonal elemental models. Lagged versions (offset by one month) of sea surface temperature and chlorophyll-*a* were compared to accommodate potential delays in biological responses (Sturrock et al. 2015, Izzo et al. 2016). The effect of the extrinsic variables on chemical signatures were produced using the ‘Effects’ package in RStudio to generate and display model predictions. Subsequently, canonical analysis of principle coordinates (CAP) were created using *Primer* (v6.0) and were used to investigate the key drivers of spatial and temporal differences between the sample groups.

RESULTS

Isotopic and elemental chronologies were developed from snapper otoliths from two regions and three cohorts in South Australia. We derived mixed-effects models that indicated the extent of intrinsic and extrinsic influences on the chemical chronologies. Increment widths of the otoliths, a proxy of somatic growth and reflective of metabolic characteristics, decreased sharply over the first 2-3 increments and then declined more gradually (Figure 5.4). The decrease in increment width was generally less steep and remained higher in the NSG compared to the SE, likely indicating somatic growth and a smaller reduction in growth by age.

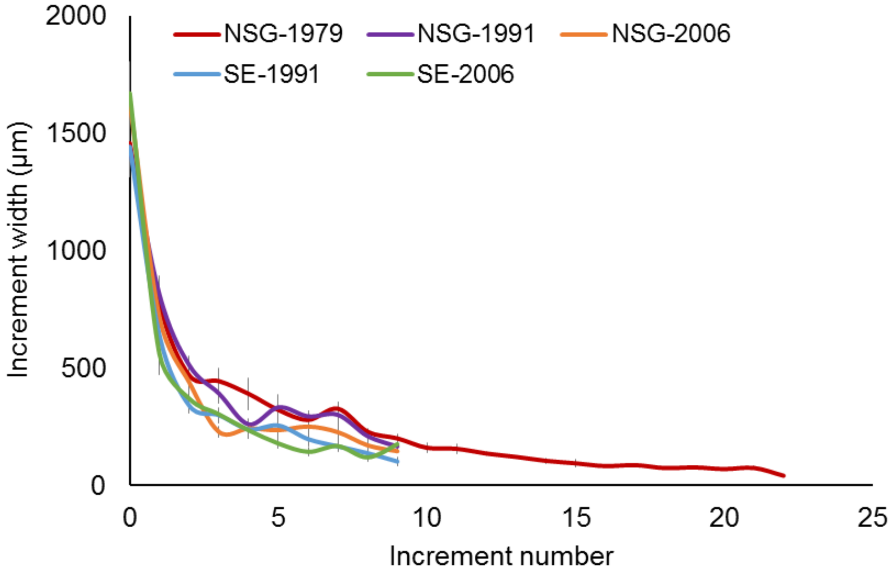

Figure 5.4 - Mean (+ standard errors) otolith increment widths along axis 1 (Figure 2) in snapper from two regions and three cohorts in South Australia.

Fish ID random intercepts was included in the best model for all chemical markers, which accounts for individual variation in chemical trends (Table 5.3, Table 5.4). Best models for all elemental markers included a random age slope which also allowed individual fish to have a unique age-dependent trajectory (Table 5.3, Table 5.4). Model estimates indicated extent of the effect sizes, with strong effect sizes indicated by *t* being higher than 2 or lower than -2 (-2>t>2), while Est indicated magnitude and direction of the effect. Chemical trajectories were all affected by age (indicating lifetime change in chemical trends), with the highest change occurring for strontium concentrations and carbon, followed by manganese. Carbon, oxygen, magnesium and strontium increased across lifetime profiles (Figure 5.5 – 5.8) while barium, manganese and lithium decreased (Figure 5.9 – Figure 5.11). Physiological characteristics influenced several chemical markers. Otolith growth had a strong positive effect on magnesium while fish length had minor negative effects on carbon, strontium and lithium. Differences in chemical signatures between Sex were detected for carbon, oxygen and magnesium, with a large effect size on magnesium. Males had higher carbon and oxygen isotopes but lower magnesium concentrations than females. Additionally, interactive fish length and sex had a minor positive effect on carbon isotopes. Apart from Age, no intrinsic parameters improved model fit over the base intrinsic model for barium or manganese.

Table 5.2 - Optimal model structures derived by ranking a series of increasingly complex mixed-effects models. Optimal fixed effects structures and random effects structures of lifetime trends in carbon isotopes ($\delta^{13}C$), oxygen isotopes ($\delta^{18}O$), magnesium (Mg:Ca), strontium (Sr:Ca) and barium (Ba:Ca) concentrations in snapper otoliths. Random slope term is indicated by x **|** y. Seasonal models are used for elemental (Mg:Ca, Sr:Ca, Ba:Ca, Mn:Ca and Li:Ca) chronologies and include Age (sAge) as discrete seasonal values (e.g. one year = four seasons old). Caudal fork length (Fish Length), increment width in otoliths (Otolith Growth) and Sex were assessed as possible fixed effects. Environmental predictors assessed include sea surface temperature (linear: SST, quadratic: SST + SST^2) and chlorophyll-*a* (linear: Chl-*a*, quadratic: Chl-*a* + Chl-a^2). Lagged versions (offset by one month) of environmental predictors were assessed to accommodate potential delays in biological responses. Absence of terms indicates that the base model was the best fit.

PARAMETER	RANDOM EFFECTS	FIXED EFFECTS (intrinsic properties)	FIXED EFFECTS (environmental predictors)
$\delta^{13}C$	1|FishID	Age, Fish Length x Sex	• SST(lagged) + SST(lagged)^2 • Chl-*a*
$\delta^{18}O$	1|FishID	Age, Sex	• SST • Chl-*a*
Mg:Ca	sAge|FishID	sAge, Otolith Growth, Sex	• SST(lagged)
Sr:Ca	sAge|FishID	sAge, Otolith Growth	
Ba:Ca	sAge|FishID	sAge	
Mn:Ca	sAge|FishID	sAge	
Li:Ca	sAge|FishID	sAge, Fish Length, Otolith Growth	

Model fits for carbon isotopes were moderate, describing up to 26% of the variance with most variation attributed to the fixed effects (Table 5.4). Model fits were low for oxygen, only describing up to 17.5% of the variation with 13% attributable to fixed effects. Model fit was high for magnesium, explaining 52.6% of the variation with 13% due to the fixed effects. Model fit was also high for strontium, explaining 69.3% of the variation with 33.5% of this from fixed effects.

The optimum model for barium concentrations explained 78% of the variation but very little was attributable to fixed effects indicating high individual variation. Model fit was high for manganese, describing 72.6% of the variation, with 44.8% attributable to fixed effects. The optimum model for lithium described a high 58.9% of the variation, with fixed effects being responsible for 14.2%.

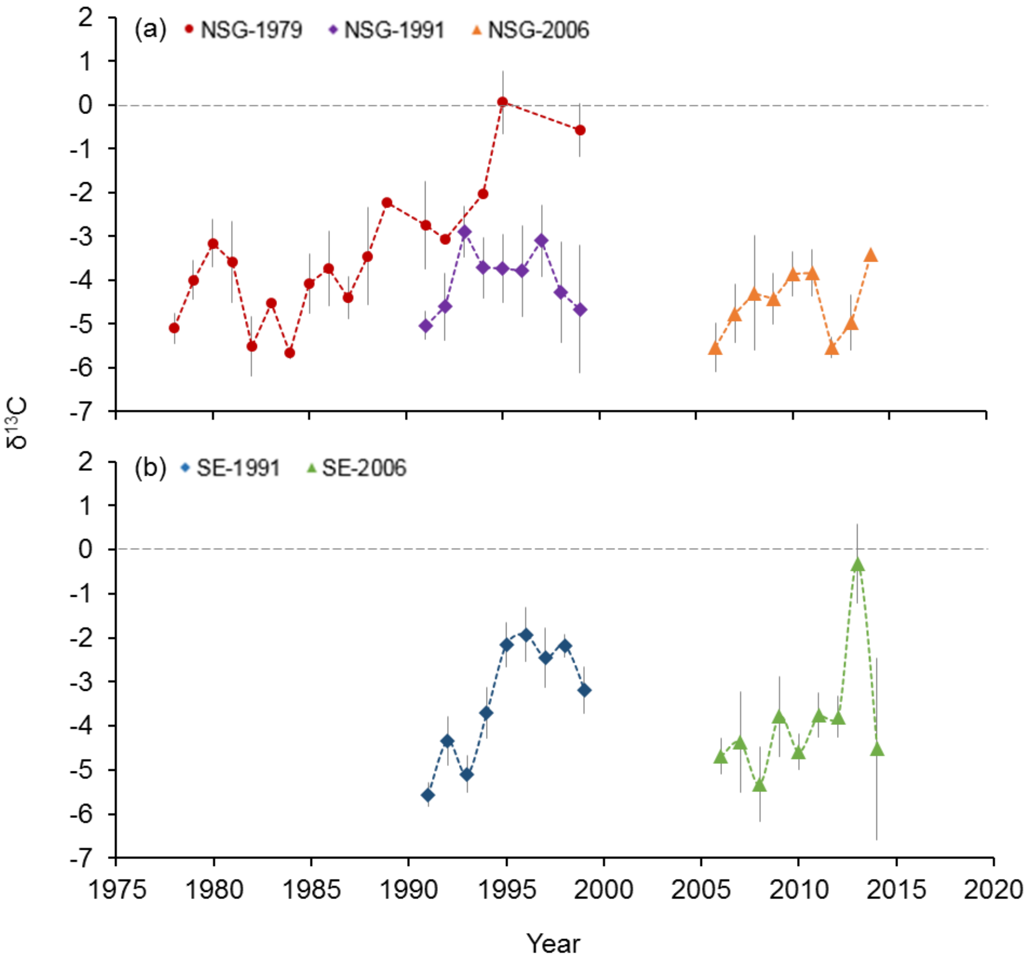

Figure 5.5 - Lifetime annual means (+ standard errors) for stable carbon isotopes ($\delta^{13}C$) in snapper otoliths from Northern Spencer Gulf (a) and South East (b) regions and three cohorts (1979, 1991, 2006) in South Australia. Absence of error bars indicates *n*<1 for the age.

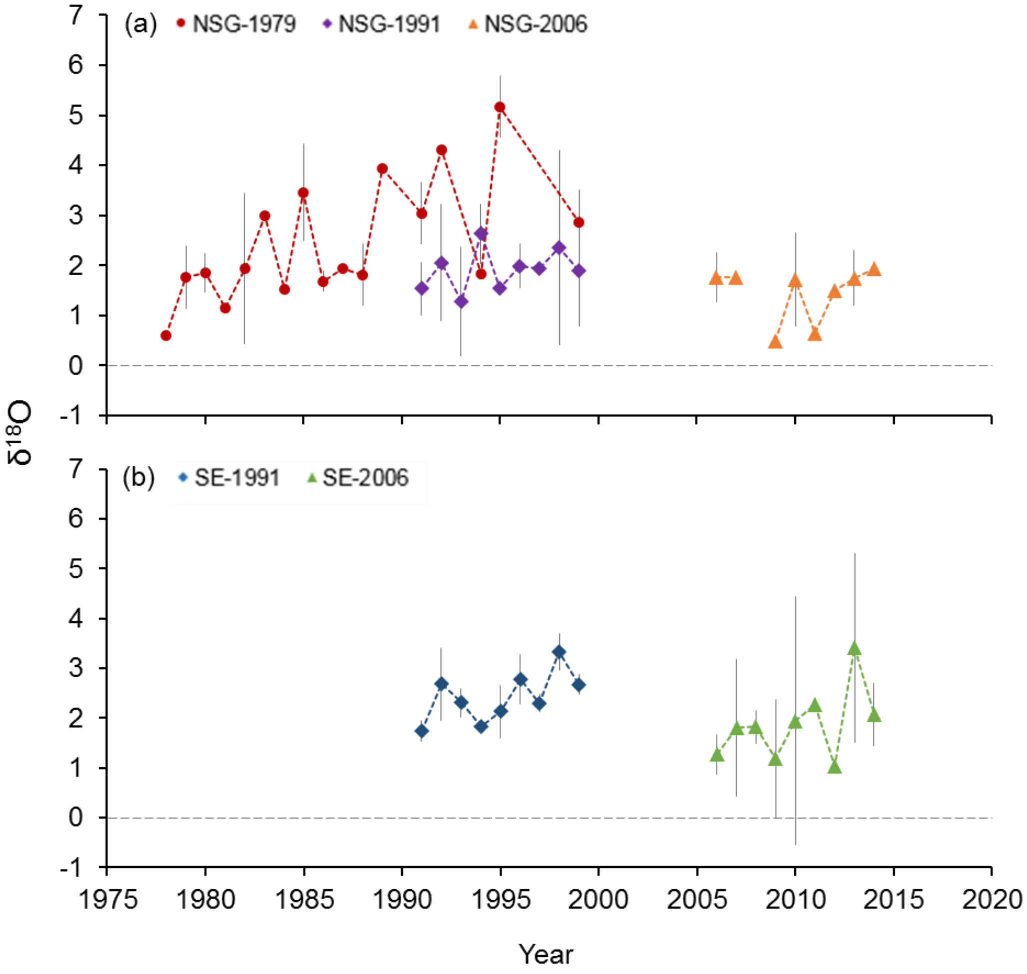

Figure 5.6 - Lifetime annual means (+ standard errors) for stable oxygen isotopes ($\delta^{18}O$) in snapper otoliths from Northern Spencer Gulf (a) and South East (b) regions and three cohorts (1979, 1991, 2006) in South Australia. Absence of error bars indicates *n*<1 for the age.

Table 5.3 - Model parameter estimates and test statistics of best models describing random effects, fixed effects and extrinsic covariates of isotope and elemental variation in snapper otoliths. Estimates are included for carbon isotopes ($\delta^{13}C$) and oxygen isotopes ($\delta^{18}O$). Presence of values indicate that inclusion of the variable improved the model fit. For fixed effects, strong effect sizes are indicated by *t* being higher than 2 or lower than -2 ($-2>t>2$), while Est indicates magnitude and direction of the effect. R^2 metrics explain model fit with R^2 (marginal) describing the proportion of variance of fixed effects and R^2 (conditional) describing the variance explained by both fixed and random effects. Environmental predictors assessed include sea surface temperature (linear: SST, quadratic: SST + SST^2) and chlorophyll-*a* (linear: Chl-*a*, quadratic: Chl-*a* + Chl-a^2).

	$\delta^{13}C$			$\delta^{18}O$		
RANDOM EFFECTS	**Var**	**SD**	**Corr**	**Var**	**SD**	**Corr**
Fish ID	0.191	0.437		0.134	0.366	
Age|Fish ID						
Season						
Region						
Cohort						
Residual	2.118	1.455		1.59	1.260	
FIXED EFFECTS	**Est**	**SE**	***t***	**Est**	**SE**	***t***
Intercept	-3.863	0.259	-14.93	1.67	0.270	6.189
Age	0.159	0.029	5.413	0.066	0.037	1.780
Sex (male)	0.196	0.331	0.592	0.417	0.318	1.313
Otolith Growth						
Fish Length	-0.001	0.002	-0.781			
Fish Length x Sex	0.004	0.002	1.716			
Otolith Growth x Sex						
MODEL FIT						
R^2 (marginal)	0.229			0.127		
R^2 (conditional)	0.259			0.175		
ENVIRONMENTAL PREDICTORS	**Est**	**SE**	***T***	**Est**	**SE**	**t**
SST				-0.090	0.198	-0.454
SST + SST^2	-0.546	0.299	-1.823			
Chl-*a*	-0.493	0.240	-2.055	-0.169	0.192	-0.878
Chl-*a* + Chl-a^2						

Table 5.4 - Model parameter estimates and test statistics of best models describing random effects, fixed effects and extrinsic covariates of isotope and elemental variation in snapper otoliths. Estimates are included for magnesium (Mg:Ca), strontium (Sr:Ca), barium (Ba:Ca) manganese (Mn:Ca) and lithium (Li:Ca). Presence of values indicate that inclusion of the variable improved model fit. For fixed effects, large effect sizes are indicated by *t* being higher than 2 or lower than -2 (-2>*t*>2), while Est indicates magnitude and direction of the effect. R^2 metrics explain model fit with R^2 (marginal) describing the proportion of variance of fixed effects and R^2 (conditional) describing the variance explained by both fixed and random effects. Environmental covariates assessed include sea surface temperature (linear: SST, quadratic: SST + SST^2) and chlorophyll-*a* (linear: Chl-*a*, quadratic: Chl-*a* + Chl-*a*^{2}).

	Mg:Ca			Sr:Ca			Ba:Ca			Mn:Ca			Li:Ca		
RANDOM EFFECTS	**Var**	**SD**	**Corr**	**Var**	**SD**	**Corr**	**Var**	**SD**	**Corr**	**Var**	**SD**	**Corr**	**Var**	**SD**	**Corr**
Fish ID	0.023	0.152		0.012	0.108		0.11	0.331		0.01445	0.12019		0.031	0.177	
Age|Fish ID	0.019	0.139	-0.19	0.016	0.127	0.31	0.065	0.254	0.36	0.0647	0.25444	0.03	0.005	0.072	0.20
Season										0.00234	0.04838				
Region															
Cohort															
Residual	0.032	0.188		0.009	0.095		0.030	0.173		0.01591	0.12615		0.026	0.162	
FIXED EFFECTS	**Est**	**SE**	***t***	**Est**	**SE**	***t***	**Est**	**SE**	***t***	**Est**	**SE**	***t***	**Est**	**SE**	***t***
Intercept	3.951	0.053	75.21	8.154	0.025	325.2	0.882	0.069	12.71	0.182	0.0261	6.973	1.412	0.040	34.59
Age	0.017	0.037	-0.446	0.158	0.027	5.8	-0.044	0.054	-0.819	-0.231	0.0542	-4.264	-0.063	0.019	-3.331
Sex (male)	-0.182	0.070	-2.59												
Otolith Growth	0.039	0.013	3.014												
Fish Length				-0.1615	0.085	-1.888							-0.230	0.155	-1.481
Fish Length x Sex															
Otolith Growth x Sex															
MODEL FIT															
R^2 (marginal)	0.168			0.335			0.007			0.4479			0.142		
R^2 (conditional)	0.526			0.693			0.780			0.7259			0.589		
ENVIRONMENTAL COVARIATE	**Est**	**SE**	***t***	**Est**	**SE**	***t***	**Est**	**SE**	***t***	**Est**	**SE**	***t***	**Est**	**SE**	***T***
SST	-0.002	0.003	-0.569												
SST + SST^2															
Chl-*a*															
Chl-*a* + Chl-*a*^{2}															

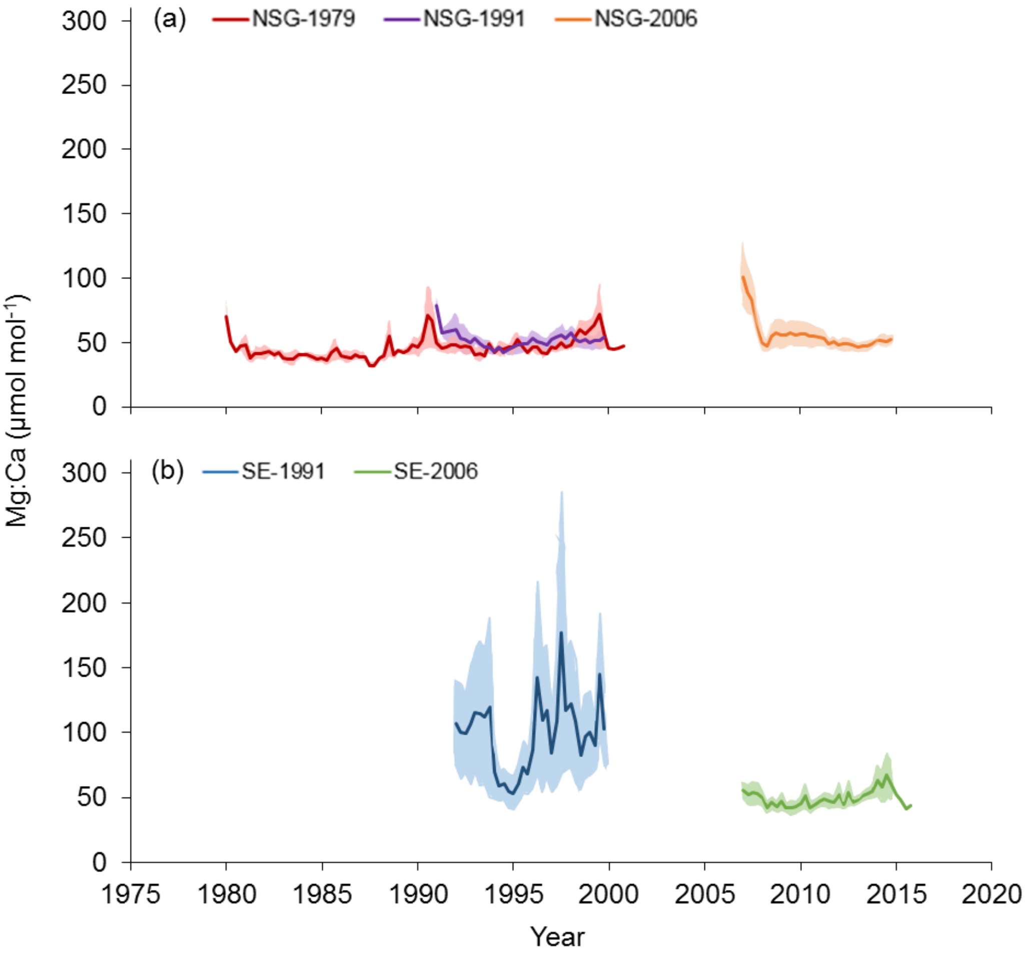

Figure 5.7 - Lifetime annual means (+ standard errors) for magnesium (Mg:Ca) in snapper otoliths from Northern Spencer Gulf (NSG) and South East (SE) regions and three cohorts (1979, 1991, 2006) in South Australia. Absence of error bars indicates *n*<1 for the age.

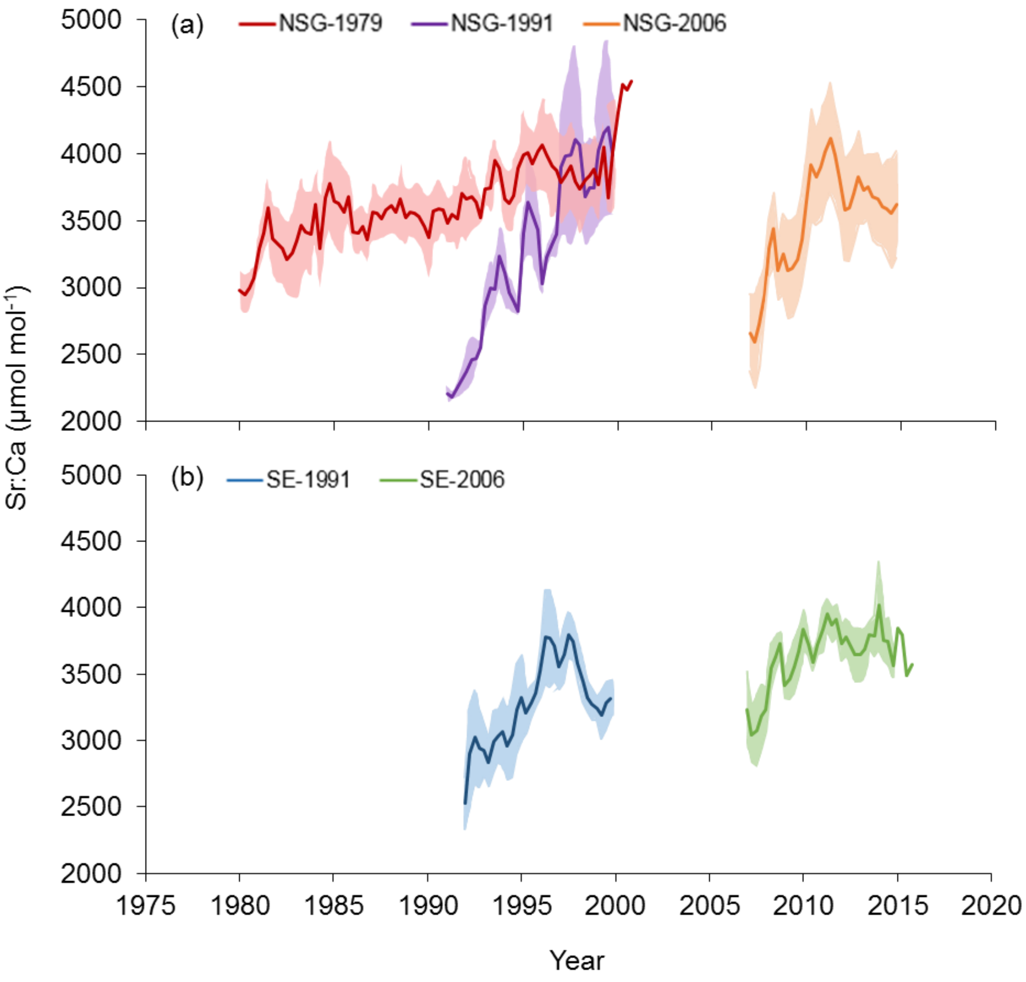

Figure 5.8 - Lifetime annual means (+ standard errors) for strontium (Sr:Ca) in snapper otoliths from Northern Spencer Gulf (NSG) and South East (SE) regions and three cohorts (1979, 1991, 2006) in South Australia. Absence of error bars indicates *n*<1 for the age.

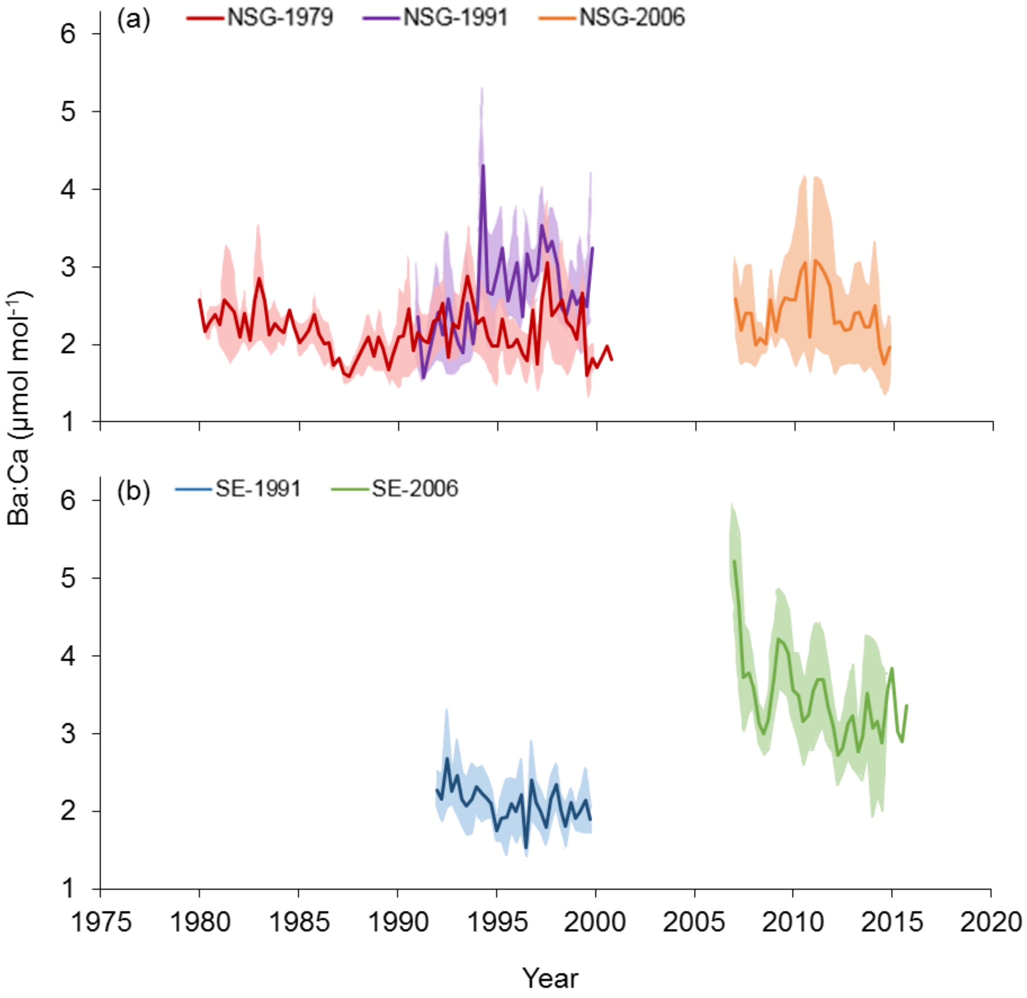

Figure 5.9 - Lifetime annual means (+ standard errors) for barium (Ba:Ca) in snapper otoliths from Northern Spencer Gulf (NSG) and South East (SE) regions and three cohorts (1979, 1991, 2006) in South Australia. Absence of error bars indicates *n*<1 for the age.

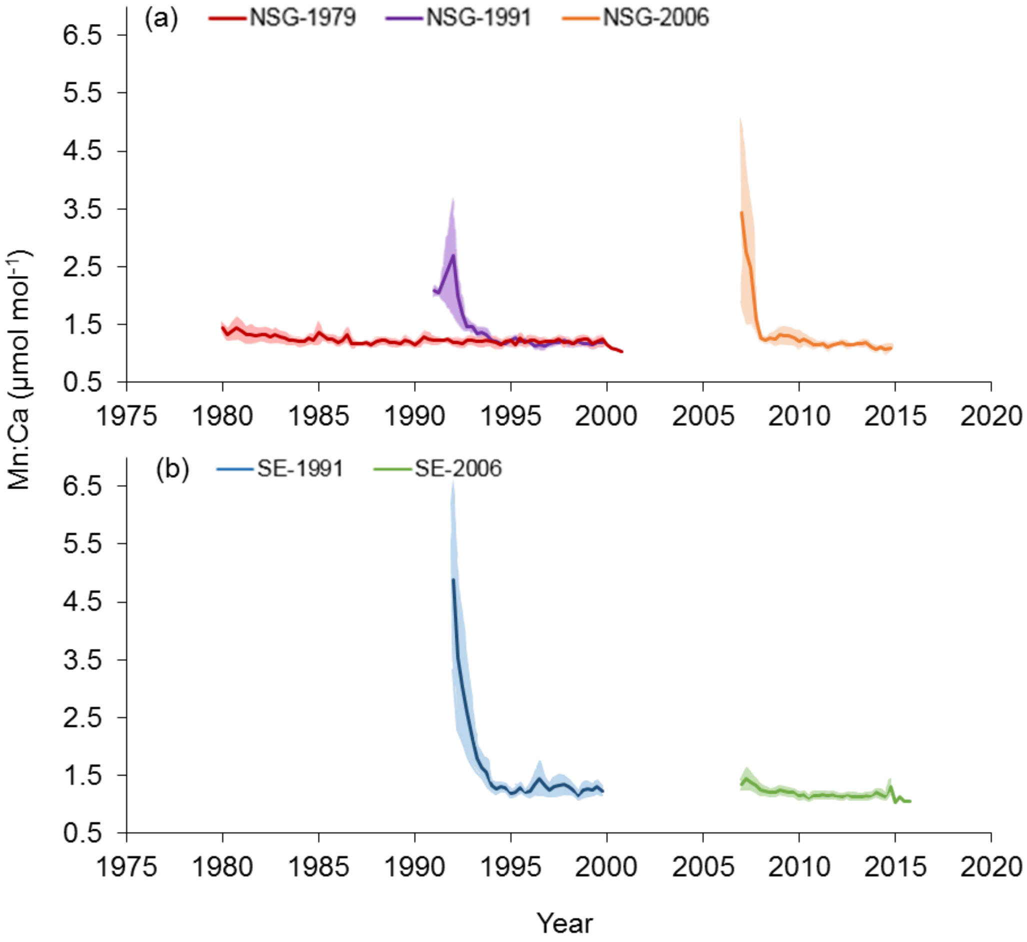

Figure 5.10 - Lifetime annual means (+ standard errors) for manganese (Mn:Ca) in snapper otoliths from Northern Spencer Gulf (NSG) and South East (SE) regions and three cohorts (1979, 1991, 2006) in South Australia. Absence of error bars indicates *n*<1 for the age.

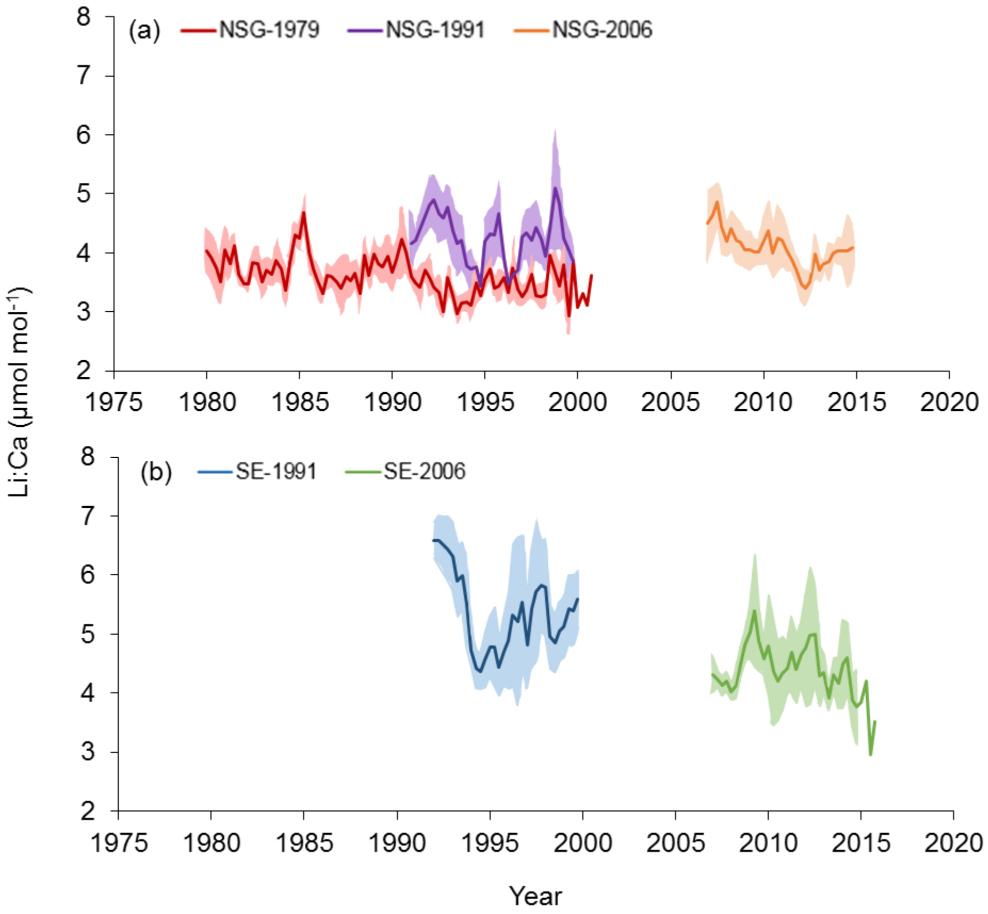

Figure 5.11 - Lifetime annual means (+ standard errors) for lithium (Li:Ca) in snapper otoliths from Northern Spencer Gulf (NSG) and South East (SE) regions and three cohorts (1979, 1991, 2006) in South Australia. Absence of error bars indicates *n*<1 for the age.

Multivariate analysis indicated differences in otolith chemistry between regions and cohorts (Figure 5.10). Lithium and magnesium accounted for the majority of the multivariate separation of the SE-1991 cohort from the NSG groups, whereas barium was responsible for separating out SE-2006 cohort. Carbon isotope signatures are more influential than oxygen isotopes and likely drove some of the difference between SE-2006 cohort and NSG cohorts. In contrast, multivariate signatures were generally consistent between the NSG cohorts.

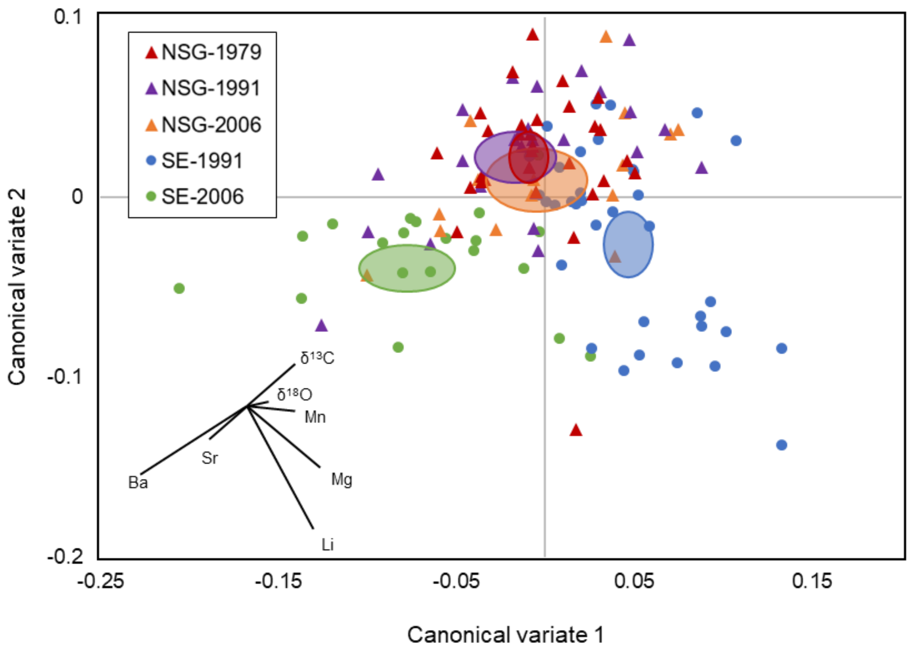

Figure 5.10 - Canonical analysis of principle coordinates (CAP) plot showing variation in chemical signatures in snapper otoliths for two regions (NSG, SE) and 3 cohorts (1979, 1991, 2006) in South Australia. Ellipses represent 95% confidence around group means. Vector diagrams show the direction and weight of individual chemical markers to sample distribution.

Environmental predictors

Sea surface temperature had minor negative predicted effects on carbon, oxygen and magnesium in otoliths (Figure 5.11). Chlorophyll-*a* had a large negative predicted effect on carbon and a minor negative predicted effect on oxygen. Lagged versions (by one month) were ranked higher in the sea surface temperature models for carbon and magnesium. Extrinsic covariates did not improve model fits over optimum base intrinsic models for strontium, barium, manganese or lithium.

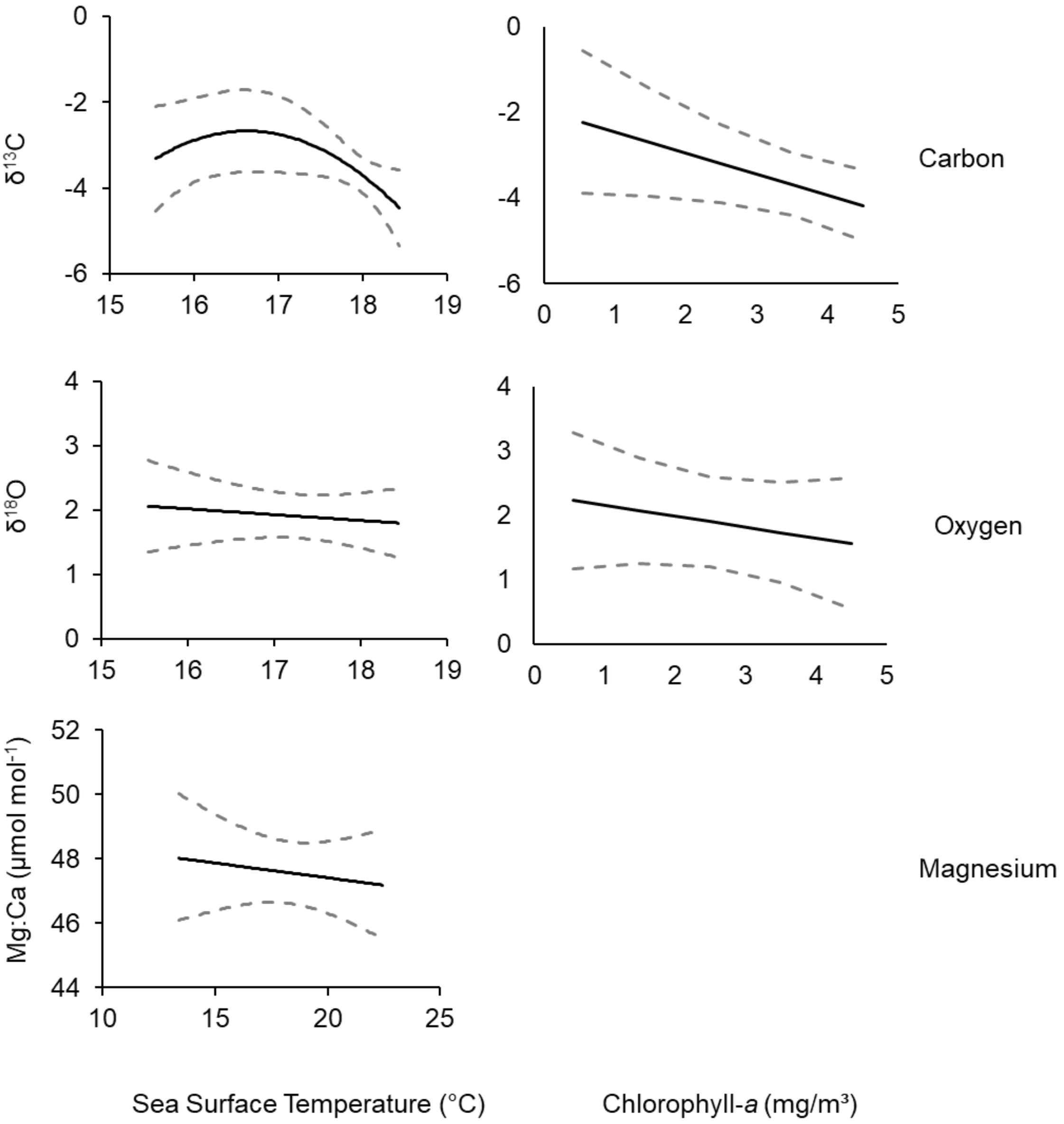

Figure 5.11 - Predicted annual variation in carbon isotopes ($\delta^{13}C$) and oxygen isotopes ($\delta^{18}O$), and seasonal variation in magnesium concentrations (Mg:Ca) in snapper otoliths due to sea surface temperature and chlorophyll-*a* across South Australia. Note that the x axis differs between isotopes and magnesium.

DISCUSSION

We reveal intrinsic and extrinsic drivers of otolith chemistry in snapper. Carbon isotopes, magnesium, strontium and lithium signatures were influenced by physiological characteristics. Carbon isotopes, oxygen isotopes and magnesium were also influenced by extrinsic variables of ocean temperatures and chlorophyll-*a*. In contrast, barium and manganese were not affected by physiological characteristics, which was evidence of a stronger environmental influence. These results refine our understanding of the influences on otolith chemistry for improved use in reconstructing physiological histories.

Investigating the potential of otolith isotopes and elements as physiological biomarkers

Despite ontogenetic trends, variation in otolith carbon isotopes among fish within specific life stages and ages suggests variation in metabolic rate. Mixed-effects modelling revealed a relationship between carbon isotopes and physiological processes through retention of intrinsic parameters of fish length, otolith growth and sex in the models. While growth (otolith and somatic) and metabolic rates are separate processes, they generally correlate and can still provide insights into the other (Yamamoto et al. 1998, Álvarez & Nicieza 2005). The mixed-effects modelling supported experimental conclusions that carbon isotopes can track metabolic rates in fish (Chung et al. 2019b, Martino unpublished). Otolith carbon arises from two sources: (1) dissolved inorganic carbon in environmental water and (2) metabolically-sourced carbon from diet (Kalish 1991, Solomon et al. 2006, Tohse & Mugiya 2008). However, differences in dissolved inorganic carbon in environmental water or diet were unlikely to be the dominant influence, as ocean waters have mostly homogenous carbon signatures and considerable changes to diet are required to significantly alter values of carbon isotopes (Kroopnick 1985, Tagliabue & Bopp 2008, Schmittner et al. 2013, Chung et al. 2019a). Higher metabolic rates likely increased the proportion of metabolically-sourced carbon into otoliths shown as lower isotope ratios in snapper otoliths, which suggests regional trends in metabolic rates. Ontogenetic trends were also prominent in carbon isotope signatures, with values for some cohorts gradually increasing with age. Increasing lifetime carbon isotopes likely indicate mass-specific metabolic rates decreasing with age. Initially high larval respiration, metabolic rates and growth likely decreased rapidly with age, plateaued and remained relatively constant as mass approached adult size (Fidhiany & Winckler 1998, Rosenfeld et al. 2015, Peck & Moyano 2016). Ontogenetic increases in carbon isotopes have been documented for other species. Most carbon isotope profiles increase steeply, and then plateau, although, there is significant variation in the steepness and duration of the initial slope (Schwarcz et al. 1998, Begg & Weidman 2001, Jamieson et al. 2004, Shephard et al. 2007, Trueman et al. 2016). High variability in carbon isotope values among individuals is also common across species, highlighting the influence of individual physiology. Differences in ontogenetic trends between species indicate species-specific physiology and different life-history strategies. For example, differences in foraging strategy and age of maturation likely impact metabolic activity and isotope values (Chung 2015). Sea surface temperature had a predicted negative influence on otolith carbon isotopes for snapper, corroborating experimental results and illustrating that metabolic rates increased under higher temperatures (Martino et al. 2019a). This relationship likely reflects the influence of temperature on fish physiology by increasing metabolic demands and respiration rates (Gillooly et al. 2001, Martino unpublished). The influence of chlorophyll-*a*, indicative of primary productive, was a similarly negative relationship and indicates higher food availabilities likely led to higher metabolic rates. This study supports the innate relationship of carbon isotopes and metabolic rates in a wild fish, with detectable dissimilarities inferring metabolic differences across regions, cohorts and life-history stages.

We found that magnesium had a strong positive relationship with otolith growth, a minor negative relationship with temperature, and no significant relationship with either carbon isotopes (representative of metabolic rates) or chlorophyll-*a* (representative of food availability). Relationships between magnesium concentrations and somatic or otolith growth have been found for other species (Martin & Thorrold 2005, Hamer & Jenkins 2007, Sturrock et al 2015, Grammer et al. 2017). Furthermore, magnesium in otoliths does not couple with environmental factors such as composition of diet or ambient water (Woodcock et al. 2012), however higher magnesium has been suggested to relate to higher metabolic activity (Limburg et al. 2018). It has been proposed that due to the large size of magnesium ions when hydrated, magnesium must be actively transported via the ionocytes through the epithelium and into the endolymph (Limburg et al. 2018). When metabolic activity is high the ionocytes are more active and thus more magnesium is incorporated into the endolymph for potential random trapping in interstitial spaces during increment formation (Thomas et al. 2017, Limburg et al. 2018). It has been further stated that the exact energetic component magnesium relates to was unknown, such as consumption, metabolism, excretion, or growth (Limburg et al. 2018). We show that magnesium incorporation is complicated and likely does not reflect metabolic rates but may more strongly relate to one of the other energetic components, such as consumption, excretion or growth. Further research, particularly experimental work, is needed to understand the mechanisms and influences of magnesium incorporation.

Strontium and barium are the prominent elements in otoliths used as environmental indicators (Bath et al. 2000, Elsdon et al. 2008, Izzo et al. 2018). We showed that fish length was related to strontium concentrations, but no physiological characteristics influenced barium concentrations. Previous studies have also demonstrated negative relationships between strontium concentrations and otolith or somatic growth, including for Australasian snapper (Hamer & Jenkins 2007, Lin et al. 2007, Grammer et al. 2017). In contrast, barium concentrations have not been related to growth or physiology, including for Australasian snapper (Bath et al. 2000, Hamer & Jenkins 2007, Miller 2009). Ambient water concentrations contribute to otolith composition for both elements, although with generally lower contributions for strontium (59 - 84%) and higher contributions for barium (62 - 98%) in marine species (Walther & Thorrold 2006, Webb et al. 2012, Doubleday et al. 2013). We showed that this difference in incorporation from water sources likely relates to differences in physiological regulation between barium and strontium. Furthermore, we have shown that neither strontium nor barium are affected by environmental water temperatures or food availability. Previous studies have documented positive, negative and no relationships between temperature and both barium and strontium otolith concentrations (Miller 2009, Sturrock et al. 2012, Izzo et al. 2018). This suggest that the effect is likely highly species- and environment-specific. While environmental influences are important factors in strontium and barium in otoliths, a proportion of strontium is likely to be physiologically regulated. Consequently, strontium concentrations along with carbon isotopes and magnesium concentrations, may be able to provide insights into fish physiology under uniform environmental conditions.

Physiological characteristics did not influence manganese in snapper otoliths, suggesting it may be an accurate tracker of environments. Previous studies have shown temperature, salinity and carbon dioxide/pH ($p\text{CO}_2$) in ambient water do not influence manganese (Martin and Thorrold 2005, Martino et al. 2017) but it has been suggested to potentially track hypoxic conditions (Limburg et al. 2015). Additionally, we show that a physiological characteristic, fish length, may have a minor influence on lithium. Lithium does not correlate with temperature or carbon dioxide/pH (Martino et al. 2017), but there are suggestions it may correlate with salinity (Hicks et al. 2010). Further research, particularly experimental work, would enhance our understanding of the influences on manganese and lithium incorporation into otoliths.

Applications and limitations

High values for carbon isotopes in SE-1991 suggest that these fish likely had comparatively lower metabolic rates than both NSG cohorts and SE-2006 fish. NSG is a warmer semiarid/Mediterranean climate, whereas the SE experiences cooler temperate meso-thermal climate (Edyvane 1999). Consequently, differences in temperature between regions may explain some of the difference in metabolic activity. However, carbon isotope ratios also differed between the SE cohorts suggesting a difference in energetic processes between these two cohorts. Large differences between these cohorts were also apparent with barium signatures, being significantly higher in the SE-2006. Previous work on snapper otolith chemistry in southern Australia has indicated that high barium concentrations likely indicate that fish are from the major nursery area of Port Phillip Bay, which is east of our study region (Hamer et al. 2006, Fowler et al. 2017). SE-2006 had high barium signatures that decreased with age, suggesting this cohort likely originated and resided in Port Phillip Bay before migrating to the SE region. Compared to SE2006, oxygen signatures in otoliths indicate SE-1991 may have resided in lower temperature/salinity areas which may have led to lower metabolic rates as suggested by carbon. However, based on previous tagging and chemistry studies, differences in barium are more likely to indicate interannual variation in water concentrations in Port Phillip Bay through differences from the chemical input source, rather than differences in spawning region (Hamer et al. 2003). In contrast, the similarities in chemical signatures between the NSG cohorts, particularly in carbon, magnesium and barium, likely indicate that NSG snapper are lifetime residents of Spencer Gulf region.

We show that males had higher carbon signatures and lower magnesium but higher oxygen signatures than females. The carbon and magnesium signatures for males indicate lower metabolic rates/energetic components than females. This could be due to increased energy requirements for females to produce eggs (Wootton 1979, McBride et al. 2015). The higher oxygen signatures indicate environmental differences. Oxygen isotopes are in equilibrium with ambient water oxygen composition and generally negatively correlated with temperature and salinity (Kalish 1991, Kim et al. 2007). Female snapper may inhabit warmer, more saline or shallower waters than male counterparts, potentially due to energy and/or behavioural differences.

This study indicates that intrinsic properties should be important considerations in sampling designs using otolith chemistry. When possible, it is important to keep age, cohort and sex of fish consistent, otherwise there is potential to confound physiological influences with environmental changes. Further, otolith chemistry is demonstrated to provide insights into physiological trends in fish. Carbon isotopes can be used as a proxy for metabolic rates, while magnesium and strontium concentrations may be able to support inferences from carbon isotopes. High or low signatures in carbon isotopes, magnesium and strontium may infer higher or lower activity/growth, which could address questions on feeding or movement habits. Furthermore, these physiological biomarkers have specific value for differentiating between fish in homogenous environments. Differences in otolith chemistry due to compositional differences in environmental water is the key approach of using otolith chemistry to track fish movements and habitat use, and clarify differences between populations or stock structure (Elsdon et al. 2008, Fowler et al. 2017, Izzo et al. 2018). However, these reconstructions are limited by the requirement of a detectable change in environmental signature, such as in salinity or elemental concentrations (Hamer et al. 2006, Izzo et al. 2018). The physiological differences in fish that enable changes in carbon isotopes, magnesium and strontium in otoliths could be used to differentiate between populations in marine environments, where water conditions, such as salinity or dissolved inorganic carbon, are relatively consistent. The use of otolith chemistry in marine environments is currently restricted by the uniformity of ocean water, compared to freshwater or estuary systems, but this approach could enhance its use. Multivariate analysis (such as canonical analysis of principal coordinates plots) combining both environmental and physiologically-driven chemical signatures is a particularly effective approach of differentiating between populations. Used in conjunction, physiological and environmental signatures in otoliths are a powerful tool to enhance our understanding of wild fish populations in marine environments.

There were some limitations with this study. For example, we were unable to distinguish between whether age effects were due to ontogenetic changes on chemical incorporation or temporal changes in the elemental concentrations in the water. Furthermore, this study was unable to account for influences from salinity or water composition (isotope ratios and elemental concentrations) as long-term continuous data were unavailable for this study. While oxygen isotopes should have a strong correlation with temperature (Kalish 1991, Kim et al. 2007), we only observed a minor effect. This may be due to salinity variations, which we have not included as a factor in our models. In particular, Northern Spencer Gulf experiences high fluctuations in salinity (Edyvane 1999). Future studies would benefit from incorporating salinity and water composition to further separate extrinsic and intrinsic drivers of otolith chemistry.

Conclusions

We show that intrinsic and extrinsic influences on otolith chemistry can be significant and that otolith chemistry can provide insights into physiological histories. Carbon isotopes, magnesium and, to a lesser extent strontium, may be able to uncover past activity, movement, and habitats and differentiate between physiologically-divergent populations. These physiological signatures have significant value in environmentally homogenous environments, such as some marine habitats. We also demonstrate mixed-effects modelling is an effective method for understanding the influence of multiple intrinsic and environmental factors on wild populations. Understanding the sources and influences on chemical markers in otoliths reinforces confidence in their accuracy in retrospective reconstructions and enhances their use for ecological applications.

CHAPTER SIX

Discussion

Intrinsic biomarkers are a powerful tool for retrospectively reconstructing past lives of fish. However, to use chemical markers confidently it is important to understand the sources and influences on their incorporation. I experimentally tested the link between physiology and intrinsic biomarkers in snapper otoliths and subsequently, applied biogeochemical and sclerochronology approaches to investigate physiological processes in wild snapper populations. In this thesis, I explored the potential of physical and chemical proxies in fish as physiological biomarkers.

Uncovering long-term growth trends using otolith chronologies

Growth is a fundamental predictor of population dynamics, productivity and biomass. I used otolith sclerochronology and mixed-effects modelling to reconstruct almost 4 decades of growth in snapper and uncovered significant inter-annual and inter-regional variation. Growth rates declined in the two most productive fishery regions and extrinsic (environmental and anthropogenic) influences were significant.

Declining growth rates of snapper in Northern Gulf St Vincent and Northern Spencer Gulf suggests that in these regions, snapper have been negatively influenced by external influences. Some fish populations respond to long-term, size-selective harvesting by selecting for slower-growing, smaller fish that mature earlier (Ernande et al. 2004, Swain et al. 2007, Olsen et al. 2009). As commercial harvesting directly removes the larger and faster growing fish, this may have skewed snapper populations towards smaller average sizes. Declining growth rates may be detrimental for snapper in the gulf regions by leading to lower stock biomass and reproductive output, and higher natural mortality (Barneche et al. 2018, Hixon et al. 2014), as well as declining success in ecological interactions such as predator-prey relationships and interspecific competition (Lewin et al. 2006, Rose et al. 2001). Commercial catch of snapper in these two regions have significantly declined in recent decades. Lower population biomass due to smaller sizes may be a contributing factor.

Exploitation of environmental resources is dependent on the available food in an ecosystem and magnitude of competition. Successful exploitation of resources shapes both immediate physiological condition and the trajectory of life-time physiological condition in fish populations (Dingemanse and Wolf 2013). I demonstrated ecosystem resources and intra- and inter-specific competition are key drivers of snapper growth, indicated through the influences of chlorophyll-*a* (indicating primary productivity), commercial catch and recruitment as significant covariates of growth. However, the relationship between fish growth and ecosystem resources was complicated and dependant on multiple factors in ecosystems. Generally, fish physiological functioning correlates with aquatic primary production (Downing et al. 1990), with the expectation that increasing food availability leads to higher growth and biomass. Primary production was positively correlated with snapper growth in some regions, but negatively correlated in others. Commercial catch, indicating removal of biomass from populations, and recruitment, indicating increase of biomass into populations, also influence food availability in local ecosystems. Similar to chlorophyll-*a* trends, catch and recruitment showed mixed relationships with growth trends, revealing region-specific, density-dependent trends in snapper growth. Identifying density-dependent processes can help predict how populations will respond to external influences that alter population size, such as predation or commercial fishing (Rose et al. 2001). Fish growth is often compensatory density-dependent, with population size negatively correlated to growth. This growth response is generally due to increased intra-specific competition, leading to less per capita food availability and reduction in an individual's feeding rate (Rose et al. 2001). Snapper growth in Northern Spencer Gulf is suggested to be compensatory density-dependence. Fortunately, this compensatory response can stabilise populations, offsetting the loss of individuals by temporarily increasing survival or reproduction of the remaining individuals and favouring an increase in population size (Anderson 2001, Fogarty et al. 1992, Rose et al. 2001). Populations can also be depensatory density-dependent, with growth positively correlated to population size. This growth response can arise when populations are reduced below a threshold where group dynamics and cooperative interactions can be impaired, limiting mating success, foraging or antipredator strategies (Lewin et al. 2006, Stephens and Sutherland 1999). Snapper growth in Northern Gulf St Vincent is suggested to be depensatory density-dependent. Unfortunately, depensatory density can destabilise populations by accelerating further population decline and delay recovery in vulnerable populations (Rose et al. 2001, Shelton and Healey 1999, Walters and Kitchell 2001). Determining density-dependence dynamics in wild populations is important for predicting how populations will respond to changes to population size. Sustainable fishery limits involve setting harvesting limits that will allow populations to continually replenish. Understanding direction and magnitude of density dependence helps us to predict population responses in snapper and inform appropriate and sustainable harvesting limits.

Few studies have applied fine scale growth profiles (Darnaude et al. 2014, Sturrock et al. 2015, Grammer et al. 2017), despite their value. I developed a novel approach of building seasonally resolved chronologies. These chronologies provided nuanced predictions of growth trends and the influence of environmental conditions. These seasonal chronologies were particularly valuable in understanding growth responses to sea surface temperature. Growth responses to temperature matched expected ectothermic responses from increasing temperature, whereby growth increased positively with temperature until reaching an optimum (pejus temperature), after which growth declined (Neuheimer et al. 2011, Pörtner and Farrell 2008). Interestingly, the pejus temperature predicted by seasonal chronologies (18-20°c) directly corresponded with optimum temperatures for juvenile snapper growth determined from aquaculture experimental work (Fielder et al. 2005). This provides confidence in the accuracy of otolith sclerochronology in reconstructing growth trends and influences on growth. It also highlights the potential applications of this technique for other ecological questions, for instance predicting pejus temperatures for difficult-to-monitor fish species such, as deep-sea or solitary fish. Consequently, seasonally-resolved chronologies present significant potential for use on other fish species to determine precise biological and environmental effects.

Clarifying the relationships between metabolic activity and chemical biomarkers

Metabolic rates drive biological processes in animals. I found that metabolic rates significantly affected chemical signatures in hard and soft tissues of snapper. I consequently demonstrated that these chemical signatures could potentially retrospectively track physiological processes and diet histories in fish.

Chemical signatures in otoliths can reflect environmental or physiological conditions. Some chemical signatures are more physiologically regulated, and incorporation may reflect fish physiology and individualised genetic makeup (Gronkjaer 2016). Physiologically-regulated chemical signatures may provide insights into past physiological trends. I validated the use of carbon isotopes in otoliths as metabolic biomarkers. Otolith carbon arises from two sources: (1) dissolved inorganic carbon in environmental water and (2) metabolically-sourced carbon from diet (Kalish 1991, Solomon et al. 2006, Tohse & Mugiya 2008). I show that shifts in carbon isotopes do not primarily reflect the trends in diet or water as these factors remained constant across treatments, but values in otoliths were significantly altered. The carbon values in otoliths significantly correlated with measured values of metabolic rate. As temperature increased, metabolic demands, higher respiration and food consumption likely increased the proportion of more depleted metabolic carbon (more negative values of carbon isotopes) incorporated into the otoliths (Kalish 1991, Solomon et al. 2006, Trueman et al. 2016). However, I show that physiological stress affected the relationship between metabolic rate and carbon isotopes, with the relationship becoming more positive with high temperatures and stress. Increased stress could have altered this relationship through physiological or chemical mechanisms that affected the pathway and uptake of carbon isotopes from water/diet to blood/endolymph and otolith.

Alternatively, temperature could also play a direct role by affecting gas solubility. My research suggests that carbon isotopes may not be a suitable tracker of metabolic rate when fish are at physiological tolerance limits, and that physiological stress is an important consideration in chemical reconstructions.

Carbon isotopes were then applied as metabolic biomarkers in wild snapper across two ecologically and climatically different regions. Carbon isotopes were distinctive enough to differentiate metabolic rates across the regions and multiple year classes. Carbon isotopes indicated that snapper in a northern gulf region of South Australia were likely to have been lifetime residents of that region, whereas in a southern region some fish had high metabolic rates and were hypothesised to have migrated from elsewhere. Very few studies have investigated the use of mixed-effects modelling on otolith chemical profiles to uncover drivers of variation (Jones & Campana 2009, Izzo et al. 2016, Grammer et al. 2017). To the best of my knowledge, I am the first to apply this approach on long-term carbon isotope chronologies. Mixed-effects modelling revealed that carbon isotopes were influenced by fish length, otolith growth and sex, further supporting its relationship with physiological processes in field conditions. Furthermore, our results add to a growing body of literature indicating that otolith magnesium and strontium concentrations are physiologically regulated in marine fishes (Brown and Severin 2009, Sturrock et al. 2014, Limburg et al. 2018). In contrast, barium concentrations and oxygen isotopes were unaffected by the physiological characteristics we examined and are suggested as accurate measures of past environmental conditions.

I demonstrate that otolith chemistry and physiological processes are inherently linked, validating the use of isotopes and elements in otoliths as physiological biomarkers. These tools may uncover metabolic trends in the wild. These physiological signatures could also be used in multivariate analyses (such as canonical analysis of principal coordinates plots) to differentiate between populations with physiological differences where no environmental gradients (such as barium or salinity concentrations) exist. Marine environments tend to be more chemically uniform than freshwater or estuarine habitats, so these approaches are likely to be particularly useful for marine fish species. My results highlight the use of chemical chronologies for reconstructing lifetime physiological trends in wild fish populations and mixed-effects modelling for understanding biological and environmental influences on otolith biominerals.

Carbon isotopes in soft-tissues have been used to track recent dietary inputs and uncover trophic pathways (Boecklen et al. 2011, Pasquaud et al. 2007, Rau et al. 1983). I showed that physiology should be a consideration when using soft-tissues to retrospectively track diet. Different temperature conditions, altering metabolic demands, influenced the incorporation of carbon isotopes in muscle and liver tissues. Increased metabolic rates may have driven increased routing of specific dietary components, altering the bulk tissue carbon signatures. As carbon isotopes increased with temperature, there may have been increased routing from more positive components such as proteins or carbohydrates. Differences in carbon values among temperature treatments could have arisen from varying metabolic rates stimulating variable food demands and amino acid requirements, consequently leading to changing balances between non-essential amino acid assimilation vs de-novo synthesis. Additionally, differences in carbon isotopes between muscle and liver tissues were likely due to structural and physiological disparities. Visceral organs such as the liver, often have higher metabolic rates but lower growth rates than supportive tissues like muscle (Dalerum and Angerbjörn 2005). Carbon isotope incorporation reflects this, showing liver isotopic composition was likely driven by high tissue turnover from metabolic rates replacing or converting existing tissues (Buchheister and Latour 2010, Carleton and Del Rio 2010, Mont'Alverne et al. 2016). Consequently, physiological differences between the soft-tissues and the effect of temperature on physiology is shown to influence isotopic incorporation in soft-tissues.

The advantages of physiological biomarkers

Intrinsic biomarkers provide many advantages over other approaches for tracking physiological processes. Otolith growth chronologies combined with mixed-effects modelling is a non-destructive approach for analysing the transverse section of otoliths, leaving them for future analyses of age and chemistry. Mixed-effects modelling is a powerful approach for determining both biological (intrinsic) and anthropogenic or environmental (extrinsic) drivers of growth, while analysing them simultaneously but allowing them to be effectively partitioned for detailed comparisons and interactions (Doubleday et al. 2015). Chemical chronologies from otoliths can also reconstruct entire life histories of fish and analytical costs are typically comparatively low, allowing for larger sample sizes. Otolith archives are also kept in research institutes and museums worldwide, providing easy access to a wide range of species, locations and year classes. Biogeochemical techniques can also be used to reconstruct histories when direct measures are not possible, such as historical or extinct species using archaeological samples (Disspain et al. 2016); or inaccessible species, such as deep-sea fish (Shephard et al. 2007, Trueman et al. 2013). Although chemical proxies may be less accurate than direct measurements via electromyogram telemetry, accelerometry or heart rate measures (Metcalfe et al. 2016), these direct approaches can have limited application due to high costs and logistics from expensive equipment and field time required. These direct measures also typically capture only a short-term 'snapshot', spanning hours to a maximum of one or two years (Butler et al. 2004). Direct measures also generally involve locating the study species in the wild and then either implanting or attaching a device. Some of these devices require recapture of the tagged individual and cannot be used on small individuals, which limits measurements of immature fish, or soft-bodied organisms such as cephalopods (Butler et al. 2004). Overall, intrinsic biomarkers can be a comparatively useful, efficient and a cost-effective alternative for investigating physiological histories.

Application of physiological biomarkers in fishery management

Long-term ecological datasets document historical change and assist in understanding the present to anticipate the future. Establishing baseline conditions can identify and isolate possible causes or change, provide context for natural variability and help to set targets for restoration efforts (Hobbie et al. 2003, Reid and Ogden 2006). Ecological datasets are valuable in fisheries management. Fishery management protects wild populations from being overfished and ensures long-term sustainability of fish stocks by setting appropriate limits on fishery activity. Effective management requires the ability to predict long-term fluctuations in abundance and biomass production due to the interactions between human perturbations or environmental variations (Shelton and Mangel 2011).

Physiological biomarkers provide high value for use in fishery management. Fishery scientists are tasked with estimating individual sizes of fish to understand population biomass, which feeds into setting sustainable catch limits. Estimates of growth and metabolic rates are important inputs for growth and bioenergetics models in stock assessments and fishery management. Models bring together pieces of information for predicting what may happen into the future, which is particularly useful for predictions under local or global environmental disruptions (Jørgensen et al. 2016). Models have been used to estimate the intensity and dynamics of predator and prey interactions (Bachiller et al. 2018, Chipps and Wahl 2008), predict population dynamics (Megrey et al. 2007), understand the accumulation of poisons (Trudel and Rasmussen 2006) and nutrient cycling (Kraft 1992). I demonstrated that inferences from intrinsic biomarkers can be used to establish potential management strategies. Snapper growth decreased in the two most productive fishery regions. I suggest that to bolster resilience against these external pressures, it is important to preserve population age-structures, which also slows down the selective pressures towards slower-growing fish that mature earlier (Brander 2007). I further suggest that age-structures can be protected through enacting maximum legal lengths of catch or establishing and increasing the number/size of marine protected areas. Physiological biomarkers provide key insights into individual biology, population dynamics and ecosystem interactions and are valuable resources for fishery management.

Future directions – advancing physiological biomarkers in fish

I investigated the use of intrinsic biomarkers for tracking physiological processes in fish. My research has provided new insight into physiological biomarkers in fish, but there is much more to explore. This thesis centres on snapper as a test species, validating physiological biomarkers under experimental conditions and applying them in wild fish. Further experimental work could expand the potential of physiological biomarkers in other species of fish.

Snapper is a temperate/sub-tropical marine fish species and these characteristics may influence chemical incorporation into otoliths. In freshwater fish, elements in otoliths are assimilated primarily through ambient water passing over the gills (Campana 1999). In contrast, the main source in marine fish is through assimilation of ambient water through the intestines (Campana 1999). Therefore, the potential for isotopic and elemental chemistry in otoliths to be applied as physiological biomarkers needs to be also validated in freshwater and diadromous species. Moreover, juvenile snapper were used in the experimental studies undertaken here, so validation of physiochemical relationships is required for the other life-history stages. My experimental work also showed that physiological stress could decouple the relationship between metabolic rate and carbon isotopes. This needs to be investigated in other species to test if this is a species-specific response, or is more widely observed. A directional change in relationship such as observed here would have significant implications for using carbon isotopes as metabolic biomarkers in the field. I also relate carbon isotopes to laboratory-measured metabolic rates. The next step may be to combine direct measures of field metabolic rate to the chemical proxies. This may further enhance carbon isotopes as metabolic biomarkers and could improve their accuracy in long-term metabolic reconstructions.

My research also provides opportunity to explore new perspectives of biominerals by providing metabolic insights into other aquatic animals. Hard-parts in molluscs could potentially be used in a similar manner. Carbon isotopes in bivalve shells and hard-parts in cephalopods such as statoliths (cephalopod equivalent to otoliths), cuttlebones or beaks have a metabolically-sourced component. Experimental work, particularly on cephalopods, is lacking and the incorporation of carbon into mollusc hard-parts is poorly understood. Consequently, there is great potential for exploring the possibility of metabolic biomarkers in other aquatic animals.

Conclusions

Long-term ecological datasets document historical change which assists in understanding the present in order to anticipate the future. Intrinsic biomarkers are a valuable tool for retrospectively creating long-term datasets that would otherwise be costly and logistically difficult to obtain through direct methods. I show chemical signatures in otoliths are valid metabolic proxies for fish within optimal physiological limits. Tracking physiology is important for addressing a wide-range of biological and ecological questions at individual, population and ecosystem levels. As such, physiological histories are a powerful tool for improving our understanding of wild populations. Fisheries provide an important food source for the global population and these techniques can inform sustainable fishery practices which will benefit fish populations, the fishing industry and general community for years to come.

REFERENCES

Adkins, J. F., McIntyre K., and Schrag. D. P. (2002) The salinity, temperature, and $\delta^{18}O$ of the glacial deep ocean. Science 298:1769-1773.

Alexandre, C.M. and Palstra, A.P. (2017) Effect of short-term regulated temperature variations on the swimming economy of Atlantic salmon smolts. Conservation Physiology 5, cox025-cox025.

Andersen, K.H. and Brander, K. (2009) Expected rate of fisheries-induced evolution is slow. Proceedings of the National Academy of Sciences 106, 11657-11660.

Anderson, T.W. (2001) Predator responses, prey refuges, and density-dependent mortality of a marine fish. Ecology 82, 245-257.

Angilletta, M.J., Wilson, R.S., Navas, C.A. and James, R.S. (2003) Tradeoffs and the evolution of thermal reaction norms. Trends in Ecology & Evolution 18, 234-240.

Audzijonyte, A., Kuparinen, A. and Fulton, E.A. (2013) How fast is fisheries-induced evolution? Quantitative analysis of modelling and empirical studies. Evolutionary Applications 6, 585-595.

Bachiller, E., Utne, K.R., Jansen, T. and Huse, G. (2018) Bioenergetics modeling of the annual consumption of zooplankton by pelagic fish feeding in the Northeast Atlantic. PLoS One 13, e0190345.

Barneche, D.R., Robertson, D.R., White, C.R. and Marshall, D.J. (2018) Fish reproductive-energy output increases disproportionately with body size. Science 360, 642-645.

Barnes, C., Jennings, S. and Barry, J.T. (2009) Environmental correlates of large-scale spatial variation in the $\delta^{13}C$ of marine animals. Estuarine Coastal and Shelf Science 81, 368-374.

Barrow, J., Ford, J., Day, R. and Morrongiello, J. (2017) Environmental drivers of growth and predicted effects of climate change on a commercially important fish, *Platycephalus laevigatus*. Marine Ecology Progress Series.

Barton, B.A. and Iwama, G.K. (1991) Physiological changes in fish from stress in aquaculture with emphasis on the response and effects of corticosteroids. Annual Review of Fish Diseases 1, 3-26.

Bastow, T.P., Jackson, G. and Edmonds, J.S. (2002) Elevated salinity and isotopic composition of fish otolith carbonate: stock delineation of pink snapper, *Pagras auratus*, in Shark Bay, Western Australia. Marine Biology 141, 801-806.

Bates, D., Maechler, M., B, B. and Walker, S. (2015) lme4: Linear Mixed-Effects Models using Eigen and S4, R package version 1.1-7. ed.

Bath, G.E., Thorrold, S.R., Jones, C.M., Campana, S.E., McLaren, J.W. and Lam, J.W.H. (2000) Strontium and barium uptake in aragonitic otoliths of marine fish. Geochimica et Cosmochimica Acta 64, 17051714.

Begg, G.A. and Weidman, C.R. (2001) Stable $d^{13}C$ and $d^{18}O$ isotopes in otoliths of haddock *Melanogrammus aeglefinus* from the northwest Atlantic Ocean. Marine Ecology Progress Series 216, 223-233.

Beitinger, T.L. and Fitzpatrick, L.C. (1979) Physiological and ecological correlates of preferred temperature in fish. American Zoologist 19, 319-329.

Bell, J.D., Watson, R.A. and Ye, Y. (2017) Global fishing capacity and fishing effort from 1950 to 2012. Fish and Fisheries 18, 489-505.

Benson, B.B. and Krause, D. (1984) The concentration and isotopic fractionation of oxygen dissolved in freshwater and seawater in equilibrium with the atmosphere. Limnology and Oceanography 29, 620-632.

Berkeley, S.A., Hixon, M.A., Larson, R.J. and Love, M.S. (2004) Fisheries sustainability via protection of age structure and spatial distribution of fish populations. Fisheries 29, 23-32.

Bettencourt, V. and Guerra, A. (1999) Carbon- and oxygen-isotope composition of the cuttlebone of *Sepia officinalis*: a tool for predicting ecological information? Marine Biology 133, 651-657.

Black, B.A., Schroeder, I.D., Sydeman, W.J., Bograd, S.J., Wells, B.K. and Schwing, F.B. (2011) Winter and summer upwelling modes and their biological importance in the California Current Ecosystem. Global Change Biology 17, 2536-2545.

Blanke, C.M., Chikaraishi, Y., Takizawa, Y., Steffan, S.A., Dharampal, P.S. and Vander Zanden, M.J. (2017) Comparing compound-specific and bulk stable nitrogen isotope trophic discrimination factors across multiple freshwater fish species and diets. Canadian Journal of Fisheries and Aquatic Sciences 74, 1291-1297.

Bloomfield, A.L., Elsdon, T.S., Walther, B.D., Gier, E.J. and Gillanders, B.M. (2011) Temperature and diet affect carbon and nitrogen isotopes of fish muscle: can amino acid nitrogen isotopes explain effects? Journal of Experimental Marine Biology and Ecology 399, 48-59.

Boecklen, W.J., Yarnes, C.T., Cook, B.A. and James, A.C. (2011) On the use of stable isotopes in trophic ecology. Annual Review of Ecology, Evolution, and Systematics 42, 411-440.

Bœuf, G. and Payan, P. (2001) How should salinity influence fish growth? Comparative Biochemistry and Physiology Part C: Toxicology & Pharmacology 130, 411-423.

Bolger, T. and Connolly, P. (1989) The selection of suitable indices for the measurement and analysis of fish condition. Journal of Fish Biology 34, 171-182.

Bonga, S.E.W. (1997) The stress response in fish. Physiological Reviews 77, 591-625.

Brander, K. (2010) Impacts of climate change on fisheries. Journal of Marine Systems 79, 389-402.

Brander, K.M. (2007) Global fish production and climate change. Proceedings of the National Academy of Sciences 104, 19709-19714.

Brett, J.R. (1969) Temperature and fish. Chesapeake Science 10, 275-276.

Brodie, J., De'Ath G., Devlin M., Furnas M., and Wright. M. (2007) Spatial and temporal patterns of nearsurface chlorophyll-*a* in the Great Barrier Reef lagoon. Marine and Freshwater Research 58:342353.

Brown, J.H., Gillooly, J.F., Allen, A.P., Savage, V.M. and West, G.B. (2004) Toward a metabolic theory of ecology. Ecology 85, 1771-1789.

Brown, R. J., and K. P. Severin. 2009. Otolith chemistry analyses indicate that water Sr:Ca is the primary factor influencing otolith Sr:Ca for freshwater and diadromous fish but not for marine fish. Canadian Journal of Fisheries and Aquatic Sciences 66, 1790-1808.

Buchheister, A. and Latour, R.J. (2010) Turnover and fractionation of carbon and nitrogen stable isotopes in tissues of a migratory coastal predator, summer flounder (*Paralichthys dentatus*). Canadian Journal of Fisheries and Aquatic Sciences 67, 445-461.

Bunn, A.G. (2008) A dendrochronology program library in R (dplR). Dendrochronologia 26, 115-124.

Bureau of Meteorology. 2017. Southern Oscillation Index (SOI) since 1876. Commonwealth of Australia, Australia.

Burnham, K.P. and Anderson, D.R. (2004) Multimodel inference: understanding AIC and BIC in model selection. Sociological Methods and Research 33, 261-304.

Butler, P.J., Green, J.A., Boyd, I.L. and Speakman, J.R. (2004) Measuring metabolic rate in the field: the pros and cons of the doubly labelled water and heart rate methods. Functional Ecology 18, 168-183.

Cai, W., Borlace, S., Lengaigne, M., van Rensch, P., Collins, M., Vecchi, G., Timmermann, A., Santoso, A., McPhaden, M.J., Wu, L., England, M.H., Wang, G., Guilyardi, E. and Jin, F.-F. (2014) Increasing frequency of extreme El Niño events due to greenhouse warming. Nature Climate Change 4, 111.

Campana, S.E. (1999) Chemistry and composition of fish otoliths: pathways, mechanisms and applications. Marine Ecology Progress Series 188, 263-297.

Campana, S.E. and Neilson, J.D. (1985) Microstructure of fish otoliths. Canadian Journal of Fisheries and Aquatic Sciences 42, 1014-1032.

Campana, S.E. and Thorrold, S.R. (2001) Otoliths, increments, and elements: keys to a comprehensive understanding of fish populations? Canadian Journal of Fisheries and Aquatic Sciences 58, 30-38.

Carleton, S.A. and Del Rio, C.M. (2010) Growth and catabolism in isotopic incorporation: a new formulation and experimental data. Functional Ecology 24, 805-812.

Chabot, D., Koenker, R. and Farrell, A.P. (2016a) The measurement of specific dynamic action in fishes. Journal of Fish Biology 88, 152-172.

Chabot, D., Steffensen, J.F. and Farrell, A.P. (2016b) The determination of standard metabolic rate in fishes. Journal of Fish Biology 88, 81-121.

Chiew, F.H.S., Piechota, T.C., Dracup, J.A. and McMahon, T.A. (1998) El Niño/Southern Oscillation and Australian rainfall, streamflow and drought: Links and potential for forecasting. Journal of Hydrology 204, 138-149.

Chipps, S.R. and Wahl, D.H. (2008) Bioenergetics modeling in the 21st century: Reviewing new insights and revisiting old constraints. Transactions of the American Fisheries Society 137, 298-313.

Chung, M.-T. (2015) Functional and life-history traits in deep-sea fishes. University of Southampton.

Chung, M.-T., C. N. Trueman, J. A. Godiksen, and P. Grønkjær. (2019a) Otolith δ^{13}C values as a metabolic proxy: approaches and mechanical underpinnings. Marine and Freshwater Research 10.1071/MF18317.

Chung, M.-T., Trueman, C. N., Godiksen J. A., Holmstrup M. E., and Grønkjær P. (2019b) Field metabolic rates of teleost fishes are recorded in otolith carbonate 2:24.

Cicchetti, D.V. (1994) Guidelines, criteria, and rules of thumb for evaluating normed and standardized assessment instruments in psychology. Psychological Assessment 6, 284.

Clark, T.D., Ryan, T., Ingram, B., Woakes, A., Butler, P. and Frappell, P.B. (2005) Factorial aerobic scope is independent of temperature and primarily modulated by heart rate in exercising Murray cod (*Maccullochella peelii peelii*). Physiological and Biochemical Zoology 78, 347-355.

Clark, T.D., Sandblom, E. and Jutfelt, F. (2013) Aerobic scope measurements of fishes in an era of climate change: respirometry, relevance and recommendations. Journal of Experimental Biology 216, 2771-2782.

Clarke, A. and Johnston, N.M. (1999) Scaling of metabolic rate with body mass and temperature in teleost fish. Journal of Animal Ecology 68, 893-905.

Cooke, S.J., Birnie-Gauvin, K., Lennox, R.J., Taylor, J.J., Rytwinski, T., Rummer, J.L., Franklin, C.E., Bennett, J.R. and Haddaway, N.R. (2017) How experimental biology and ecology can support evidence-based decision-making in conservation: avoiding pitfalls and enabling application. Conservation Physiology 5, cox043.

Cooke, S.J., Thorstad, E.B. and Hinch, S.G. (2004) Activity and energetics of free-swimming fish: insights from electromyogram telemetry. Fish and Fisheries 5, 21-52.

Crook, D.A., Buckle, D.J., Allsop, Q., Baldwin, W., Saunders, T.M., Kyne, P.M., Woodhead, J.D., Maas, R., Roberts, B. and Douglas, M.M. (2017) Use of otolith chemistry and acoustic telemetry to elucidate migratory contingents in barramundi *Lates calcarifer*. Marine and Freshwater Research. 68, 1554-1566.

Dalerum, F. and Angerbjörn, A. (2005) Resolving temporal variation in vertebrate diets using naturally occurring stable isotopes. Oecologia 144, 647-658.

Darnaude, A.M., Sturrock, A., Trueman, C.N., Mouillot, D., Campana, S.E., Hunter, E. and Eimf (2014) Listening in on the past: What can otolith delta O-18 values really tell us about the environmental history of fishes? PLoS One 9, 17.

DeNiro, M.J. and Epstein, S. (1977) Mechanism of carbon isotope fractionation associated with lipid synthesis. Science 197, 261-263.

DeNiro, M.J. and Epstein, S. (1978) Influence of diet on the distribution of carbon isotopes in animals. Geochimica et Cosmochimica Acta 42, 495-506.

Dierking, J., Morat, F., Letourneur, Y. and Harmelin-Vivien, M. (2012) Fingerprints of lagoonal life: Migration of the marine flatfish *Solea solea* assessed by stable isotopes and otolith microchemistry. Estuarine, Coastal and Shelf Science 104-105, 23-32.

DiMaria, R., Miller, J. and Hurst, T. (2010) Temperature and growth effects on otolith elemental chemistry of larval Pacific cod, *Gadus macrocephalus*. Environmental Biology of Fishes 89, 453-462.

Dingemanse, N.J. and Wolf, M. (2013) Between-individual differences in behavioural plasticity within populations: causes and consequences. Animal Behaviour 85, 1031-1039.

Disspain, M.C.F., Ulm, S. and Gillanders, B.M. (2016) Otoliths in archaeology: Methods, applications and future prospects. Journal of Archaeological Science: Reports 6, 623-632.

Do Souto, M., Spinelli, M.L., Brown, D.R., Pájaro, M., Diaz, M.V. and Capitanio, F.L. (2018) Benefits of frontal waters for the growth of *Engraulis anchoita* larvae: The influence of food availability. Fisheries Research 204, 181-188.

Donnellan, S.C. and McGlennon, D. (1996) Stock identification and discrimination in snapper (*Pagrus auratus*) in southern Australia. SARDI.

Doubleday, Z.A., Harris, H.H., Izzo, C. and Gillanders, B.M. (2014) Strontium randomly substituting for calcium in fish otolith aragonite. Analytical Chemistry 86, 865-869.

Doubleday, Z.A., Izzo, C., Haddy, J.A., Lyle, J.M., Ye, Q. and Gillanders, B.M. (2015) Long-term patterns in estuarine fish growth across two climatically divergent regions. Oecologia, 1-12.

Doubleday, Z.A., Izzo, C., Woodcock, S.H. and Gillanders, B.M. (2013) Relative contribution of water and diet to otolith chemistry in freshwater fish. Aquatic Biology 18, 271-280.

Downing, J.A., Plante, C. and Lalonde, S. (1990) Fish production correlated with primary productivity, not the morphoedaphic index. Canadian Journal of Fisheries and Aquatic Sciences 47, 1929-1936.

Edyvane, K.S. (1999) Conserving marine biodiversity in South Australia - Part 2 - Identification of areas of high conservation values in South Australia.

Elsdon, T.S. and Gillanders, B.M. (2002) Interactive effects of temperature and salinity on otolith chemistry: challenges for determining environmental histories of fish. Canadian Journal of Fisheries and Aquatic Sciences 59, 1796-1808.

Elsdon, T.S. and Gillanders, B.M. (2004) Fish otolith chemistry influenced by exposure to multiple environmental variables. Journal of Experimental Marine Biology and Ecology 313, 269-284.

Elsdon, T.S. and Gillanders, B.M. (2005) Alternative life-history patterns of estuarine fish: barium in otoliths elucidates freshwater residency. Canadian Journal of Fisheries and Aquatic Sciences 62, 11431152.

Elsdon, T.S., Ayvazian, S., McMahon, K.W. and Thorrold, S.R. (2010) Experimental evaluation of stable isotope fractionation in fish muscle and otoliths. Marine Ecology Progress Series 408, 195-205.

Elsdon, T.S., Wells, B.K., Campana, S.E., Gillanders, B.M., Jones, C.M., Limburg, K.E., Secor, D.H., Thorrold, S.R. and Walther, B.D. (2008) Otolith chemistry to describe movements and life-history parameters of fishes: Hypotheses, assumptions, limitations and inferences, in: Gibson, R.N., Atkinson, R.J.A., Gordon, J.D.M. (Eds.), Oceanography and Marine Biology: An Annual Review, Vol 46, pp. 297-330.

Eppley, R.W. (1972) Temperature and phytoplankton growth in the sea. Fishery Bulletin 70, 1063-1085.

Epstein, S., Buchsbaum, R., Lowenstam, H. and Urey, H.C. (1951) Carbonate-water isotopic temperature scale. Geological Society of America Bulletin 62, 417-426.

Ernande, B., Dieckmann, U. and Heino, M. (2004) Adaptive changes in harvested populations: plasticity and evolution of age and size at maturation. Proceedings of the Royal Society of London B: Biological Sciences 271, 415-423.

Ferrell, D.J., Henry, G.W., Bell, J.D. and Quartararo, N. (1992) Validation of annual marks in the otoliths of young snapper, *Pagrus auratus* (sparidae). Australian Journal of Marine and Freshwater Research 43, 1051-1055.

Fidhiany, L. and Winckler, K. (1998) Influence of body mass, age, and maturation on specific oxygen consumption in a freshwater cichlid fish, *Cichlasoma nigrofasciatum* (Günther, 1869)*. Comparative Biochemistry and Physiology Part A: Molecular & Integrative Physiology 119, 613619.

Fielder, D.S., Bardsley, W.J., Allan, G.L. and Pankhurst, P.M. (2005) The effects of salinity and temperature on growth and survival of Australian snapper, *Pagrus auratus* larvae. Aquaculture 250, 201-214.

Fogarty, M., Rosenberg, A. and Sissenwine, M. (1992) ES&T Series: Fisheries risk assessment sources of uncertainty: A case study of Georges Bank haddock. Environmental Science and Technology 26, 440-447.

Fowler, A.J. (2000) Snapper (*Pagrus auratus*), Fishery assessment report to PIRSA for the MSF fishery management committee. SARDI.

Fowler, A.J. and McGlennon, D. (2011) Variation in productivity of a key snapper, *Chrysophrys auratus*, fishery related to recruitment and fleet dynamics. Fisheries Management and Ecology. 18, 411423.

Fowler, A.J., Gillanders, B.M. and Hall, K.C. (2004) Adult migration, population replenishment and geographic structure for snapper in South Australia South Australian Research and Development Institute (Aquatic Sciences), p. 152.

Fowler, A.J., Gillanders, B.M. and Hall, K.C. (2005) Relationship between elemental concentration and age from otoliths of adult snapper (*Pagrus auratus*, Sparidae): implications for movement and stock structure. Marine and Freshwater Research. 56, 661-676.

Fowler, A.J., Hamer, P.A. and Kemp, J. (2017) Age-related otolith chemistry profiles help resolve demographics and meta-population structure of a widely-dispersed, coastal fishery species. Fisheries Research. 189, 77-94.

Fowler, A.J., McGarvey, R., Carroll, J., Feenstra, J.E., Jackson, W.B. and Lloyd, M.T. (2016) Snapper (*Chrysophrus auratus*) Fishery. Fishery Assessment Report to PIRSA Fisheries and Aquaculture. South Australian Research and Development Institute (Aquatic Sciences), Adelaide.

Fox, J. (2003) Effect displays in R for generalised linear models. Journal of Statistical Software 8, 1-27.

Francis, M. and Pankhurst, N. (1988) Juvenile sex inversion in the New Zealand snapper *Chrysophrys auratus* (Bloch and Schneider, 1801)(Sparidae). Marine and Freshwater Research. 39, 625-631.

Fusco, G. and Minelli, A. (2010) Phenotypic plasticity in development and evolution: facts and concepts. Introduction. Philosophical transactions of the Royal Society of London. Series B, Biological sciences 365, 547-556.

Gallahar, N. and Kingsford, M. (1996) Factors influencing Sr/Ca ratios in otoliths of *Girella elevata*: an experimental investigation. Journal of Fish Biology 48, 174-186.

Gannes, L.Z., del Rio, C.M., and Koch, P. (1998) Natural abundance variations in stable isotopes and their potential uses in animal physiological ecology. Comparative Biochemistry and Physiology Part A: Molecular & Integrative Physiology 119, 725-737.

Gaston, T.F. and Suthers, I.M. (2004) Spatial variation in $\delta^{13}C$ and $\delta^{15}N$ of liver, muscle and bone in a rocky reef planktivorous fish: the relative contribution of sewage. Journal of Experimental Marine Biology and Ecology 304, 17-33.

Gastwirth, J.L., Gel, Y.R. and Miao, W. (2009) The impact of Levene's test of equality of variances on statistical theory and practice. Statistical Science, 343-360.

Gillanders, B.M., Black, B.A., Meekan, M.G. and Morrison, M.A. (2012) Climatic effects on the growth of a temperate reef fish from the Southern Hemisphere: a biochronological approach. Marine Biology 159, 1327-1333.

Gillooly, J.F., Brown, J.H., West, G.B., Savage, V.M. and Charnov, E.L. (2001) Effects of size and temperature on metabolic rate. Science 293, 2248-2251.

Gilmore, K.L., Doubleday, Z.A. and Gillanders, B.M. (2018) Testing hypoxia: physiological effects of longterm exposure in two freshwater fishes. Oecologia 186, 37-47.

Gomon, M.F., Bray, D.J. and Kuiter, R.H. (2008) Fishes of Australia's southern coast. Reed New Holland, Musuem Victoria, Chatswood, N.S.W.

Grammer, G.L., Morrongiello, J.R., Izzo, C., Hawthorne, P.J., Middleton, J.F. and Gillanders, B.M. (2017) Coupling biogeochemical tracers with fish growth reveals physiological and environmental controls on otolith chemistry. Ecological Monographs 87, 487-507.

Gronkjaer, P. (2016) Otoliths as individual indicators: a reappraisal of the link between fish physiology and otolith characteristics. Marine and Freshwater Research. 67, 881-888.

Gronkjaer, P., Pedersen, J.B., Ankjaero, T.T., Kjeldsen, H., Heinemeier, J., Steingrund, P., Nielsen, J.M. and Christensen, J.T. (2013) Stable N and C isotopes in the organic matrix of fish otoliths: validation of a new approach for studying spatial and temporal changes in the trophic structure of aquatic ecosystems. Canadian Journal of Fisheries and Aquatic Sciences 70, 143-146.

Hamer, P.A. and Jenkins, G.P. (2007) Comparison of spatial variation in otolith chemistry of two fish species and relationships with water chemistry and otolith growth. Journal of Fish Biology 71, 1035-1055.

Hamer, P.A., Jenkins, G.P. and Coutin, P. (2006) Barium variation in *Pagrus auratus* (Sparidae) otoliths: A potential indicator of migration between an embayment and ocean waters in south-eastern Australia. Estuarine, Coastal and Shelf Science 68, 686-702.

Hamer, P. A., Jenkins G. P., and Gillanders. B. M. (2003) Otolith chemistry of juvenile snapper *Pagrus auratus* in Victorian waters: natural chemical tags and their temporal variation. Marine Ecology Progress Series 263:261-273.

Hansen, M. J., D. Boisclair, S. B. Brandt, S. W. Hewett, J. F. Kitchell, M. C. Lucas, and J. J. Ney. 1993. Applications of bioenergetics models to fish ecology and management: Where do we go from here? Transactions of the American Fisheries Society 122:1019-1030.

Hanson, J.M. and Leggett, W.C. (1985) Experimental and field evidence for inter- and intraspecific competition in two freshwater fishes. Canadian Journal of Fisheries and Aquatic Sciences 42, 280286.

Harley, C.D., Randall Hughes, A., Hultgren, K.M., Miner, B.G., Sorte, C.J., Thornber, C.S., Rodriguez, L.F., Tomanek, L. and Williams, S.L. (2006) The impacts of climate change in coastal marine systems. Ecology Letters 9, 228-241.

Hellstrom, J., Paton, C., Woodhead, J. and Hergt, J. (2008) Iolite: software for spatially resolved LA-(quad and MC) ICPMS analysis. Mineralogical Association of Canada short course series 40, 343-348.

Helser, T.E., Lai, H.-l. and Black, B.A. (2012) Bayesian hierarchical modeling of Pacific geoduck growth increment data and climate indices. Ecological Modelling 247, 210-220.

Henderson, R.A. and Price, G.D. (2012) Paleoenvironment and paleoecology inferred from oxygen and carbon isotopes of subtropical mollusks from the Late Cretaceous (Cenomanian) of Bathurst Island, Australia. Palaios 27, 617-626.

Hicks, A. S., Closs, G. P. and Swearer. S. E. (2010) Otolith microchemistry of two amphidromous galaxiids across an experimental salinity gradient: A multi-element approach for tracking diadromous migrations. Journal of Experimental Marine Biology and Ecology 394:86-97.

Hixon, M.A., Johnson, D.W. and Sogard, S.M. (2014) BOFFFFs: on the importance of conserving old-growth age structure in fishery populations. ICES Journal of Marine Science 71, 2171-2185.

Hobbie, J.E., Carpenter, S.R., Grimm, N.B., Gosz, J.R. and Seastedt, T.R. (2003) The US Long Term Ecological Research Program. BioScience 53, 21-32.

Høie, H., Andersson, C., Folkvord, A. and Karlsen, Ø. (2004) Precision and accuracy of stable isotope signals in otoliths of pen-reared cod (*Gadus morhua*) when sampled with a high-resolution micromill. Marine Biology 144, 1039-1049.

Høie, H., Folkvord, A. and Otterlei, E. (2003) Effect of somatic and otolith growth rate on stable isotopic composition of early juvenile cod (*Gadus morhua* L) otoliths. Journal of Experimental Marine Biology and Ecology 289, 41-58.

Hulbert, A. and Else, P.L. (2000) Mechanisms underlying the cost of living in animals. Annual review of physiology 62, 207-235.

Immenhauser, A., Schöne, B.R., Hoffmann, R. and Niedermayr, A. (2016) Mollusc and brachiopod skeletal hard parts: Intricate archives of their marine environment. Sedimentology 63, 1-59.

IMOS. 2017a. IMOS - SRS - MODIS - 01 day - Chlorophyll-*a* concentration (OC3 model). Australian Ocean Data Network.

IMOS. 2017b. IMOS - SRS SATELLITE - SST L3S - 03 day composite - night time. Australian Ocean Data Network.

Inoue, H. and Sugimura, Y. (1986) Distribution of $p\mathrm{CO}_2$ and $\delta^{13}\mathrm{C}$ in the air and surface sea water in the Southern Ocean, south of Australia. Memoirs of National Institute of Polar Research. Special issue 40, 454-461.

IPCC (2014) Climate change 2014: Synthesis report. Contribution of Working Groups I, II and III to the fifth assessment report of the Intergovernmental Panel on Climate Change. IPCC, Geneva, Switzerland.

Izzo, C., Doubleday, Z.A., Grammer, G.L., Disspain, M.C.F., Ye, Q. and Gillanders, B.M. (2016) Seasonally resolved environmental reconstructions using fish otoliths. Canadian Journal of Fisheries and Aquatic Sciences 74, 23-31.

Izzo, C., Reis-Santos, P. and Gillanders, B.M. (2018) Otolith chemistry does not just reflect environmental conditions: A meta-analytic evaluation. Fish and Fisheries 19, 441-454.

Jamieson, R.E., Schwarcz, H.P. and Brattey, J. (2004) Carbon isotopic records from the otoliths of Atlantic cod (*Gadus morhua*) from eastern Newfoundland, Canada. Fish Res. 68, 83-97.

Jones, J.B. and Campana, S.E. (2009) Stable oxygen isotope reconstruction of ambient temperature during the collapse of a cod (*Gadus morhua*) fishery. Ecological Applications 19, 1500-1514.

Jørgensen, C., Enberg, K. and Mangel, M. (2016) Modelling and interpreting fish bioenergetics: a role for behaviour, life-history traits and survival trade-offs. Journal of Fish Biology 88, 389-402.

Kalish, J.M. (1991a) C-13 and O-18 isotopic disequilibria in fish otoliths - metabolic and kinetic effects. Marine Ecology Progress Series 75, 191-203.

Kalish, J.M. (1991b) Oxygen and carbon stable isotopes in the otoliths of wild and laboratory-reared Australian salmon (*Arripis trutta*). Marine Biology 110, 37-47.

Kelly, L.J. and del Rio, C.M. (2010) The fate of carbon in growing fish: an experimental study of isotopic routing. Physiological and Biochemical Zoology 83, 473-480.

Kiljunen, M., Grey, J., Sinisalo, T., Harrod, C., Immonen, H. and Jones, R.I. (2006) A revised model for lipidnormalizing δ13C values from aquatic organisms, with implications for isotope mixing models. Journal of Applied Ecology 43, 1213-1222.

Kim, S.-T., O'Neil, J.R., Hillaire-Marcel, C. and Mucci, A. (2007) Oxygen isotope fractionation between synthetic aragonite and water: Influence of temperature and Mg2+ concentration. Geochim. Cosmochim. Acta 71, 4704-4715.

Kitagawa, T., Ishimura, T., Uozato, R., Shirai, K., Amano, Y., Shinoda, A., Otake, T., Tsunogai, U. and Kimura, S. (2013) Otolith delta O-18 of Pacific bluefin tuna *Thunnus orientalis* as an indicator of ambient water temperature. Marine Ecology Progress Series 481, 199-209.

Kitchell, J. F., Stewart D. J., and Weininger D. (1977) Applications of a bioenergetics model to yellow perch (*Perca flavescens*) and walleye (*Stizostedion vitreum vitreum*). Journal of the Fisheries Board of Canada 34:1922-1935.

Kitchens, L.L., Rooker, J.R., Reynal, L., Falterman, B.J., Saillant, E. and Murua, H. (2018) Discriminating among yellowfin tuna *Thunnus albacares* nursery areas in the Atlantic Ocean using otolith chemistry. Marine Ecology Progress Series 603, 201-213.

Koch, G.G. (2004) Intraclass correlation coefficient. Encyclopedia of statistical sciences 6.

Kraft, C.E. (1992) Estimates of phosphorus and nitrogen cycling by fish using a bioenergetics approach. Canadian Journal of Fisheries and Aquatic Sciences 49, 2596-2604.

Kroopnick, P. (1985) The distribution of 13C of ΣCO2 in the world oceans. Deep Sea Research Part A. Oceanographic Research Papers 32, 57-84.

Laikre, L., Schwartz, M.K., Waples, R.S. and Ryman, N. (2010) Compromising genetic diversity in the wild: unmonitored large-scale release of plants and animals. Trends in Ecology & Evolution 25, 520-529.

Last, P.R., White, W.T., Gledhill, D.C., Hobday, A.J., Brown, R., Edgar, G.J. and Pecl, G. (2011) Long-term shifts in abundance and distribution of a temperate fish fauna: a response to climate change and fishing practices. Global Ecology and Biogeography 20, 58-72.

Lehodey, P., Alheit, J., Barange, M., Baumgartner, T., Beaugrand, G., Drinkwater, K., Fromentin, J.-M., Hare, S., Ottersen, G. and Perry, R. (2006) Climate variability, fish, and fisheries. Journal of Climate 19, 50095030.

Lewin, W.-C., Arlinghaus, R. and Mehner, T. (2006) Documented and potential biological impacts of recreational fishing: insights for management and conservation. Reviews in Fisheries Science 14, 305-367.

Limburg, K. E., Walther B. D., Lu Z., Jackman G., Mohan J., Walther Y., Nissling A., Weber P. K., and Schmitt A. K. (2015) In search of the dead zone: Use of otoliths for tracking fish exposure to hypoxia. Journal of Marine Systems 141:167-178.

Limburg, K.E., Wuenschel, M.J., Hüssy, K., Heimbrand, Y. and Samson, M. (2018) Making the otolith magnesium chemical calendar-clock tick: Plausible mechanism and empirical evidence. Reviews in Fisheries Science & Aquaculture 26, 479-493.

Lin, S.-H., Chang, C.-W., Iizuka, Y. and Tzeng, W.-N. (2007) Salinities, not diets, affect strontium/calcium ratios in otoliths of *Anguilla japonica*. Journal of Experimental Marine Biology and Ecology 341, 254-263.

Loeppky, A.R. and Davoren, G.K. (2018) Temperature and salinity influence the chemistry in the pre-hatch otolith region of capelin, *Mallotus villosus*, during lab and field egg incubation experiments. Journal of Experimental Marine Biology and Ecology 501, 65-73.

Lorenzen, K. (2016) Toward a new paradigm for growth modeling in fisheries stock assessments: Embracing plasticity and its consequences. Fisheries Research. 180, 4-22.

Maceina, M. (1997) Simple application of using residuals from catch-curve regressions to assess year-class strength in fish. Fisheries Research. 32, 115-121.

Macfarlane, R., Ralston, S., Royer, C. and Norton, E.C. (2005) Juvenile chinook salmon (*Oncorhynchus tshawytscha*) growth on the central California coast during the 1998 El Niño and 1999 La Niña. Fisheries Oceanography 14, 321-332.

Martin, G.B. and Thorrold, S.R. (2005) Temperature and salinity effects on magnesium, manganese, and barium incorporation in otoliths of larval and early juvenile spot *Leiostomus xanthurus*. Marine Ecology Progress Series 293, 223-232.

Martino, J., Doubleday Z. A., Woodcock S. H., and Gillanders. B. M. (2017) Elevated carbon dioxide and temperature affects otolith development, but not chemistry, in a diadromous fish. Journal of Experimental Marine Biology and Ecology 495:57-64.

Martino, J.C., Doubleday, Z.A. and Gillanders, B.M. (2019a) Metabolic effects on carbon isotope biomarkers in fish. Ecological Indicators 97, 10-16.

Martino, J.C., Fowler, A.J., Doubleday, Z.A., Grammer, G.L. and Gillanders, B.M. (2019b) Using otolith chronologies to understand long-term trends and extrinsic drivers of growth in fisheries. Ecosphere 10, e02553.

Mazerolle, M. (2015) AICcmodavg: Model selection and multimodel inference based on (Q)AIC(c). , R package version 2.0-3 ed.

McConnaughey, T.A., Burdett, J., Whelan, J.F. and Paull, C.K. (1997) Carbon isotopes in biological carbonates: Respiration and photosynthesis. Geochimica et Cosmochimica Acta 61, 611-622.

McCue, M.D. (2006) Specific dynamic action: A century of investigation. Comparative Biochemistry and Physiology Part A: Molecular & Integrative Physiology 144, 381-394.

McGinnity, P., Jennings, E., Allott, N., Samuelsson, P., Rogan, G., Whelan, K. and Cross, T. (2009) Impact of naturally spawning captive-bred Atlantic salmon on wild populations: depressed recruitment and increased risk of climate-mediated extinction. Proceedings of the Royal Society of London B: Biological Sciences, rspb20090799.

McMahon, K.W., Fogel, M.L., Elsdon, T.S. and Thorrold, S.R. (2010) Carbon isotope fractionation of amino acids in fish muscle reflects biosynthesis and isotopic routing from dietary protein. Journal of Animal Ecology 79, 1132-1141.

Megrey, B.A., Rose, K.A., Klumb, R.A., Hay, D.E., Werner, F.E., Eslinger, D.L. and Smith, S.L. (2007) A bioenergetics-based population dynamics model of Pacific herring (Clupea harengus pallasi) coupled to a lower trophic level nutrient–phytoplankton–zooplankton model: Description, calibration, and sensitivity analysis. Ecological Modelling 202, 144-164.

Metcalfe, J., Wright, S., Tudorache, C. and Wilson, R. (2016) Recent advances in telemetry for estimating the energy metabolism of wild fishes. Journal of Fish Biology 88, 284-297.

Middleton, J.F. and Cirano, M. (2002) A northern boundary current along Australia's southern shelves: The Flinders Current. Journal of Geophysical Research: Oceans 107, 12-11-12-11.

Miles, N.G., Butler, G.L., Diamond, S.L., Bishop, D.P., van der Meulen, D.E., Reinfelds, I. and Walsh, C.T. (2018) Combining otolith chemistry and telemetry to assess diadromous migration in pinkeye mullet, *Trachystoma petardi* (Actinopterygii, Mugiliformes). Hydrobiologia 808, 265-281.

Miller, J. (2009) The effects of temperature and water concentration on the otolith incorporation of barium and manganese in black rockfish *Sebastes melanops*. Journal of Fish Biology 75, 39-60.

Mont'Alverne, R., Jardine, T.D., Pereyra, P.E.R., Oliveira, M.C.L.M., Medeiros, R.S., Sampaio, L.A., Tesser, M.B. and Garcia, A.M. (2016) Elemental turnover rates and isotopic discrimination in a euryhaline fish reared under different salinities: Implications for movement studies. Journal of Experimental Marine Biology and Ecology 480, 36-44.

Moreira, C., Froufe, E., Sial, A.N., Caeiro, A., Vaz-Pires, P. and Correia, A.T. (2018) Population structure of the blue jack mackerel (*Trachurus picturatus*) in the NE Atlantic inferred from otolith microchemistry. Fisheries Research. 197, 113-122.

Morrongiello, J.R. and Thresher, R.E. (2015) A statistical framework to explore ontogenetic growth variation among individuals and populations: a marine fish example. Ecological Monographs 85, 93-115.

Morrongiello, J.R., Thresher, R.E. and Smith, D.C. (2012) Aquatic biochronologies and climate change. Nature Climate Change 2, 849-857.

Morrongiello, J.R., Walsh, C.T., Gray, C.A., Stocks, J.R. and Crook, D.A. (2014) Environmental change drives long-term recruitment and growth variation in an estuarine fish. Global Change Biology 20, 18441860.

Nagy, K.A. (2005) Field metabolic rate and body size. Journal of Experimental Biology 208, 1621-1625.

Nelson, J.A. (2016) Oxygen consumption rate v. rate of energy utilization of fishes: a comparison and brief history of the two measurements. Journal of Fish Biology 88, 10-25.

Neuheimer, A.B., Thresher, R.E., Lyle, J.M. and Semmens, J.M. (2011) Tolerance limit for fish growth exceeded by warming waters. Nature Climate Change 1, 110-113.

Newsome, S.D., Fogel, M.L., Kelly, L. and del Rio, C.M. (2011) Contributions of direct incorporation from diet and microbial amino acids to protein synthesis in Nile tilapia. Functional Ecology 25, 1051-1062.

Norin, T. and Clark, T.D. (2016) Measurement and relevance of maximum metabolic rate in fishes. Journal of Fish Biology 88, 122-151.

Norriss, J.V. and Crisafulli, B. (2010) Longevity in Australian snapper *Pagrus auratus* (Sparidae). Journal of the Royal Society of Western Australia 93, 129-132.

Olsen, E.M., Carlson, S.M., Gjøsæter, J. and Stenseth, N.C. (2009) Nine decades of decreasing phenotypic variability in Atlantic cod. Ecology Letters 12, 622-631.

Ong, J.J.L., Rountrey, A.N., Black, B.A., Nguyen, H.M., Coulson, P.G., Newman, S.J., Wakefield, C.B., Meeuwig, J.J. and Meekan, M.G. (2018) A boundary current drives synchronous growth of marine fishes across tropical and temperate latitudes. Global Change Biology 24, 1894-1903.

Ottersen, G., Hjermann, D.Ø. and Stenseth, N.C. (2006) Changes in spawning stock structure strengthen the link between climate and recruitment in a heavily fished cod (*Gadus morhua*) stock. Fisheries Oceanography 15, 230-243.

Pasquaud, S., Lobry, J. and Elie, P. (2007) Facing the necessity of describing estuarine ecosystems: a review of food web ecology study techniques. Hydrobiologia 588, 159-172.

Paton, C., Hellstrom, J., Paul, B., Woodhead, J. and Hergt, J. (2011) Iolite: Freeware for the visualisation and processing of mass spectrometric data. Journal of Analytical Atomic Spectrometry 26, 2508-2518.

Pauly, D. and Zeller, D. (2016) Catch reconstructions reveal that global marine fisheries catches are higher than reported and declining. Nature Communications 7, ncomms10244.

Peck, M. and Moyano, M. (2016) Measuring respiration rates in marine fish larvae: challenges and advances. Journal of Fish Biology 88, 173-205.

Pecl, G.T., Ward, T., Doubleday, Z., Clarke, S., Day, J., Dixon, C., Frusher, S., Gibbs, P., Hobday, A., Hutchinson, N., Jennings, S., Jones, K., Li, X., D, D.S. and Stoklosa, R. (2011) Risk assessment of impacts of climate change for key marine species in south eastern Australia. Part 1: Fisheries and aquaculture risk assessment. Fisheries Research and Development Corporation, p. Project 2009/2070.

Peterson, B.J. and Fry, B. (1987) Stable isotopes in ecosystem studies. Annual review of ecology and systematics 18, 293-320.

Pörtner, H.O. and Farrell, A.P. (2008) Physiology and Climate Change. Science 322, 690-692.

Post, D.M., Layman, C.A., Arrington, D.A., Takimoto, G., Quattrochi, J. and Montaña, C.G. (2007) Getting to the fat of the matter: models, methods and assumptions for dealing with lipids in stable isotope analyses. Oecologia 152, 179-189.

Price, G.D., Twitchett, R.J., Smale, C. and Marks, V. (2009) Isotopic analysis of the life history of the enigmatic squid *Spirula spirula*, with implications for studies of fossil cephalopods. Palaios 24, 273-279.

Price, T.D., Qvarnström, A. and Irwin, D.E. (2003) The role of phenotypic plasticity in driving genetic evolution. Proceedings of the Royal Society of London B: Biological Sciences 270, 1433-1440.

Quintella, B., Póvoa, I. and Almeida, P.R. (2009) Swimming behaviour of upriver migrating sea lamprey assessed by electromyogram telemetry. Journal of Applied Ichthyology 25, 46-54.

Radtke, R.L., Lenz, P., Showers, W. and Moksness, E. (1996) Environmental information stored in otoliths: insights from stable isotopes. Marine Biology 127, 161-170.

Rahman, M.M. and Verdegem, M. (2010) Effects of intra- and interspecific competition on diet, growth and behaviour of *Labeo calbasu* (Hamilton) and *Cirrhinus cirrhosus* (Bloch). Applied Animal Behaviour Science 128, 103-108.

Rau, G., Mearns, A., Young, D., Olson, R., Schafer, H. and Kaplan, I. (1983) Animal $^{13}C/^{12}C$ correlates with trophic level in pelagic food webs. Ecology 64, 1314-1318.

Regan, M.D. and Richards, J.G. (2017) Rates of hypoxia induction alter mechanisms of O_2 uptake and the critical O_2 tension of goldfish. Journal of Experimental Biology.

Reid, M.A. and Ogden, R.W. (2006) Trend, variability or extreme event? The importance of long-term perspectives in river ecology. River Research and Applications 22, 167-177.

Reis-Santos, P., Vasconcelos, R.P., Tanner, S.E., Fonseca, V.F., Cabral, H.N. and Gillanders, B.M. (2018) Extrinsic and intrinsic factors shape the ability of using otolith chemistry to characterize estuarine environmental histories. Marine Environmental Research 140, 332-341.

Resplandy, L., Keeling, R.F., Eddebbar, Y., Brooks, M.K., Wang, R., Bopp, L., Long, M.C., Dunne, J.P., Koeve, W. and Oschlies, A. (2018) Quantification of ocean heat uptake from changes in atmospheric O_2 and CO_2 composition. Nature 563, 105-108.

Rexfort, A. and Mutterlose, J. (2009) The role of biogeography and ecology on the isotope signature of cuttlefishes (Cephalopoda, Sepiidae) and the impact on belemnite studies. Palaeogeography, Palaeoclimatology, Palaeoecology 284, 153-163.

Richardson, A.J. and Poloczanska, E.S. (2008) Under-Resourced, Under Threat. Science 320, 1294-1295.

Roberts, C.M., Bohnsack, J.A., Gell, F., Hawkins, J.P. and Goodridge, R. (2001) Effects of Marine Reserves on Adjacent Fisheries. Science 294, 1920-1923.

Roche, D.G., Binning, S.A., Bosiger, Y., Johansen, J.L. and Rummer, J.L. (2013) Finding the best estimates of metabolic rates in a coral reef fish. Journal of Experimental Biology 216, 2103-2110.

Romanek, C.S., Grossman, E.L. and Morse, J.W. (1992) Carbon isotopic fractionation in synthetic aragonite and calcite: Effects of temperature and precipitation rate. Geochimica et Cosmochimica Acta 56, 419-430.

Rose, K.A., Cowan, J.H., Winemiller, K.O., Myers, R.A. and Hilborn, R. (2001) Compensatory density dependence in fish populations: importance, controversy, understanding and prognosis. Fish and Fisheries 2, 293-327.

Rosenfeld, J., Van Leeuwen, T., Richards, J. and Allen, D. (2015) Relationship between growth and standard metabolic rate: measurement artefacts and implications for habitat use and life-history adaptation in salmonids. Journal of Animal Ecology 84, 4-20.

Rosenfeld, J.S., Leiter, T., Lindner, G. and Rothman, L. (2005) Food abundance and fish density alters habitat selection, growth, and habitat suitability curves for juvenile coho salmon (*Oncorhynchus kisutch*). Canadian Journal of Fisheries and Aquatic Sciences 62, 1691-1701.

Rubenstein, D.R. and Hobson, K.A. (2004) From birds to butterflies: animal movement patterns and stable isotopes. Trends in Ecology & Evolution 19, 256-263.

Rungruangsak-Torrissen, K., Pringle, G., Moss, R. and Houlihan, D. (1998) Effects of varying rearing temperatures on expression of different trypsin isozymes, feed conversion efficiency and growth in Atlantic salmon (shape *Salmo salar* L.). Fish Physiology and Biochemistry 19, 247-255.

Saunders, R.J., Fowler, A.J. and Gillanders, B.M. (2012) The spawning dynamics of snapper (*Chrysophrys auratus*) in northern Spencer Gulf, South Australia. N. Z. J. Marine and Freshwater Research. 46, 491-510.

Schmittner, A., Gruber, N., Mix, A.C., Key, R.M., Tagliabue, A. and Westberry, T.K. (2013) Biology and air-sea gas exchange controls on the distribution of carbon isotope ratios ($\delta^{13}C$) in the ocean. Biogeosciences 10, 5793-5816.

Schöne, B.R., Schmitt, K. and Maus, M. (2017) Effects of sample pretreatment and external contamination on bivalve shell and Carrara marble $\delta^{18}O$ and $\delta^{13}C$ signatures. Palaeogeography, Palaeoclimatology, Palaeoecology 484, 22-32.

Schöne, B.R., Wanamaker Jr, A.D., Fiebig, J., Thébault, J. and Kreutz, K. (2011) Annually resolved $\delta^{13}C$ shell chronologies of long-lived bivalve mollusks (*Arctica islandica*) reveal oceanic carbon dynamics in the temperate North Atlantic during recent centuries. Palaeogeography, Palaeoclimatology, Palaeoecology 302, 31-42.

Schulte, P.M., Healy, T.M. and Fangue, N.A. (2011) Thermal performance curves, phenotypic plasticity, and the time scales of temperature exposure. Integrative and Comparative Biology 51, 691-702.

Schwarcz, H.P. (1991) Some theoretical aspects of isotope paleodiet studies. Journal of Archaeological Science 18, 261-275.

Schwarcz, H.P., Gao, Y., Campana, S., Browne, D., Knyf, M. and Brand, U. (1998) Stable carbon isotope variations in otoliths of Atlantic cod (*Gadus morhua*). Canadian Journal of Fisheries and Aquatic Sciences 55, 1798-1806.

Sebens, K.P. (1987) The ecology of indeterminate growth in animals. Annual Review of Ecology and Systematics 18, 371-407.

Shelton, A.O. and Mangel, M. (2011) Fluctuations of fish populations and the magnifying effects of fishing. Proceedings of the National Academy of Sciences of the United States of America. 108, 7075-7080.

Shelton, P.A. and Healey, B.P. (1999) Should depensation be dismissed as a possible explanation for the lack of recovery of the northern cod (*Gadus morhua*) stock? Canadian Journal of Fisheries and Aquatic Sciences 56, 1521-1524.

Shephard, S., Trueman, C., Rickaby, R. and Rogan, E. (2007) Juvenile life history of NE Atlantic orange roughy from otolith stable isotopes. Deep Sea Research Part I: Oceanographic Research Papers 54, 12211230.

Sherwood, G.D. and Rose, G.A. (2003) Influence of swimming form on otolith $\delta^{13}C$ in marine fish. Marine Ecology Progress Series 258, 283-289.

Shirai, K., Otake, T., Amano, Y., Kuroki, M., Ushikubo, T., Kita, N.T., Murayama, M., Tsukamoto, K. and Valley, J.W. (2018) Temperature and depth distribution of Japanese eel eggs estimated using otolith oxygen stable isotopes. Geochimica et Cosmochimica Acta 236, 373-383.

Skinner, M.M., Martin, A.A. and Moore, B.C. (2016) Is lipid correction necessary in the stable isotope analysis of fish tissues? Rapid Communications in Mass Spectrometry 30, 881-889.

Smith, P.J., Francis, R.I.C.C. and McVeagh, M. (1991) Loss of genetic diversity due to fishing pressure. Fisheries Research. 10, 309-316.

Smoliński, S. and Mirny, Z. (2017) Otolith biochronology as an indicator of marine fish responses to hydroclimatic conditions and ecosystem regime shifts. Ecological Indicators 79, 286-294.

Solomon, C.T., Weber, P.K., Cech, J.J.J., Ingram, B.L., Conrad, M.E., Machavaram, M.V., Pogodina, A.R. and Franklin, R.L. (2006) Experimental determination of the sources of otolith carbon and associated isotopic fractionation. Canadian Journal of Fisheries and Aquatic Sciences 63, 79-89.

Steffensen, J.F. (1989) Some errors in respirometry of aquatic breathers: How to avoid and correct for them. Fish Physiology and Biochemistry 6, 49-59.

Stephens, P.A. and Sutherland, W.J. (1999) Consequences of the Allee effect for behaviour, ecology and conservation. Trends in Ecology & Evolution 14, 401-405.

Sturrock, A.M., Hunter, E., Milton, J.A., Johnson, R.C., Waring, C.P. and Trueman, C.N. (2015) Quantifying physiological influences on otolith microchemistry. Methods in Ecology and Evolution 6, 806-816.

Sturrock, A.M., Trueman, C.N., Milton, J.A., Waring, C.P., Cooper, M.J. and Hunter, E. (2014) Physiological influences can outweigh environmental signals in otolith microchemistry research. Marine Ecology Progress Series 500, 245-264.

Sturrock, A.M., Trueman, C.N., Darnaude, A.M. and Hunter, E. (2012) Can otolith elemental chemistry retrospectively track migrations in fully marine fishes? Journal of Fish Biology 81, 766-795.

Svendsen, M.B.S., Bushnell, P.G. and Steffensen, J.F. (2016) Design and setup of intermittent-flow respirometry system for aquatic organisms. Journal of Fish Biology 88, 26-50.

Swain, D.P., Sinclair, A.F. and Mark Hanson, J. (2007) Evolutionary response to size-selective mortality in an exploited fish population. Proceedings of the Royal Society B: Biological Sciences 274, 10151022.

Sweeting, C., Barry, J., Polunin, N. and Jennings, S. (2007) Effects of body size and environment on diet tissue δ^{13}C fractionation in fishes. Journal of Experimental Marine Biology and Ecology 352, 165176.

Team, R.D.C. (2014) R: A language and environment for statistical computing. R Foundation for Statistical Computing, Vienna.

Thomas, O.R., Ganio, K., Roberts, B.R. and Swearer, S.E. (2017) Trace element–protein interactions in endolymph from the inner ear of fish: implications for environmental reconstructions using fish otolith chemistry. Metallomics 9, 239-249.

Thorarensen, H., Gallaugher, P.E. and Farrell, A.P. (1996) The limitations of heart rate as a predictor of metabolic rate in fish. Journal of Fish Biology 49, 226-236.

Thorrold, S.R., Campana, S.E., Jones, C.M. and Swart, P.K. (1997) Factors determining δ^{13}C and δ^{18}O fractionation in aragonitic otoliths of marine fish. Geochimica et Cosmochimica Acta 61, 29092919.

Tohse, H. and Mugiya, Y. (2008) Sources of otolith carbonate: experimental determination of carbon incorporation rates from water and metabolic CO_2, and their diel variations. Aquatic Biology 1, 259-268.

Tohse, H., Ando, H. and Mugiya, Y. (2004) Biochemical properties and immunohistochemical localization of carbonic anhydrase in the sacculus of the inner ear in the salmon *Oncorhynchus masou*. Comparative Biochemistry and Physiology Part A: Molecular & Integrative Physiology 137, 87-94.

Tolkamp, B.J., Emmans, G.C., Yearsley, J. and Kyriazakis, I. (2002) Optimization of short-term animal behaviour and the currency of time. Animal Behaviour 64, 945-953.

Treberg, J.R., Killen, S.S., MacCormack, T.J., Lamarre, S.G. and Enders, E.C. (2016) Estimates of metabolic rate and major constituents of metabolic demand in fishes under field conditions: Methods, proxies, and new perspectives. Comparative Biochemistry and Physiology Part A: Molecular & Integrative Physiology 202, 10-22.

Trippel, E.A. (1998) Egg size and viability and seasonal offspring production of young Atlantic cod. Transactions of the American Fisheries Society 127, 339-359.

Trudel, M. and Rasmussen, J.B. (2006) Bioenergetics and mercury dynamics in fish: a modelling perspective. Canadian Journal of Fisheries and Aquatic Sciences 63, 1890-1902.

Trueman, C.N., Chung, M.-T. and Shores, D. (2016) Ecogeochemistry potential in deep time biodiversity illustrated using a modern deep-water case study. Philosophical Transactions of the Royal Society B: Biological Sciences 371.

Trueman, C.N., Rickaby, R.E.M. and Shephard, S. (2013) Thermal, trophic and metabolic life histories of inaccessible fishes revealed from stable- isotope analyses: a case study using orange roughy *Hoplostethus atlanticus*. Journal of Fish Biology 83, 1613-1636.

Van de Pol, M. and Wright, J. (2009) A simple method for distinguishing within-versus between-subject effects using mixed models. Animal Behaviour 77, 753-758.

van der Walt, B. and Faragher, R.A. (2003) Otolith marking of rainbow trout fry by immersion in low concentrations of alizarin complexone. North American Journal of Fisheries Management 23, 141148.

Venturelli, P.A., Shuter, B.J. and Murphy, C.A. (2009) Evidence for harvest-induced maternal influences on the reproductive rates of fish populations. Proceedings of the Royal Society B: Biological Sciences 276, 919-924.

Wada, E., Mizutani, H. and Minagawa, M. (1991) The use of stable isotopes for food web analysis. Critical Reviews in Food Science and Nutrition 30, 361-371.

Wakefield, C.B., Potter, I.C., Hall, N.G., Lenanton, R.C. and Hesp, S.A. (2017) Timing of growth zone formations in otoliths of the snapper, *Chrysophrys auratus*, in subtropical and temperate waters differ and growth follows a parabolic relationship with latitude. ICES Journal of Marine Science 74, 180-192.

Walters, C. and Kitchell, J.F. (2001) Cultivation/depensation effects on juvenile survival and recruitment: implications for the theory of fishing. Canadian Journal of Fisheries and Aquatic Sciences 58, 3950.

Walther, B.D. and Thorrold, S.R. (2006) Water, not food, contributes the majority of strontium and barium deposited in the otoliths of a marine fish. Marine Ecology Progress Series 311, 125-130.

Wang, T. and Overgaard, J. (2007) The heartbreak of adapting to global warming. Science 315, 49.

Watanabe, F., Alcântara, E., Rodrigues, T., Imai, N., Barbosa, C. and Rotta, L. (2015) Estimation of chlorophyll-*a* concentration and the trophic state of the Barra Bonita hydroelectric reservoir using OLI/landsat-8 images. International Journal of Environmental Research and Public Health 12, 10391.

Watanabe, S., Kodama, M. and Fukuda, M. (2009) Nitrogen stable isotope ratio in the manila clam, *Ruditapes philippinarum*, reflects eutrophication levels in tidal flats. Marine Pollution Bulletin 58, 1447-1453.

Webb, S.D., Woodcock, S.H. and Gillanders, B.M. (2012) Sources of otolith barium and strontium in estuarine fish and the influence of salinity and temperature. Marine Ecology Progress Series 453, 189-199.

Wei, T., and Simko, V. (2017). R package "corrplot": Visualization of a Correlation Matrix (Version 0.84). Available from https://github.com/taiyun/corrplot.

Weidman, C.R. and Millner, R. (2000) High-resolution stable isotope records from North Atlantic cod. Fish Res. 46, 327-342.

Weisberg, S. (1993) Using hard-part increment data to estimate age and environmental effects. Canadian Journal of Fisheries and Aquatic Sciences 50, 1229-1237.

Weisberg, S., Spangler, G. and Richmond, L.S. (2010) Mixed effects models for fish growth. Canadian Journal of Fisheries and Aquatic Sciences 67, 269-277.

Whitledge, G.W. (2009) Otolith microchemistry and isotopic composition as potential indicators of fish movement between the Illinois River drainage and Lake Michigan. Journal of Great Lakes Research 35, 101-106.

Wikelski, M. and Cooke, S.J. (2006) Conservation physiology. Trends in Ecology & Evolution 21, 38-46.

Woodcock, S.H., Munro, A.R., Crook, D.A. and Gillanders, B.M. (2012) Incorporation of magnesium into fish otoliths: Determining contribution from water and diet. Geochim. Cosmochim. Acta 94, 12-21.

Woodson, L. E., Wells B. K., Grimes C. B., Franks R. P., Santora J. A., and Carr. M. H. (2013) Water and otolith chemistry identify exposure of juvenile rockfish to upwelled waters in an open coastal system. Marine Ecology Progress Series 473:261-273.

Worm, B. (2016) Averting a global fisheries disaster. Proceedings of the National Academy of Sciences 113, 4895-4897.

Wright, K. (2012) corrgram: Plot a correlogram. R package version 1.

Wright, P.J., Régnier, T., Gibb, F.M., Augley, J. and Devalla, S. (2018) Assessing the role of ontogenetic movement in maintaining population structure in fish using otolith microchemistry. Ecology and Evolution 8, 7907-7920.

Wurster, C., and Patterson, W. (2003). Metabolic rate of late Holocene freshwater fish: Evidence from $\delta^{13}C$ values of otoliths. Paleobiology, 29(4), 492-505.

Wurster, C.M., Patterson, W.P., Stewart, D.J, Bowlby, J.N., and Stewart, T.J. (2005). Thermal histories, stress, and metabolic rates of chinook salmon (*Oncorhynchus tshawytscha*) in Lake Ontario: evidence from intra-otolith stable isotope analyses. Canadian Journal of Fisheries and Aquatic Sciences 62, 700713.

Zuur, A., Ieno, E., Walker, N., Saveliev, A. and Smith, G. (2009) Mixed effects models and extensions in ecology with R. Springer, New York, NY.

SUPPLEMENTARY INFORMATION

SUPPLEMENTARY INFORMATION S2

CHAPTER TWO – Using otolith chronologies to understand long-term trends and drivers of growth in fisheries

GRAPHICAL ABSTRACT

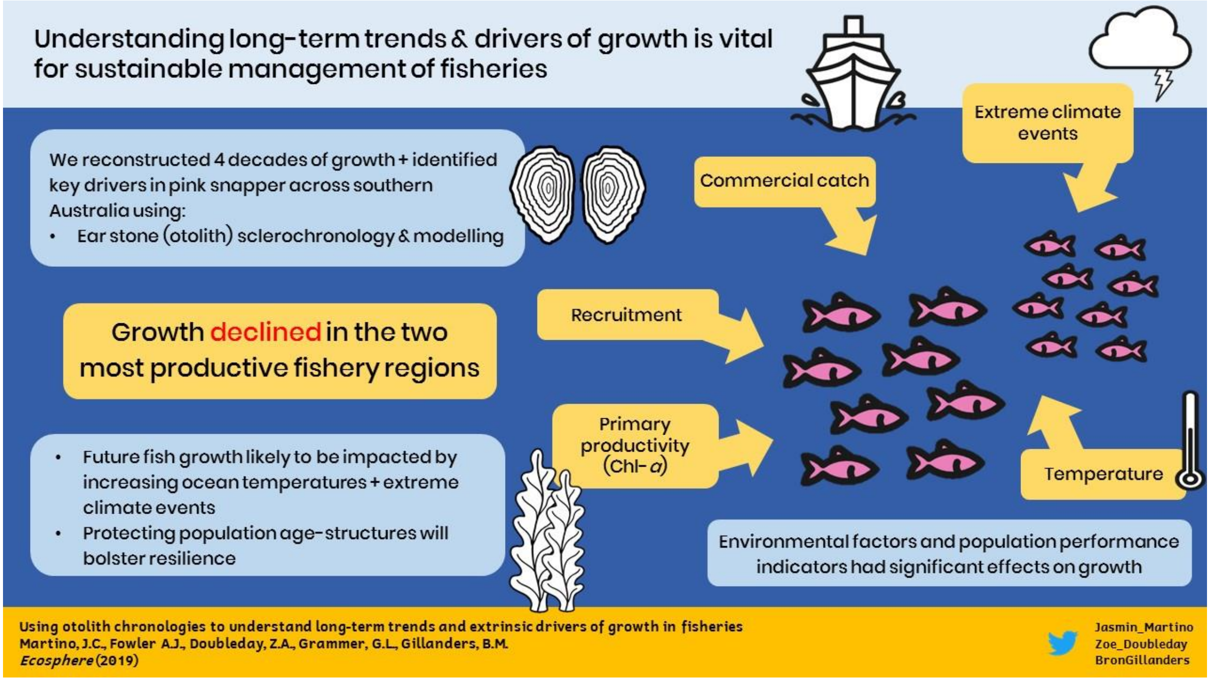

Understanding long-term trends & drivers of growth is vital for sustainable management of fisheries

We reconstructed 4 decades of growth + identified key drivers in pink snapper across southern Australia using:

- Ear stone (otolith) sclerochronology & modelling

Growth declined in the two most productive fishery regions

- Future fish growth likely to be impacted by increasing ocean temperatures + extreme climate events
- Protecting population age-structures will bolster resilience

Environmental factors and population performance indicators had significant effects on growth

Using otolith chronologies to understand long-term trends and extrinsic drivers of growth in fisheries
Martino, J.C., Fowler A.J., Doubleday, Z.A., Grammer, G.L., Gillanders, B.M.
***Ecosphere* (2019)**

Jasmin_Martino
Zoe_Doubleday
BronGillanders

APPENDIX S2.1 - REGIONAL SPECIFIC RESULTS

Northern Gulf St Vincent

The Northern Gulf St Vincent (NGSV) region had high levels of SST, chl-*a* (productivity) and Catch. Growth of snapper significantly decreased from 2000. SST, productivity and recruitment were positively correlated with growth while catch was negatively correlated. Growth declines aligned with periods of high catch in years 2005 - 2015. SOI was found to decrease growth at index extremes (El Niño and La Niña events). Depensatory density-dependent effects on growth were apparent.

Northern Spencer Gulf

Northern Spencer Gulf (NSG) experienced high productivity, SST and Catch. Snapper growth in NSG declined through the chronology. SST, productivity and Catch were significant drivers that increased growth while recruitment decreased growth. Growth declines particularly aligned with periods of high catch from years 1979 - 2004. Snapper in NSG were strongly influenced by the high temperatures and the fish are likely near their optimum thermal maxima, which limits growth. Contrasting within-individual and among–individual variation in SST coefficients are likely explained by genetic differences or individual-specific past experiences. Compensatory density-dependent effects on growth were apparent.

South East

The South East (SE) experienced the lowest SST and productivity and also low catch levels. Growth significantly fluctuated from year to year and there was no significant temporal trend. SST and productivity increased growth. While SST were low, it had significant effects on growth and it is likely SE fish are near the beginning of their thermal performance curve. High growth synchrony may have been driven by strong climate signal, characterized by distinctive cold-water climate with high upwelling.

West Coast

The West Coast (WC) experienced moderate levels of SST and low levels of productivity and catch. High variation in growth trends were found through the chronology. SST and productivity increased growth. SOI was found to decrease growth at index extremes (El Niño and La Niña events). Low growth synchrony and high growth variation may indicate that WC is less influenced by broad climatic drivers and more driven by microhabits or small-scale population dynamics.

SUPPLEMENTARY INFORMATION S2 – TABLES

Table S2.1 - Optimal fixed effects structure, random effects structure and environmental drivers of growth for the whole South Australian region (broad-scale), separated into Annual and Seasonal measurements. Random slope term is indicated by x **|** y, nested terms are indicated by x:y and inclusion of lagged (by one month) environmental variable is indicated by an asterix.

Region	Fixed effects	Random effects	Environmental Drivers
Annual			
Broad-scale	Age	Age|FishID, Age|Region:Year, 1|Region, Age|Region:Cohort	Chl-*a** x SST
Seasonal			
Broad-scale	sAge + sAgeCap	sAge|FishID, sAge|Season, 1|Region	Chl-*a** x SST*

Table S2.2 - Indications of significant temporal trends for environmental variables by linear regression. Significant values are indicated in **bold**.

Variable	F	DF*1*	DF2	R^2	*p*
SST					
NGSV	2.34	1	22	0.06	0.14
NSG	1.47	1	22	0.02	0.24
SE	3.95	1	22	0.11	0.06
WC	1.263	1	22	0.011	0.27
Chl-*a*					
NGSV	4.22	1	14	0.18	0.06
NSG	5.5	1	14	0.23	**0.03**
SE	6.8	1	14	0.28	**0.02**
WC	7.3	1	14	0.29	**0.017**
SOI					
Broad	2.364	1	36	0.04	0.13
Catch					
NGSV	40.63	1	31	0.55	**4.25E-07**
NSG	18.31	1	31	0.35	**0.00017**
SE	9.327	1	31	0.21	**0.005**
WC	3.021	1	31	0.06	0.092
Recruitment					
NGSV	0.054	1	24	-0.04	0.8
NSG	2.396	1	28	0.05	0.13
SE	0.2398	1	16	-0.05	0.63

Table S2.3 - Predicted effects of extrinsic predictors on snapper growth across a range and per extrinsic unit for Annual and Seasonal models.

	Extrinsic factor	**Region**	**Predictor range**		**Growth predicted effects (%)**	
			MIN	**MAX**	**Across range**	**Per unit**
ANNUAL	**SST**	**Broad**	16.58	17.76	5.34	4.54
		NGSV	16.90	17.84	12.85	13.73
		NSG	17.60	18.43	1.28	1.54
		SE	15.06	16.65	33.92	21.35
		WC	16.51	18.13	5.306	3.29
	Chl-*a*	**Broad**	1.702	2.72	18.98	18.52
		NGSV	2.73	4.37	21.66	13.19
		NSG	2.95	4.46	9.19	6.085
		SE	0.443	1.12	34.26	50.26
		WC	0.60	1.12	25.94	49.94
	SOI	**Broad**	-13.83	13.64	10.49	0.38
		NGSV	-13.83	13.64	16.63	0.60
		WC	-11.93	13.3	17.69	0.70
	Catch	**Broad**	194.97	911.47	20.45	0.028
		NGSV	9.07	416.45	25.73	0.063
		NSG	46.28	360.41	9.50	0.030
	Recruitment	**NGSV**	-2.46	1.64	2.43	0.59
		NSG	-1.51	1.25	1.15	0.41
		SE	-0.70	1.34	4.33	2.11
SEASONAL	**SST**	**Broad**	13.71	20.64	245.54	35.45
		NGSV	13.29	21.48	219.79	26.85
		NSG	13.81	22.43	178.03	20.64
		SE	13.35	18.05	253.98	54.042
		WC	14.59	20.06	305.00	55.75
	Chl-*a*	**Broad**	1.430	3.56	220.71	103.25
		NGSV	2.35	6.68	134.68	31.16
		NSG	2.45	5.88	75.85	22.12
		SE	0.38	1.72	33.87	25.44
		WC	1.09	1.72	99.85	158.02
	SOI	**NGSV**	-24.2	21.4	37.42	0.820

Table S2.4 - Output summary for selection of best random effects and best extrinsic fixed effects structures for snapper growth in the broad South Australia region (All), Northern Gulf St Vincent (NGSV), Northern Spencer Gulf (NSG), South East (SE) and West Coast (WC).

	Region	**Model #**	**Random effects structure**	**AICc**	**R^2 (C)**	**R^2 (M)**
ANNUAL	**ALL**	M5g	(Age|FishID) + (Age|Region:Year) + (1|Region) + (Age|Region:Cohort)	2137.69	0.845	0.7625
	NGSV	M4d	(Age|FishID) + (Age|Year) + (Age|Cohort)	622.75	0.8507	0.7930
	NSG	M4d	(Age|FishID) + (Age|Year) + (Age|Cohort)	721.86	0.8526	0.7462
	SE	M4d	(Age|FishID) + (Age|Year) + (Age|Cohort)	224.59	0.8502	0.7891
	WC	M4d	(Age|FishID) + (Age|Year) + (Age|Cohort)	529.32	0.7984	0.7288
SEASONAL	**ALL**	M4b	(iAge.seas|FishID) + (iAge|Season) + (1|Region)	4523.89	0.9067	0.4517
	NGSV	M3a	(Age|FishID) + (Age|Year)	1447.54	0.9202	0.5031
	NSG	M3a	(Age|FishID) + (Age|Year)	1740.80	0.9214	0.4604
	SE	M3a	(Age|FishID) + (Age|Year)	147.65	0.9187	0.5355
	WC	M3a	(Age|FishID) + (Age|Year)	1525.16	0.8864	0.4740
	Region	**Model #**	**Extrinsic fixed effects structure**	**AICc**	**R^2 (C)**	**R^2 (M)**
ANNUAL	**ALL**	e11	SST * Chl-*a*(l)	992.27	0.7762	0.8507
	NGSV	e27	Recruitment * Chl-*a*	162.88	0.8829	0.9235
	NSG	e30	Recruitment * Chl-*a*(l)	167.29	0.6373	0.8171
	SE	e27	Recruitment * Chl-*a*	114.79	0.6752	0.8248
	WC	e3	Chl-*a*	295.73	0.7979	0.8477
SEASONAL	**ALL**	e18	SST(l) * Chl-*a*(l)	1480.43	0.7830	0.9086
	NGSV	e18	SST(l) * Chl-*a*(l)	86.30	0.8290	0.9426
	NSG	e11	SST * Chl-*a*(l)	509.39	0.6454	0.9063
	SE	e8	SST * Chl-*a*	-65.63	0.7960	0.8952
	WC	e13	Chl-*a* * SST(l)	607.71	0.7524	0.9231

Table S2.5 - Selection of optimal random effects structures (highlighted in **bold**) in annually resolved models. Random slope term designated with x **|** y. Nested terms designated by x : y.

Region	Model #	Random effects structure	AICc	R^2 (C)	R^2 (M)
All	M1a	(1|FishID)	3238.12	0.7983	0.7519
	M1b	(Age|FishID)	2651.51	0.8126	0.7603
	M2a	(Age|FishID) + (1|Year)	2473.34	0.8261	0.7428
	M2b	(Age|FishID) + (1|Cohort)	2618.46	0.8131	0.7556
	M3a	(Age|FishID) + (Age|Year)	2404.25	0.8131	0.6831
	M3b	(Age|FishID) + (Age|Cohort)	2537.33	0.8448	0.8023
	M5a	(Age|FishID) + (1|Region:Year) + (1|Region) + (1|Region:Cohort)	2371.48	0.8383	0.7317
	M5b	(Age|FishID) + (Age|Region:Year) + (Age|Region) + (Age|Region:Cohort)	2141.71	0.8448	0.7625
	M5c	(Age|FishID) + (Age|Region:Year) + (1|Region) + (1|Region:Cohort)	2279.25	0.8345	0.7121
	M5d	(Age|FishID) + (1|Region:Year) + (Age|Region) + (1|Region:Cohort)	2369.31	0.8363	0.7353
	M5e	(Age|FishID) + (1|Region:Year) + (1|Region) + (Age|Region:Cohort)	2258.24	0.8511	0.7581
	M5f	(Age|FishID) + (Age|Region:Year) + (Age|Region) + (1|Region:Cohort)	2282.15	0.8332	0.715
	M5g	**(Age|FishID) + (Age|Region:Year) + (1|Region) + (Age|Region:Cohort)**	**2137.69**	**0.845**	**0.7625**
	M5h	(Age|FishID) + (1|Region:Year) + (Age|Region) + (Age|Region:Cohort)	2265.12	0.8497	0.7578
	M5i	(Age|FishID) + (Age|Region:Year) + (AgeCap|Region) + (Age|Region:Cohort)	2141.60	0.845	0.762
	M5j	(Age|FishID) + (1|Region:Year) + (AgeCap|Region) + (Age|Region:Cohort)	2262.22	0.8511	0.7584
	M5k	(Age|FishID) + (Age|Region:Year) + (AgeCap|Region) + (1|Region:Cohort)	2283.10	0.8346	0.7117
	M5l	(Age|FishID) + (1|Region:Year) + (AgeCap|Region) + (1|Region:Cohort)	2375.46	0.8383	0.732
NGSV	M1a	(1|FishID)	952.63	0.8320	0.8001
	M1b	(Age|FishID)	762.13	0.8404	0.8066
	M2a	(Age|FishID) + (1|Year)	722.25	0.8483	0.7793
	M2b	(Age|FishID) + (1|Cohort)	752.09	0.8411	0.8070
	M3a	(Age|FishID) + (Age|Year)	704.26	0.8445	0.7308
	M3b	(Age|FishID) + (Age|Cohort)	734.89	0.8444	0.8115
	M4a	(Age|FishID) + (1|Year) + (1|Cohort)	718.09	0.8484	0.7739
	M4b	(Age|FishID) + (Age|Year) + (1|Cohort)	693.99	0.8445	0.7217
	M4c	(Age|FishID) + (1|Year) + (Age|Cohort)	687.70	0.8608	0.7620
	M4d	**(Age|FishID) + (Age|Year) + (Age|Cohort)**	**622.75**	**0.8507**	**0.7930**
NSG	M1a	(1|FishID)	1024.93	0.8164	0.7620
	M1b	(Age|FishID)	808.72	0.8300	0.7518
	M2a	(Age|FishID) + (1|Year)	790.018	0.8409	0.7105
	M2b	(Age|FishID) + (1|Cohort)	809.97	0.8298	0.7514
	M3a	(Age|FishID) + (Age|Year)	771.23	0.8348	0.6770
	M3b	(Age|FishID) + (Age|Cohort)	755.98	0.8512	0.7872
	M4a	(Age|FishID) + (1|Year) + (1|Cohort)	784.18	0.8437	0.6590
	M4b	(Age|FishID) + (Age|Year) + (1|Cohort)	767.90	0.8365	0.6519
	M4c	(Age|FishID) + (1|Year) + (Age|Cohort)	739.23	0.8628	0.7652
	M4d	**(Age|FishID) + (Age|Year) + (Age|Cohort)**	**721.86**	**0.8526**	**0.7462**
SE	M1a	(1|FishID)	467.04	0.7721	0.7056
	M1b	(Age|FishID)	419.00	0.7754	0.7230
	M2a	(Age|FishID) + (1|Year)	267.63	0.8384	0.7644
	M2b	(Age|FishID) + (1|Cohort)	403.23	0.7848	0.6935
	M3a	(Age|FishID) + (Age|Year)	226.38	0.8373	0.7684
	M3b	(Age|FishID) + (Age|Cohort)	393.64	0.8134	0.7595
	M4a	(Age|FishID) + (1|Year) + (1|Cohort)	259.78	0.8418	0.7433
	M4b	(Age|FishID) + (Age|Year) + (1|Cohort)	227.74	0.8362	0.7576
	M4c	(Age|FishID) + (1|Year) + (Age|Cohort)	242.70	0.8524	0.7901
	M4d	**(Age|FishID) + (Age|Year) + (Age|Cohort)**	**224.59**	**0.8502**	**0.7891**
WC	M1a	(1|FishID)	600.97	0.7460	0.6990
	M1b	(Age|FishID)	555.51	0.7618	0.7078
	M2a	(Age|FishID) + (1|Year)	544.17	0.7781	0.7075
	M2b	(Age|FishID) + (1|Cohort)	557.43	0.7621	0.7076

M3a	(Age|FishID) + (Age|Year)	530.51	0.7898	0.7150
M3b	(Age|FishID) + (Age|Cohort)	556.91	0.7782	0.7289
M4a	(Age|FishID) + (1|Year) + (1|Cohort)	546.220	0.7781	0.7075
M4b	(Age|FishID) + (Age|Year) + (1|Cohort)	532.15	0.7894	0.7133
M4c	(Age|FishID) + (1|Year) + (Age|Cohort)	548.73	0.7885	0.7179
M4d	**(Age|FishID) + (Age|Year) + (Age|Cohort)**	**529.326804**	**0.7984**	**0.7288**

Table S2.6 - Selection of optimal random effects structures (highlighted in **bold**) in seasonally resolved models. Random slope term designated with x **\|** y.

Region	Model #	Random effects structure	AICc	R^2 (C)	R^2 (M)
All	M1a	(1|FishID)	29589.97	0.6383	0.6069
	M1b	(iAge.seas|FishID)	28918.39	0.6261	0.5897
	M2a	(iAge.seas|FishID) + (1|Season)	5221.38	0.9084	0.4748
	M3a	(iAge.seas|FishID) + (Age|Season)	4564.73	0.9045	0.4557
	M4a	(iAge.seas|FishID) + (1|Season) + (1|Region)	5178.79	0.9117	0.4643
	M4b	**(iAge.seas|FishID) + (iAge|Season) + (1|Region)**	**4523.89**	**0.9067**	**0.4517**
NGSV	M1a	(1|FishID)	8290.86	0.6907	0.6671
	M1b	(Age|FishID)	8070.06	0.6761	0.6508
	M2a	(Age|FishID) + (1|Season)	1644.96	0.9249	0.4734
	M3a	**(Age|FishID) + (Age|Year)**	**1447.54**	**0.9202**	**0.5031**
NSG	M1a	(1|FishID)	8879.66	0.6664	0.6307
	M1b	(Age|FishID)	8659.62	0.6421	0.5843
	M2a	(Age|FishID) + (1|Season)	1843.021	0.9197	0.4448
	M3a	**(Age|FishID) + (Age|Year)**	**1740.80**	**0.9214**	**0.4604**
SE	M1a	(1|FishID)	7152.44	0.5448	0.5137
	M1b	(Age|FishID)	7101.36	0.5510	0.5250
	M2a	(Age|FishID) + (1|Season)	362.60	0.9140	0.5240
	M3a	**(Age|FishID) + (Age|Year)**	**147.65**	**0.9187**	**0.5355**
WC	M1a	(1|FishID)	5103.21	0.5857	0.5504
	M1b	(Age|FishID)	5021.43	0.5954	0.5564
	M2a	(Age|FishID) + (1|Season)	1599.33	0.8842	0.4574
	M3a	**(Age|FishID) + (Age|Year)**	**1525.16**	**0.8864**	**0.4740**

Table S2.7 - Selection of extrinsic covariate fits (highlighted in **bold**) in annually and seasonal models. Selection of base model indicates there is a lack of evidence that the extrinsic factor affects fish growth.

	Region	Fit	AICC
SST			
ANNUAL	**NGSV**	Base	614.2
		Linear	475.4
		Curvilinear	**473.3**
	NSG	Base	712.4
		Linear	**551.6**
		Curvilinear	552.4
	SE	Optimal	214.2
		Linear	**201.4**
		Curvilinear	203.5
	WC	Optimal	529.3
		Linear	**528.1**
		Curvilinear	529.3
SEASONAL	**NGSV**	Base	1433.4
		Linear	804.8
		Curvilinear	**766.6**
	NSG	Base	1433.4
		Linear	1121.6
		Curvilinear	**1091.3**
	SE	Base	137.5
		Linear	**0.6485**
		Curvilinear	1.770
	WC	Base	1515.81
		Linear	1426.63
		Curvilinear	**1421.07**
Chl-*a*			
ANNUAL	NGSV	Base	614.23
		Linear	289.58
		Curvilinear	**287.91**
	NSG	Base	712.43
		Linear	**235.82**
		Curvilinear	237.20
	SE	Base	214.25
		Linear	162.35
		Curvilinear	**161.63**
	WC	Base	529.32
		Linear	**295.73**
		Curvilinear	297.83
SEASONAL	**NGSV**	Base	1433.45
		Linear	164.31
		Curvilinear	**162.70**
	NSG	Base	1433.45
		Linear	541.08
		Curvilinear	**539.91**
	SE	Optimal	137.56
		Linear	**13.91**
		Curvilinear	14.52
	WC	Base	1515.80
		Linear	**675.60**
		Curvilinear	677.53
SOI			
ANNUAL	**NGSV**	Base	614.23
		Linear	615.71
		Curvilinear	**611.92**
	NSG	**Base**	**712.43**
		Linear	713.93
		Curvilinear	715.97
	SE	**Base**	**214.25**
		Linear	216.27
		Curvilinear	217.14
	WC	Base	529.32
		Linear	531.35
		Curvilinear	**524.78**
SEASONAL	**NGSV**	Base	1433.45
		Linear	1435.35
		Curvilinear	**1432.23**
	NSG	**Base**	**1433.45**
		Linear	1728.64
		Curvilinear	1728.83

	SE	**Base**	**137.56**
		Linear	139.48
		Curvilinear	143.31
	WC	Optimal	1515.80
		Linear	**675.60**
		Curvilinear	677.53
Recruitment			
ANNUAL	NGSV	Base	614.23
		Linear	**448.61**
		Curvilinear	450.26
	NSG	Base	712.43
		Linear	**633.24**
		Curvilinear	635.04
	SE	Optimal	214.25
		Linear	**157.18**
		Curvilinear	158.11
	NGSV	Base	614.23
Catch			
ANNUAL		**Linear**	**575.64**
		Curvilinear	576.26
	NSG	Base	712.43
		Linear	**648.91**
		Curvilinear	650.94
	SE	**Base**	**214.25**
		Linear	216.12
		Curvilinear	216.98
	WC	**Base**	**529.32**
		Linear	530.28
		Curvilinear	530.43

Table S2.8 - Selection for best extrinsic variable (highlighted in **bold**) for annually resolved models. Inclusion of a lagged term is indicated by (l). Blank rows indicate interactions that were removed from comparison due to significant correlation (linear regression = *p*>0.05) between terms.

Region	Model #	Fixed Effects Structure	AICc	R^2 (C)	R^2 (M)
All	e1	Growth – optimal base model	2127.2	0.7643	0.8445
	e2	SST	1823.56	0.7878	0.8622
	e3	Chl-*a*	995.17	0.7740	0.8513
	e4	SOI	2128.42	0.7630	0.8446
	e33	Catch	2026	0.7806	0.8497
	e5	SST(l)	1822.9	0.7881	0.8621
	e6	Chl-*a*(l)	993.05	0.7752	0.8515
	e7	SOI(l)	2128.2	0.7635	0.8447
	e8	SST * Chl-*a*	992.89	0.7754	0.8504
	e9	SST * SOI	1827.3	0.7869	0.8619
	e10	Chl-*a* * SOI			
	e11	**SST *** Chl-*a***(l)**	**992.27**	**0.7762**	**0.8507**
	e12	SST * SOI(l)	1827.4	0.7869	0.8620
	e13	Chl-*a* * SST(l)	993.7	0.7751	0.8503
	e14	Chl-*a* * SOI(l)			
	e15	Chl-*a*(l) * SOI			
	e16	SST(l) * SOI	1825.6	0.7875	0.8618
	e17	SST(l) * SOI(l)	1826	0.7871	0.8618
	e18	SST(l) * Chl-*a*(l)	992.39	0.7761	0.8506
	e19	SOI(l) * Chl-*a*(l)			
	e20	Catch * SST	1809.8	0.7920	0.860893
	e21	Catch * Chl-*a*			
	e22	Catch * SOI			
	e23	Catch * SST(l)	1808.2	0.7916	0.8607
	e24	Catch * Chl-*a*(l)			
	e25	Catch * SOI (l)			
NGSV	e1	Growth – optimal base model	614.24	0.7941	0.8505
	e2	SST	475.46	0.8561	0.8991

	e3	Chl-*a*	289.58	0.8407	0.8994
	e4	SOI	615.71	0.7927	0.8503
	e32	Recruitment	448.61	0.7960	0.8499
	e33	Catch	575.64	0.8147	0.8651
	e5	SST(l)	474.4	0.8573	0.8995
	e6	Chl-*a*(l)	289.76	0.8406	0.9001
	e7	SOI(l)	615.11	0.7917	0.8503
	e8	SST * ClA.OC3M	287.99	0.8430	0.9068
	e9	SST * Chl-*a*	479.3	0.8562	0.8990
	e10	SST * SOI			
	e11	Chl-*a* * SOI	288.13	0.8434	0.9064
	e12	SST * Chl-*a*(l)	479.56	0.8561	0.8990
	e13	SST * SOI(l)	287.09	0.8422	0.9088
	e14	Chl-*a* * SST(l)			
	e15	Chl-*a* * SOI(l)	290.23	0.8419	0.9042
	e16	Chl-*a*(l) * SOI	477.53	0.8578	0.8996
	e17	SST(l) * SOI	478.08	0.8578	0.8995
	e18	SST(l) * SOI(l)	287.21	0.8428	0.9083
	e19	SST(l) * Chl-*a*(l)			
	e20	SOI(l) * Chl-*a*(l)	463.44	0.8542	0.8944
	e21	Catch * SST			
	e22	Catch * Chl-*a*	579.68	0.8144	0.8649
	e23	Catch * SOI	463.37	0.8551	0.8945
	e24	Catch * SST(l)			
	e25	Catch * Chl-*a*(l)	579.72	0.8148	0.8650
	e26	Catch * SOI (l)	345.11	0.8701	0.8995
	e27	**Recruitment * Chl-*a***	**162.88**	**0.8829**	**0.9235**
	e28	Recruitment * SOI	448.21	0.8125	0.8518
	e29	Recruitment * SST(l)	344.3	0.8706	0.8991
	e30	Recruitment * Chl-*a*(l)	163.7	0.8823	0.9238
	e31	Recruitment * SOI(l)	448.51	0.8112	0.8511
NSG	e1	Growth – optimal base model	712.43	0.7470	0.8523
	e2	SST	551.63	0.7812	0.8732
	e3	Chl-*a*	235.82	0.5116	0.7877
	e4	SOI	713.93	0.7541	0.8514
	e32	Recruitment	633.24	0.7198	0.8627
	e33	Catch	648.92	0.7980	0.8618
	e5	SST(l)	551.19	0.7845	0.8734
	e6	Chl-*a*(l)	235.28	0.5109	0.7872
	e7	SOI(l)	714.16	0.7528	0.8515
	e8	SST * ClA.OC3M	238.67	0.5106	0.7881
	e9	SST * Chl-*a*	553.8	0.7734	0.8742
	e10	SST * SOI			
	e11	Chl-*a* * SOI	239.63	0.5100	0.7871
	e12	SST * Chl-*a*(l)	553.41	0.7705	0.8742
	e13	SST * SOI(l)	239.16	0.5110	0.7883
	e14	Chl-*a* * SST(l)			
	e15	Chl-*a* * SOI(l)			
	e16	Chl-*a*(l) * SOI	553.64	0.7862	0.8746
	e17	SST(l) * SOI	557.66	0.8013	0.8722
	e18	SST(l) * SOI(l)	239.54	0.5098	0.7876
	e19	SST(l) * Chl-*a*(l)			
	e20	SOI(l) * Chl-*a*(l)	552.10	0.7931	0.8722
	e21	Catch * SST	240.17	0.5128	0.7880
	e22	Catch * Chl-*a*	652.17	0.7988	0.8622
	e23	Catch * SOI	551.75	0.7943	0.8724
	e24	Catch * SST(l)	239.56	0.5110	0.7885
	e25	Catch * Chl-*a*(l)	652.31	0.7985	0.8620
	e26	Catch * SOI (l)	476.11	0.7910	0.8854
	e27	Recruitment * Chl-*a*	167.82	0.6374	0.8152
	e28	Recruitment * SOI	636.58	0.7352	0.8609

	e29	Recruitment * SST(l)	475.94	0.7949	0.8857
	e30	Recruitment * Chl-*a*(l)	**167.29**	**0.6373**	**0.8171**
	e31	Recruitment * SOI(l)	636.70	0.7334	0.8611
SE	e1	Growth – optimal base model	214.26	0.7893	0.8496
	e2	SST	201.5	0.7801	0.8372
	e3	Chl-*a*	162.36	0.7604	0.8288
	e4	SOI	216.28	0.7881	0.8493
	e32	Recruitment	157.19	0.7633	0.8440
	e33	Catch	216.13	0.7919	0.8509
	e5	SST(l)	199.79	0.7796	0.8361
	e6	Chl-*a*(l)	161.93	0.7592	0.8261
	e7	SOI(l)	215.97	0.7851	0.8482
	e8	SST * ClA.OC3M	156.51	0.7548	0.8093
	e9	SST * Chl-*a*	204.82	0.7806	0.8358
	e10	SST * SOI			
	e11	Chl-*a* * SOI	156.28	0.7537	0.8080
	e12	SST * Chl-*a*(l)	204.58	0.7782	0.8345
	e13	SST * SOI(l)	152.66	0.7509	0.8038
	e14	Chl-*a* * SST(l)			
	e15	Chl-*a* * SOI(l)			
	e16	Chl-*a*(l) * SOI	201.55	0.7829	0.8346
	e17	SST(l) * SOI	201.56	0.7801	0.8332
	e18	SST(l) * SOI(l)	152.23	0.7465	0.7986
	e19	SST(l) * Chl-*a*(l)			
	e20	SOI(l) * Chl-*a*(l)	203.48	0.7881	0.8409
	e21	Catch * SST	163.68	0.7475	0.8235
	e22	Catch * Chl-*a*			
	e23	Catch * SOI	200.85	0.7888	0.8401
	e24	Catch * SST(l)	163.88	0.7461	0.8236
	e25	Catch * Chl-*a*(l)			
	e26	Catch * SOI (l)	152.05	0.7176	0.8215
	e27	**Recruitment * Chl-*a***	**114.79**	**0.6752**	**0.8248**
	e28	Recruitment * SOI	159.75	0.7600	0.8420
	e29	Recruitment * SST(l)	153.17	0.7608	0.8313
	e30	Recruitment * Chl-*a*(l)	114.94	0.6712	0.8266
	e31	Recruitment * SOI(l)	158.91	0.7570	0.840105
WC	e1	Growth – optimal base model	529.32	0.7288	0.7984
	e2	SST	528.18	0.7209	0.7920
	e3	**Chl-*a***	**295.73**	**0.7979**	**0.8477**
	e4	SOI	531.35	0.7291	0.7984
	e33	Catch	530.28	0.7310	0.7981
	e5	SST(l)	528.25	0.7210	0.7921
	e6	Chl-*a*(l)	296.64	0.7974	0.8476
	e7	SOI(l)	531.36	0.7291	0.7984
	e8	SST * Chl-*a*	295.80	0.8026	0.8508
	e9	SST * SOI	527.30	0.7288	0.7882
	e10	Chl-a * SOI	299.68	0.7989	0.8480
	e11	SST * Chl-*a*(l)	296.57	0.8023	0.8508
	e12	SST * SOI(l)	528.10	0.7291	0.7894
	e13	Chl-*a* * SST(l)	296.59	0.8008	0.8495
	e14	Chl-*a* * SOI(l)	299.96	0.7983	0.8479
	e15	Chl-*a*(l) * SOI	300.57	0.7984	0.8479
	e16	SST(l) * SOI	529.95	0.7255	0.7889
	e17	SST(l) * SOI(l)	530.38	0.7245	0.7894
	e18	SST(l) * Chl-*a*(l)	297.53	0.8004	0.8494
	e19	SOI(l) * Chl-*a*(l)	300.87	0.7976	0.8477
	e20	Catch * SST	530.84	0.7258	0.7912
	e21	Catch * Chl-*a*	299.12	0.7970	0.8466
	e22	Catch * SOI	533.10	0.7312	0.7962
	e23	Catch * SST(l)	531.06	0.7252	0.7912
	e24	Catch * Chl-*a*(l)	299.71	0.7966	0.8464

e25	Catch * SOI (l)	533.66	0.7308	0.7966

Table S2.9 - Selection for best extrinsic variable (highlighted in **bold**) for seasonally resolved models. Inclusion of a lagged term is indicated by (l). Blank rows indicate interactions that were removed from comparison due to significant correlation (linear regression = p>0.05) between terms.

Region	Model #	**Fixed Effects Structure**	**AICc**	**R^2 (C)**	**R^2 (M)**
ALL	e1	Growth – optimal base model	4523.89	0.4517	0.9067
	e2	SST	3473.74	0.6878	0.9101
	e3	Chl-*a*	1552.94	0.4916	0.9065
	e4	SOI	4534.97	0.4509	0.9069
	e5	SST(l)	3455.38	0.7073	0.9102
	e6	Chl-*a*(l)	1555.49	0.4754	0.9084
	e7	SOI(l)	4534.83	0.4538	0.9068
	e8	SST * Chl-*a*	1527.97	0.6918	0.9040
	e9	SST * SOI	3498.52	0.6855	0.9103
	e10	Chl-*a* * SOI	1570.72	0.4859	0.9077
	e11	SST * Chl-*a*(l)	1522.64	0.7077	0.9043
	e12	SST * SOI(l)	3499.00	0.6861	0.9103
	e13	Chl-*a* * SST(l)			
	e14	Chl-*a* * SOI(l)	1570.27	0.4951	0.9064
	e15	Chl-*a*(l) * SOI	1572.48	0.4753	0.9098
	e16	SST(l) * SOI	3480.34	0.7058	0.9104
	e17	SST(l) * SOI(l)	3480.47	0.7031	0.9101
	e18	**SST(l) * Chl-a(l)**	**1480.43**	**0.7830**	**0.9086**
	e19	SOI(l) * Chl-*a*(l)	1574.44	0.4727	0.9086
NGSV	e1	Growth – optimal base model	1433.45	0.5047	0.9199
	e2	SST	804.80	0.6923	0.9281
	e3	Chl-*a*	164.31	0.5824	0.9396
	e4	SOI	1435.35	0.5051	0.9200
	e5	SST(l)	780.023	0.7346	0.9279
	e6	Chl-*a*(l)	165.170	0.5793	0.9391
	e7	SOI(l)	1432.63	0.5115	0.9204
	e8	SST * Chl-*a*	125.400	0.7626	0.9406
	e9	SST * SOI	808.31	0.6938	0.9281
	e10	Chl-*a* * SOI	166.76	0.5879	0.9397
	e11	SST * Chl-*a*(l)			
	e12	SST * SOI(l)	808.24	0.6926	0.9281
	e13	Chl-*a* * SST(l)			
	e14	Chl-*a* * SOI(l)	168.24	0.5819	0.9397
	e15	Chl-*a*(l) * SOI	167.67	0.5853	0.9393
	e16	SST(l) * SOI	783.11	0.7356	0.9280
	e17	SST(l) * SOI(l)	783.60	0.7331	0.9279
	e18	**SST(l) * Chl-a(l)**	**86.30**	**0.8290**	**0.9426**
	e19	SOI(l) * Chl-*a*(l)	168.86	0.5805	0.9390
NSG	e1	Growth – optimal base model	1726.64	0.4621	0.9211
	e2	SST	1121.67	0.6381	0.9217
	e3	Chl-*a*	541.084	0.4589	0.9025
	e4	SOI	1728.64	0.4622	0.9211
	e5	SST(l)	1101.62	0.6759	0.9207
	e6	Chl-*a*(l)	538.86	0.4680	0.9053
	e7	SOI(l)	1727.63	0.4651	0.9210
	e8	SST * Chl-*a*			
	e9	SST * SOI	1125.10	0.6386	0.9217
	e10	Chl-*a* * SOI	544.40	0.4608	0.9023
	e11	**SST** * Chl-*a*(**l**)	**509.39**	**0.6454**	**0.9063**
	e12	SST * SOI(l)	1125.19	0.6396	0.9216
	e13	Chl-*a* * SST(l)			
	e14	Chl-*a* * SOI(l)	544.77	0.4664	0.9028

	e15	Chl-*a*(l) * SOI	540.84	0.4739	0.9048
	e16	SST(l) * SOI	1105.37	0.6764	0.9206
	e17	SST(l) * SOI(l)	1105.35	0.6765	0.9206
	e18	SST(l) * Chl-*a*(l)			
	e19	SOI(l) * Chl-*a*(l)	542.86	0.4668	0.9048
SE	e1	Growth – optimal base model	137.56	0.5373	0.9184
	e2	SST	0.6485	0.8057	0.9174
	e3	Chl-*a*	13.91	0.4552	0.9043
	e4	SOI	139.48	0.5379	0.9185
	e5	SST(l)	47.34	0.7388	0.9154
	e6	Chl-*a*(l)	14.87	0.4611	0.9075
	e7	SOI(l)	138.15	0.5269	0.9176
	e8	**SST * Chl-*a***	**-65.63**	**0.7960**	**0.8952**
	e9	SST * SOI	3.66	0.8075	0.9177
	e10	Chl-*a* * SOI	15.91	0.4570	0.9049
	e11	SST * Chl-*a*(l)	-65.39	0.7990	0.8957
	e12	SST * SOI(l)	3.705	0.8077	0.9177
	e13	Chl-*a* * SST(l)			
	e14	Chl-*a* * SOI(l)	14.71	0.4342	0.9026
	e15	Chl-*a*(l) * SOI	17.75	0.4582	0.9084
	e16	SST(l) * SOI	51.13	0.7395	0.9155
	e17	SST(l) * SOI(l)	47.35	0.7437	0.9150
	e18	SST(l) * Chl-*a*(l)	-49.45	0.7821	0.8995
	e19	SOI(l) * Chl-*a*(l)	16.71	0.4384	0.9064
WC	e1	Growth – optimal base model	1515.80	0.4759	0.8861
	e2	SST	1426.63	0.7062	0.8864
	e3	Chl-*a*	675.60	0.5077	0.9133
	e4	SOI	1517.75	0.4757	0.8861
	e5	SST(l)	1421.34	0.7182	0.8866
	e6	Chl-*a*(l)	676.99	0.5108	0.9145
	e7	SOI(l)	1516.85	0.4789	0.8873
	e8	SST * Chl-*a*	620.61	0.7271	0.9207
	e9	SST * SOI	1429.51	0.7084	0.8865
	e10	Chl-*a* * SOI	678.93	0.5083	0.9136
	e11	SST * Chl-*a*(l)	612.41	0.7609	0.9261
	e12	SST * SOI(l)	1429.85	0.7073	0.8870
	e13	**Chl-*a* * SST(l)**	**607.71**	**0.7524**	**0.9231**
	e14	Chl-*a* * SOI(l)	678.58	0.5055	0.9131
	e15	Chl-*a*(l) * SOI	679.48	0.5120	0.9146
	e16	SST(l) * SOI	1423.64	0.7211	0.8869
	e17	SST(l) * SOI(l)	1424.75	0.7217	0.8872
	e18	SST(l) * Chl-*a*(l)			
	e19	SOI(l) * Chl-*a*(l)	677.79	0.5181	0.9147

Table S2.10 - Selection of optimal fixed effects structures (highlighted in **bold**).

		Fixed Effect Structure	**AICc**	**R^2 (C)**	**R^2 (M)**
ANNUAL	**Broad**	Age	2127.19	0.8445	0.7643
		Age + AgeCap	2129.20	0.8444	0.7640
	NGSV	**Age**	**614.23**	**0.8505**	**0.7941**
		Age + AgeCap	616.24	0.8500	0.7930
	NSG	**Age**	**712.43**	**0.8523**	**0.7470**
		Age + AgeCap	714.40	0.8516	0.7425
	SE	**Age**	**214.25**	**0.8496**	**0.7893**
		Age + AgeCap	214.82	0.8487	0.7884
	WC	**Age**	**529.32**	**0.7984**	**0.7288**
		Age + AgeCap	530.54	0.8010	0.7329
SEASONAL	**Broad**	Age	4532.68	0.9014	0.4458
		Age + AgeCap	**4523.83**	**0.9067**	**0.4517**
	NGSV	Age	1437.17	0.9168	0.4895
		Age + AgeCap	**1433.45**	**0.9199**	**0.5047**
	NSG	Age	1741.56	0.9120	0.4287
		Age + AgeCap	**1726.64**	**0.9211**	**0.4621**
	SE	**Age**	**137.56**	**0.9184**	**0.5373**
		Age + AgeCap	139.40	0.9184	0.5371
	WC	**Age**	**1515.8**	**0.8861**	**0.4759**
		Age + AgeCap	1517.01	0.8873	0.4802

Table S2.11 - Selection of optimal temporal fits (highlighted in **bold**) in annually and seasonally resolved models.

	Region	Fit	AICC
ANNUAL			
	Broad	Base	2127.2
		Linear	**2099.9**
		Curvilinear	2101.4
	NGSV	Base	614.24
		Linear	608.51
		Curvilinear	**596.83**
	NSG	Base	712.44
		Linear	**666.38**
		Curvilinear	667.77
	SE	**Optimal**	**214.26**
		Linear	215.34
		Curvilinear	216.66
	WC	Optimal	529.33
		Linear	531.14
		Curvilinear	**527.74**
SEASONAL			
	Broad	Base	4508.01
		Linear	4502.83
		Curvilinear	**4489.84**
	NGSV	Base	1433.46
		Linear	1431.68
		Curvilinear	**1429.85**
	NSG	Base	1726.65
		Linear	**1701.29**
		Curvilinear	1703.24
	SE	Optimal	137.57
		Linear	138.46
		Curvilinear	**136.53**
	WC	Optimal	1515.81
		Linear	**1515.44**
		Curvilinear	1515.93

Table S2.12 - Among-individual (amongIDV; representing facultative environmental responses) and within-individual (withinIDV; representing evolutionary fixed phenotypically-plastic responses) variation in annual models with best model highlighted in **bold**. Random slope term designated with x | y.

Region	Fit	Extra Terms	AICC
All	Base		2137.7
	Model 8	amongIDV, withinIDV	**1214.1**
	Model 9	amongIDV, withinIDV, withinIDV|FishID	1219.14
NGSV	Base		622.75
	Model 8	amongIDV, withinIDV	**353.87**
	Model 9	amongIDV, withinIDV, withinIDV|FishID	356.61
NSG	Base		721.86
	Model 8	amongIDV, withinIDV	**317.66**
	Model 9	amongIDV, withinIDV, withinIDV|FishID	323.06
SE	Base		224.59
	Model 8	amongIDV, withinIDV	**171.81**
	Model 9	amongIDV, withinIDV, withinIDV|FishID	177.76
WC	Base		539.08
	Model 8	amongIDV, withinIDV	**371.1**
	Model 9	amongIDV, withinIDV, withinIDV|FishID	377.4

SUPPLEMENTARY INFORMATION S2 - FIGURES

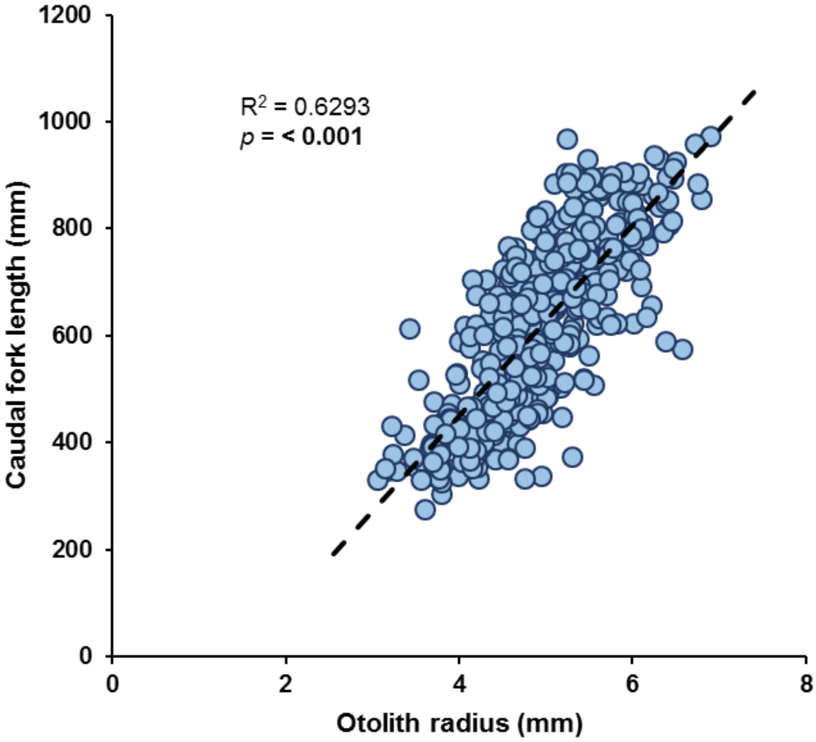

Figure S2.1 - Relationship between caudal fork length (CFL) and otolith width in South Australian snapper (*n* = 541) aged 5 to 27 years.

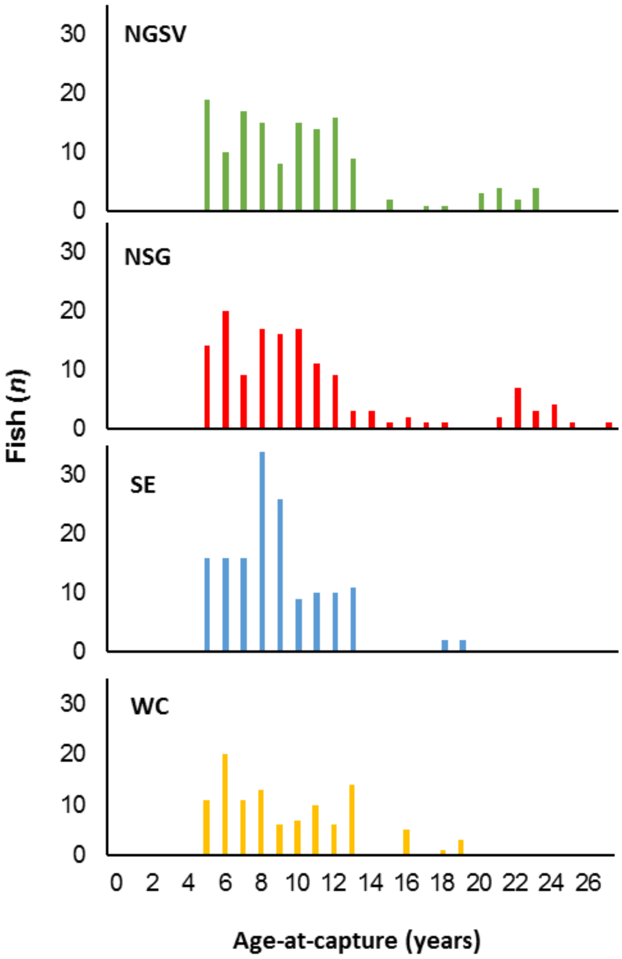

Figure S2.2 - Range of Age-at-capture of snapper of individual sampling regions North Gulf St Vincent (Green), Northern Spencer Gulf (Red), the South East (SE) and West Coast (Yellow).

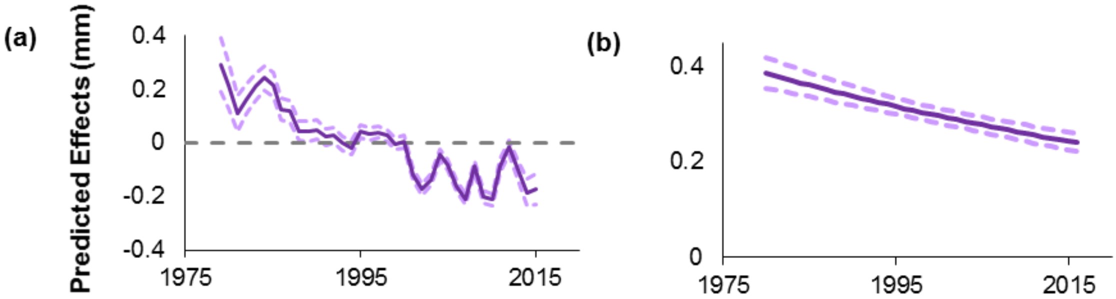

Figure S2.3 - Predicted inter-annual growth variation (a – e) and temporal trends (f - j) of snapper in the broad-scale South Australian region (Broad).

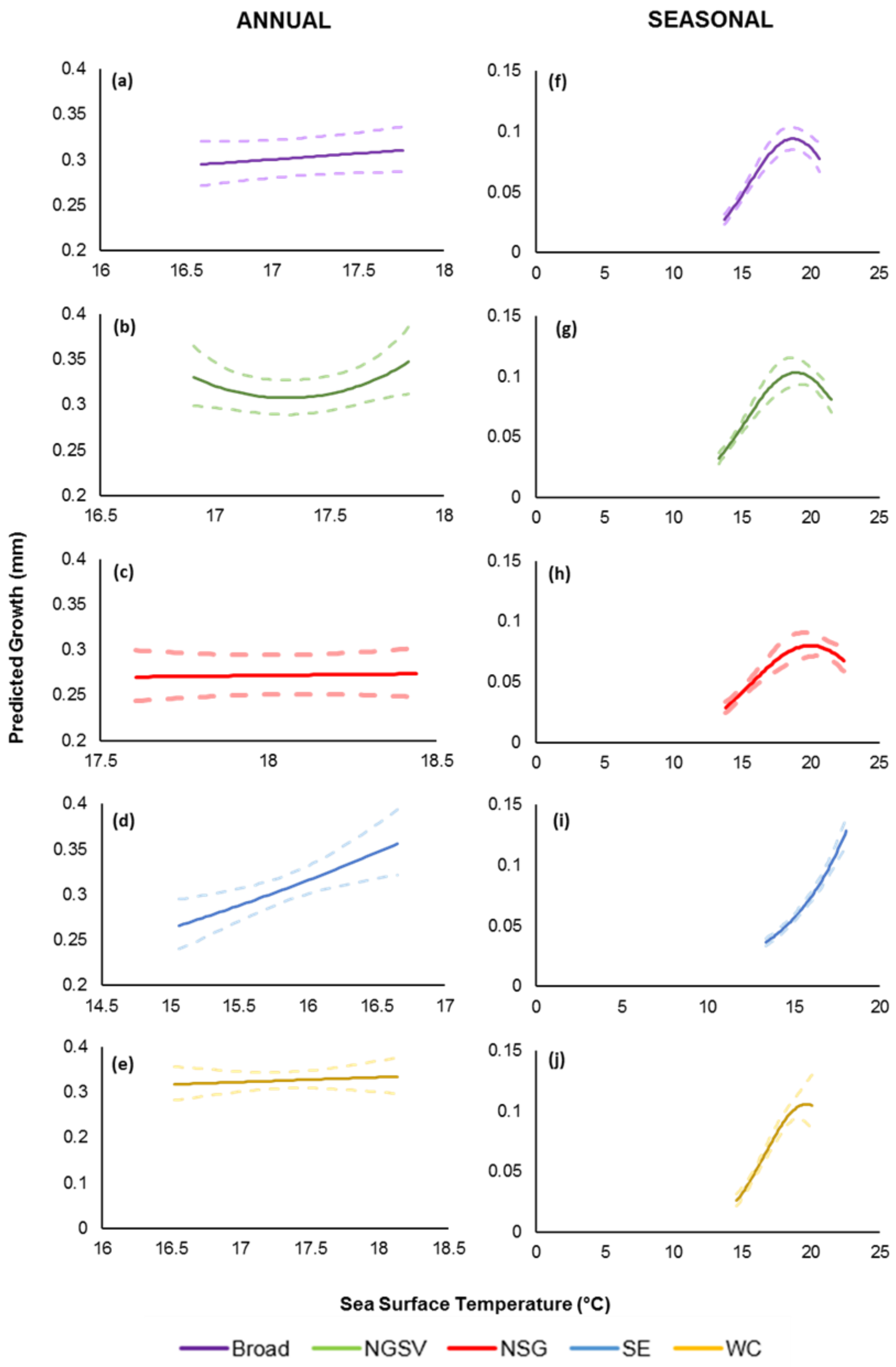

Figure S2.4 - Predicted annual and seasonal growth variation Mean (+ SE) of Sea Surface Temperature for the broad South Australian region (purple), Northern Gulf St Vincent (Green), Northern Spencer Gulf (Red), South East (Blue) and West Coast (Yellow).

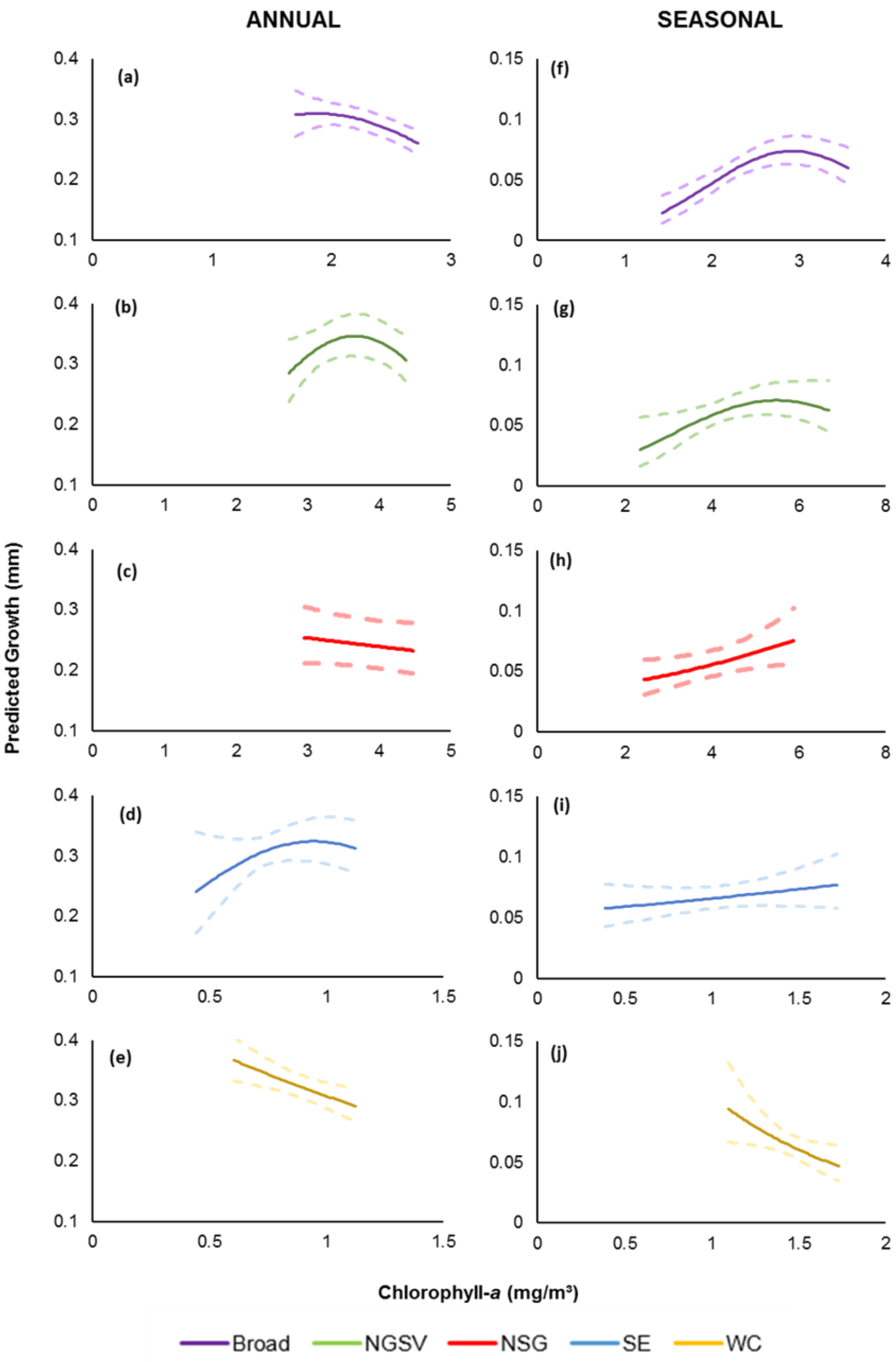

Figure S2.5 - Predicted annual growth variation Mean (+ SE) of Chlorophyll-*a* for the broad South Australian region (purple), Northern Gulf St Vincent (Green), Northern Spencer Gulf (Red), South East (Blue) and West Coast (Yellow).

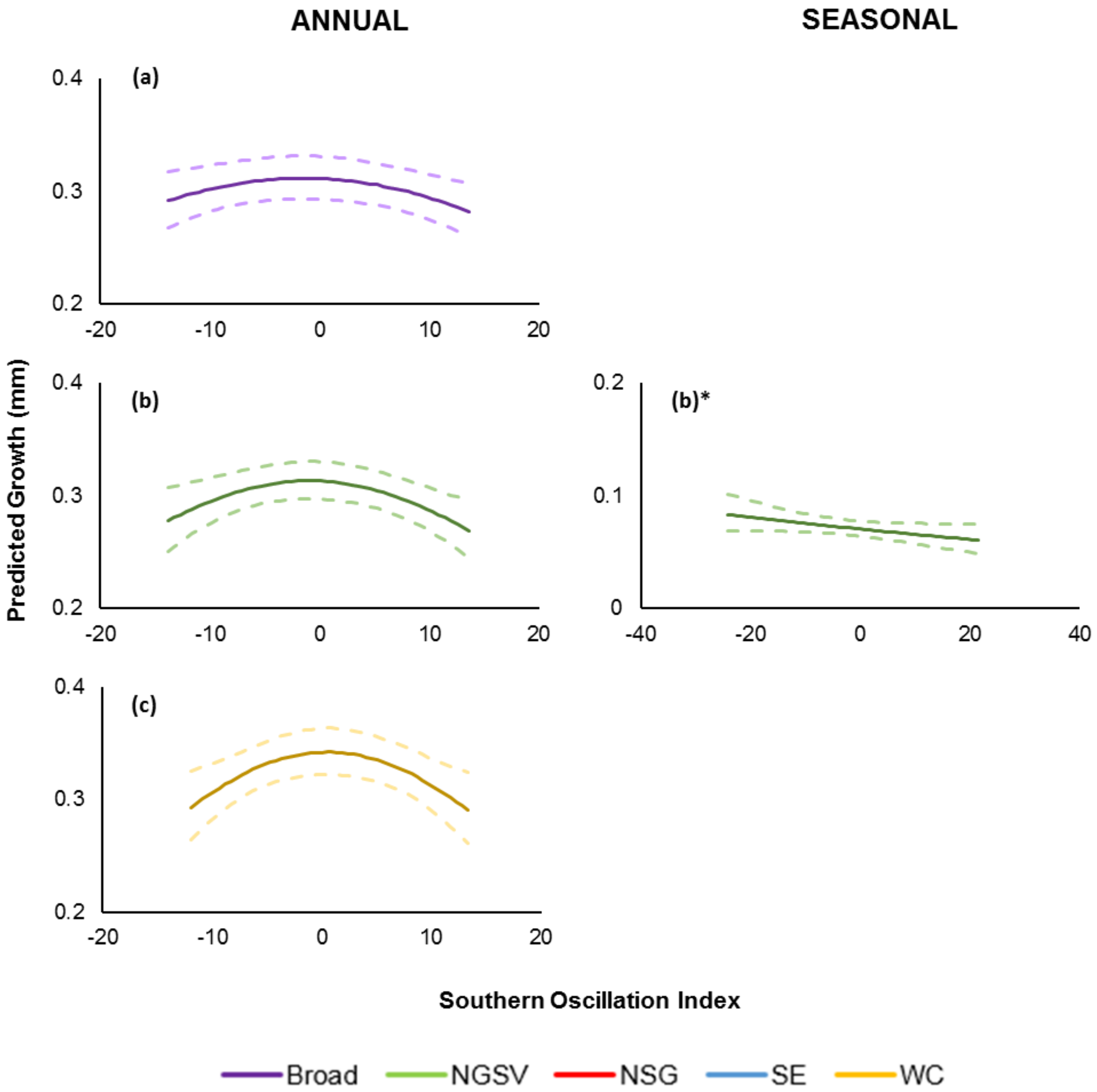

Figure S2.6 - Predicted annual growth variation Mean (+ SE) of Southern Oscillation Index for the broad South Australian region (purple), Northern Gulf St Vincent (Green), Northern and West Coast (Yellow).

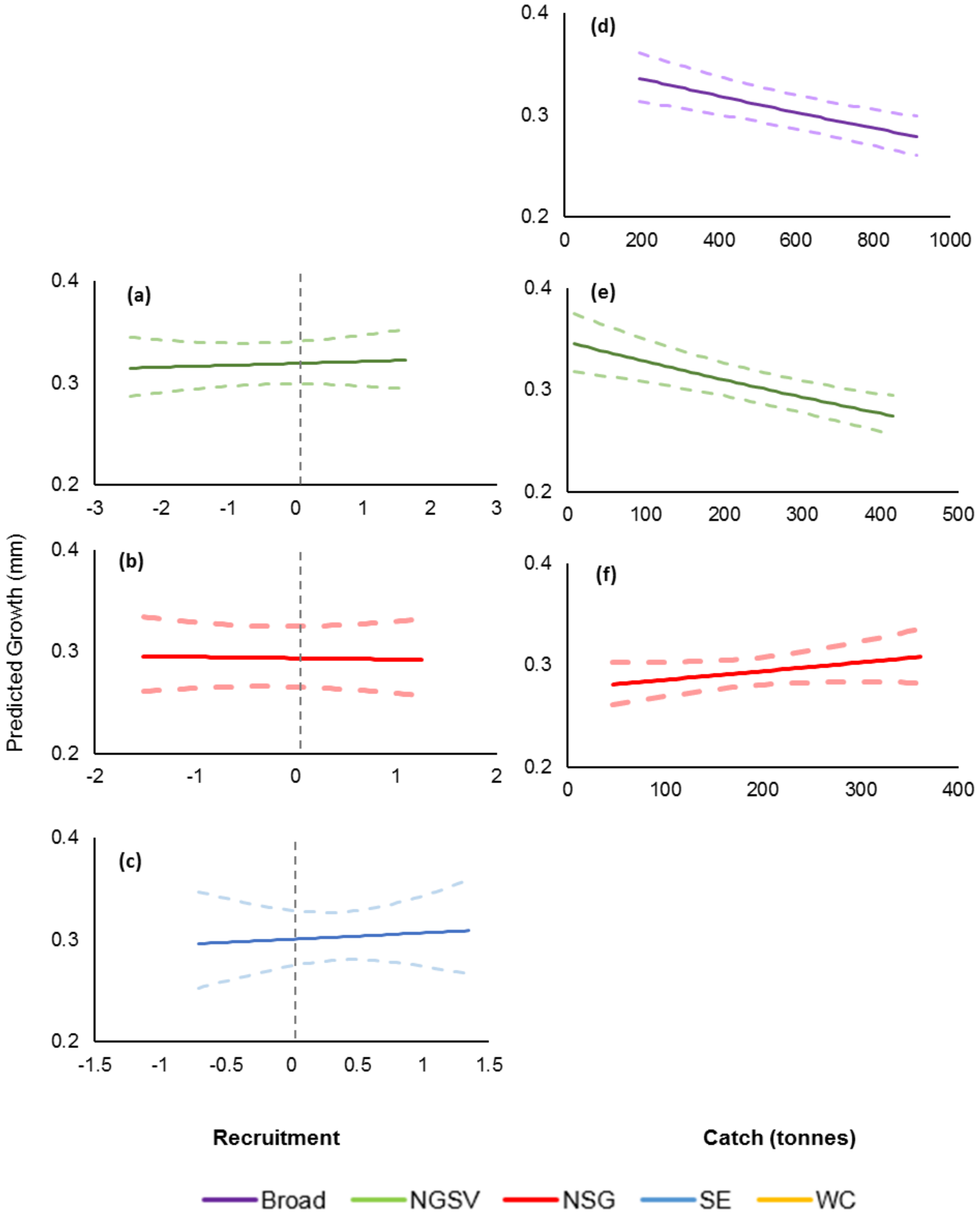

Figure S2.7 - Predicted annual growth variation Mean (+ SE) of Recruitment or Catch for the broad South Australian region (purple), Northern Gulf St Vincent (Green), Northern Spencer Gulf (Red) and South East (Blue).

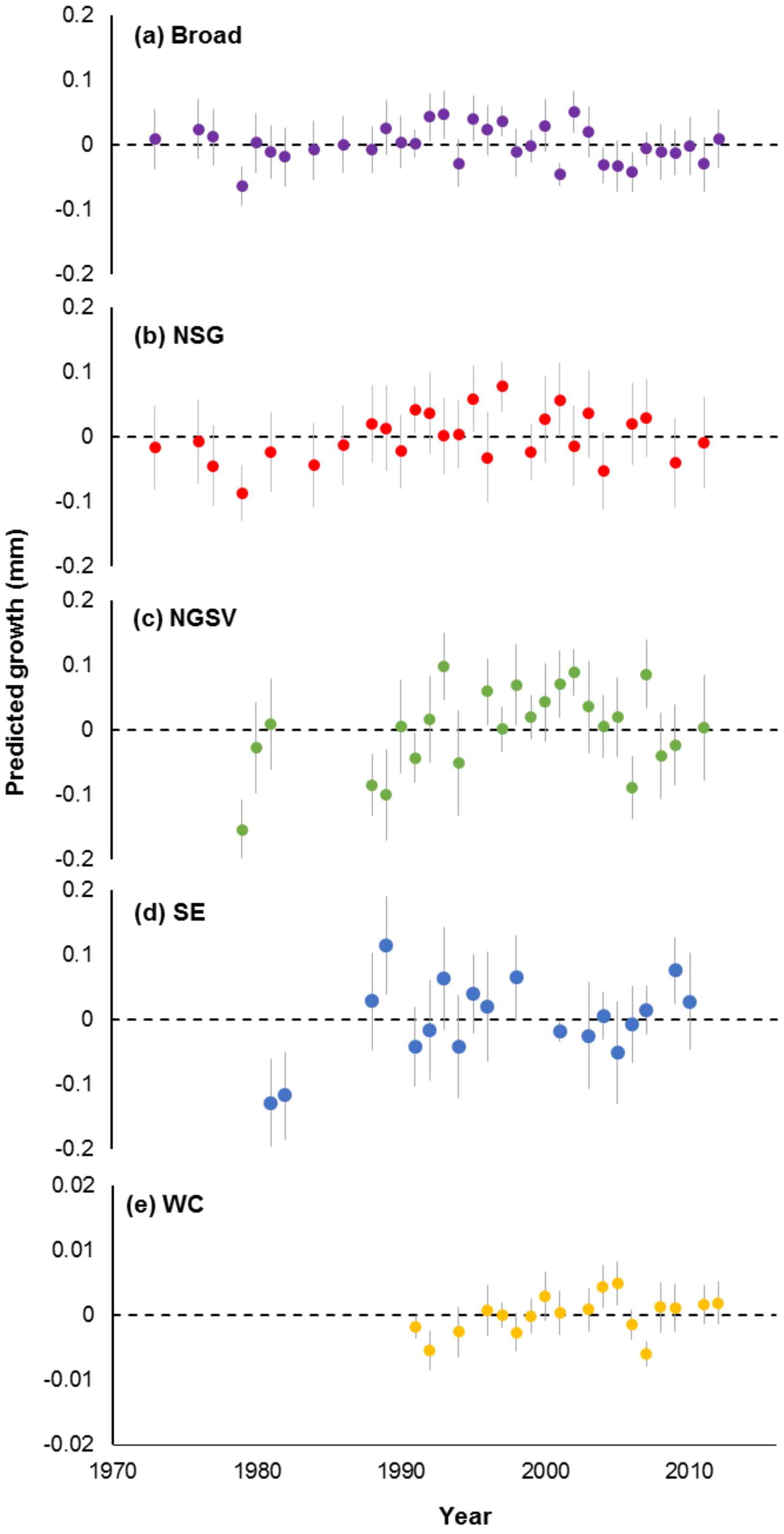

Figure S2.8 - Predicted average growth variation for Cohort represented by best linear unbiased predictors (BLUPS ± SE) in the broad South Australian region (purple), Northern Gulf St Vincent (Green), Northern Spencer Gulf (Red), South East (Blue) and West Coast (Yellow). Note different scales on the *y*-axes.

SUPPLEMENTARY INFORMATION S3

CHAPTER 3 - Metabolic effects on carbon isotope biomarkers in fish

GRAPHICAL ABSTRACT

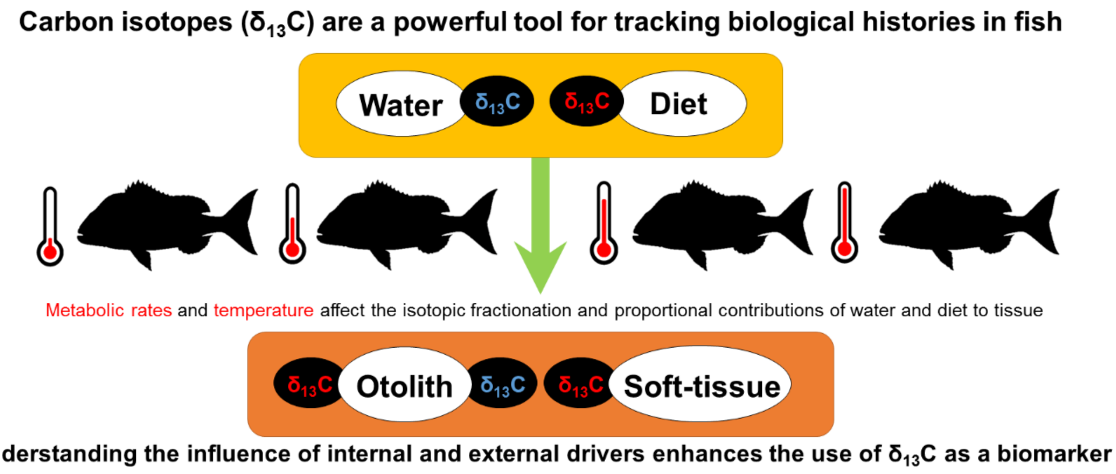

SUPPLEMENTARY INFORMATION S3 - TABLES

Table S3.1 - Analysis of variance comparing carbon isotope composition in fish tissues (otolith, muscle and liver), the proportion of metabolic carbon (*M*) and dissolved inorganic carbon (DIC) in tank water across temperature treatments. Significant values are bolded.

SOURCE		df	MS	*F*	*P*
OTOLITH					
	Temperature	3	9.6126	11.943	**0.001**
	Tank (Temperature)	11	0.81374	1.1263	0.354
	Residual	40	0.72249		
MUSCLE					
	Temperature	3	0.39538	6.726	**0.009**
	Tank (Temperature)	11	5.94E-02	1.1462	0.359
	Residual	40	5.19E-02		
LIVER					
	Temperature	3	17.886	9.959	**0.004**
	Tank (Temperature)	11	1.6752	0.51257	0.898
	Residual	40	3.2683		
M	Temperature	3	8.24E-03	0.66224	0.638
	Tank (Temperature)	11	1.40E-02	10.108	**0.001**
	Residual	40	1.38E-03		
***M* (pooled)**	Temperature	3	109.22	2.6683	**0.047**
	Residual	51	40.934		
Tank DIC	Temperature	3	1.9984	0.83249	0.468
	Residual	12	2.4005		

Table S3.2 - Analysis of variance comparing carbon isotope composition across whole and lipid-normalised fish tissues (muscle and liver) and temperature treatments. Significant values are bolded.

SOURCE		df	MS	*F*	*P*
Lipid-extracted vs Lipid whole Muscle					
	Temperature	3	0.47137	7.1332	**0.008**
	Tissue method	1	12.518	184.27	**0.001**
	Tank (Temperature)	12	6.58E-02	0.9609	0.501
	Temperature x tissue method	3	4.89E-02	0.72065	0.537
	Residual	76	6.85E-02		
Liver					
	Temperature	3	1.4673	2.1339	0.15
	Tissue method	1	786.32	428.75	**0.001**
	Tank (Temperature)	11	0.57108	0.27084	0.986
	Temperature x tissue method	3	23.452	12.828	**0.001**
	Residual	76	2.1086		

Table S3.3 - Analysis of variance comparing carbon isotope diet to tissue fractionation in fish soft tissues (muscle and liver) and DIC to otolith fractionation across temperature treatments. Significant values are bolded.

SOURCE		df	MS	*F*	*P*
Fractionation					
	Soft Tissue	1	108.45	125.36	**0.001**
	Temperature	3	6.6447	6.6605	**0.016**
	Tank (Temperature)	12	0.91241	0.54962	0.856
	Soft tissue x Temperature	3	9.8369	12.094	**0.001**
	Residual	76	1.6601		
DIC-to-otolith fractionation	Temperature	3	3.5012	0.51663	0.668
	Tank (Temperature)	11	7.6838	16.837	**0.001**
	Residual	41	0.45637		
DIC-to-otolith fractionation (pooled)	Temperature	3	6.4421	3.245	**0.029**
	Residual	52	1.9852		

Table S3.4 - Mean (± SE) body mass measurement of snapper in each temperature treatment prior to ANCOVA-adjustment for fish age.

Treatment (°C)	Weight	Length	Height	Girth
20	15.8±2.4	77.5±3.8	33.5±1.93	9.6±0.7
24	13.2±1.3	73.9±2.8	32.4±1.24	9.4±0.47
28	9.2±0.9	64.5±2.5	29.3±1.4	8.2±0.6
32	6.3±1.2	56.1±2.8	24.8±1.7	6.8±0.8

Table S3.5 - Analysis of covariance comparing fish size among temperature treatments, with the removal of the effects of covariate, fish age. Significant values are bolded.

SOURCE		**df**	**MS**	***F***	***P***
WEIGHT					
	Fish age	1	545.460	24.302	**<0.001**
	Temperature	3	27.484	1.225	0.311
	Residual	56	22.445		
LENGTH					
	Fish age	1	3270.143	49.332	**<0.001**
	Temperature	3	62.799	0.947	0.425
	Residual	56	66.288		
HEIGHT					
	Fish age	1	786.920	44.663	**<0.001**
	Temperature	3	3.755	0.213	0.887
	Residual	56	17.619		
GIRTH					
	Fish age	1	40.373	9.068	**0.004**
	Temperature	3	0.832	0.187	0.905
	Residual	56	4.452		

Table S3.6 - Correlations between fish size (length, weight, height, girth) and M (metabolically sourced carbon in otoliths) and carbon isotope values ($\delta^{13}C$) in otoliths, muscle and liver tissues.

	SOURCE	t	df	*P*	R^2
M					
	Length	-1.60	56	0.12	0.05
	Weight	-1.76	56	0.08	0.06
	Height	-1.19	56	0.24	0.03
	Girth	-1.12	56	0.27	0.02
$\delta^{13}C$ in otoliths					
	Length	-0.09	56	0.93	-0.01
	Weight	0.67	56	0.52	0.09
	Height	-0.41	56	0.69	-0.06
	Girth	-0.11	56	0.91	-0.02
$\delta^{13}C$ in muscle	Length	-4.58	56	**<0.001**	0.27
	Weight	-3.89	56	**<0.001**	0.21
	Height	-5.52	56	**<0.001**	0.35
	Girth	-5.84	56	**<0.001**	0.37
$\delta^{13}C$ in liver	Length	-1.28	56	0.21	0.01
	Weight	-1.01	56	0.32	0.001
	Height	-1.67	56	0.10	0.04
	Girth	-0.28	56	0.06	0.06

SUPPLEMENTAY INFORMATION S3 - FIGURES

Figure S3.1 - Mean (± SE) ANCOVA-adjusted fish size (weight, length, girth, height) for temperature treatments 20°C (white), 24°C (light grey), 28°C (mid grey) and 32°C (dark grey), with fish age as the covariate.

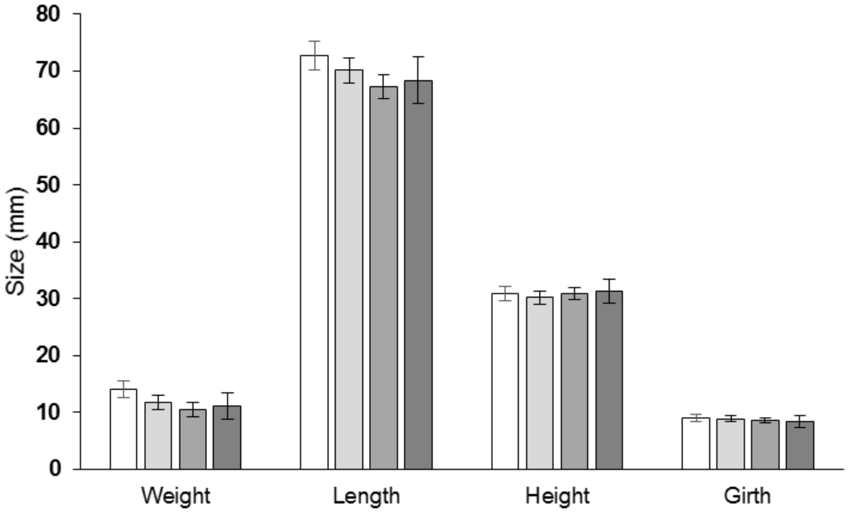

SUPPLEMENTARY INFORMATION S4

CHAPTER 4 - Biominerals track metabolic rates in fish

SUPPLEMENTARY INFORMATION S4 - TABLES

Table S4.1 - Average (± SE) tank conditions for the experimental period and treatment averages of carbon isotopes (δ^{13}C), oxygen isotopes (δ^{18}O), standard metabolic rates (SMR), maximum metabolic rates (MMR) and absolute aerobic scope (AAS).

Temperature Treatment	Temperature (°C)	Salinity (psu)	Carbon (± SE)	Oxygen (± SE)	SMR (± SE)	MMR (± SE)	AAS (± SE)
20	19.8 ±0.06	35.5 ±0.3	-8.13 ±0.086	-0.07 ±0.22	21.85 ±1.2	39.37 ±1.77	17.52 ±1.36
24	23.9 ±0.07	35.7 ±0.3	-8.97 ±0.085	-0.82 ±0.16	28.15 ±1.16	47.00 ±1.2	18.65 ±0.91
28	28.0 ±0.03	35.1 ±0.4	-10.03 ±0.218	-1.78 ±0.153	32.21 ±3.44	47.5 ±4.6	12.31 ±3.08
32	32.0 ±0.1	34.9 ±1.4					

Table S4.2 - Analysis of variance comparing isotopes [carbon (δ^{13}C) and oxygen (δ^{18}O)], metabolic rates [standard metabolic rates (SMR), maximum metabolic rates (MMR) and absolute aerobic scope (AAS)], proportion of metabolic carbon (M), dissolved inorganic carbon in treatment tanks (DIC) and fish size (length and weight) and condition (Fulton's k) across temperature treatments. Significant values are bolded.

Source		Df	MS	*F*	*P*
δ^{13}C	Temperature	2	6.31	67.1	**0.001**
	Tank (Temperature)	8	8.80E-02	0.69	0.709
	Residual	20	0.13		
δ^{18}O	Temperature	2	5.32	10.53	**0.004**
	Tank (Temperature)	8	0.53	1.42	0.260
	Residual	20	0.37		
SMR	Temperature	2	201.97	3.24	0.099
	Tank (Temperature)	8	67.89	2.16	0.086
	Residual	20	31.38		
	Temperature	2	316.1	7.56	**0.002**
	Residual	28	41.81		
MMR	Temperature	2	85.95	0.81	0.474

	Tank (Temperature)	8	119.03	3.74	**0.006**
	Residual		31.834		
AAS	Temperature	2	107.3	2.99	0.138
	Tank (Temperature)	8	39.93	2.98	**0.020**
	Residual	20	13.38		
M	Temperature	2	70.13	0.53	0.633
	Tank (Temperature)	8	155.05	38.01	**0.001**
	Residual	20	4.078		
DIC	Temperature	2	1.32	0.62	0.540
	Residual	9	2.12		
Fish length (mm)	Temperature	2	182.08	1.82	0.228
	Tank (Temperature)	8	107.89	1.89	0.116
	Residual	20	57.03		
Fish weight (g)	Temperature	2	88.12	2.33	0.149
	Tank (Temperature)	8	39.22	1.32	0.270
	Residual	20	29.78		
Fulton’s k	Temperature	2	5.65E-02	0.81	0.470
	Tank (Temperature)	8	7.37E-02	1.51	0.234
	Residual	20	4.87E-02		

SUPPLEMENTARY INFORMATION S4 - FIGURES

Figure S4.1 - Schematic of intermittent-flow respirometry system. The respirometry system consisted of four chambers with a maximum of three chambers at a time used to measure fish oxygen consumption (mg/L [ppm]) and the fourth used to measure background respiration (BR). Each chamber was a closed system attached to a pump (approximately 250 ml/s), to continuously recirculate water through the system loop, and an oxygen meter. Each respirometry cycle consisted of three stages: a 3-min flush stage where the flush pump pushed oxygenated water through each system; a 30-sec wait stage where the system is closed awaiting oxygen measurement; and a 12-min measuring period where the flush pump was off, the loop was closed and oxygen was measured.

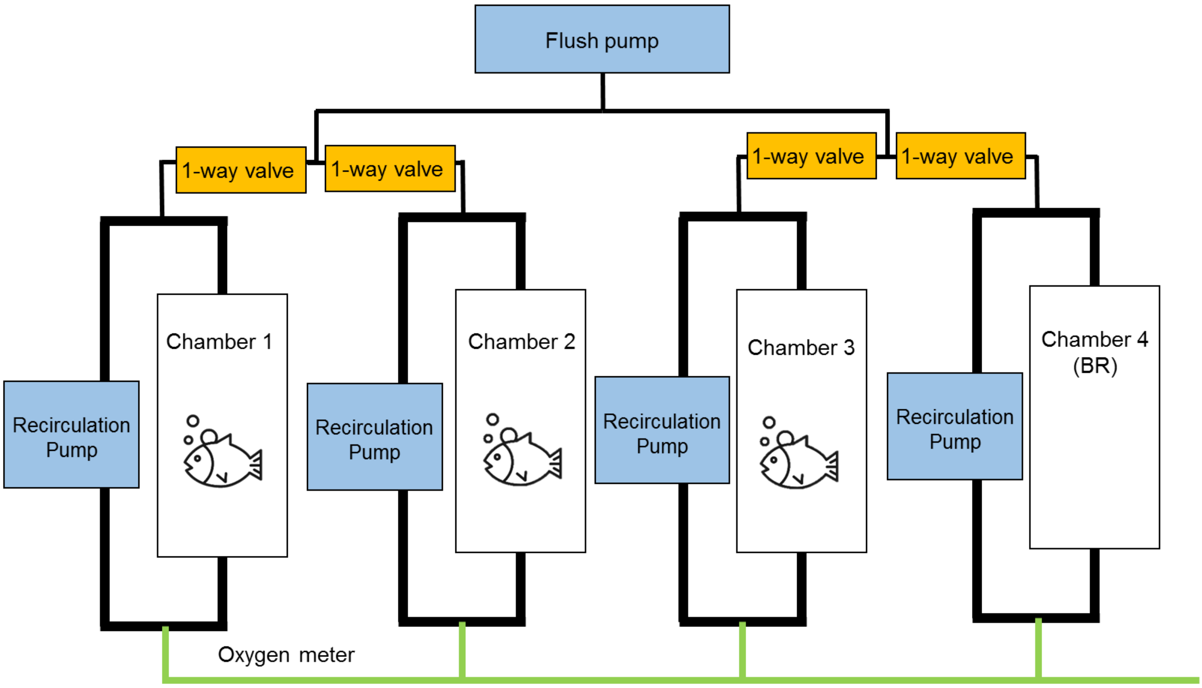

Figure S4.2 - Relationships between carbon isotopes in otoliths ($\delta^{13}C$), oxygen isotopes in otoliths ($\delta^{18}O$), standard metabolic rates (SMR), maximum metabolic rates (MMR), absolute aerobic scope (AAS), fish length, fish weight, Fulton's k and proportional contributions of metabolic carbon (*M*) to otolith $\delta^{13}C$. Spread of data and best fit line are indicated by the bottom panel, with narrower ellipses indicating stronger relationships. The top panel provides R^2 values of the relationships derived by linear regression with significant relationships ($p<0.05$) coloured red. Correlation matrix was created using package *corrgram* in R.

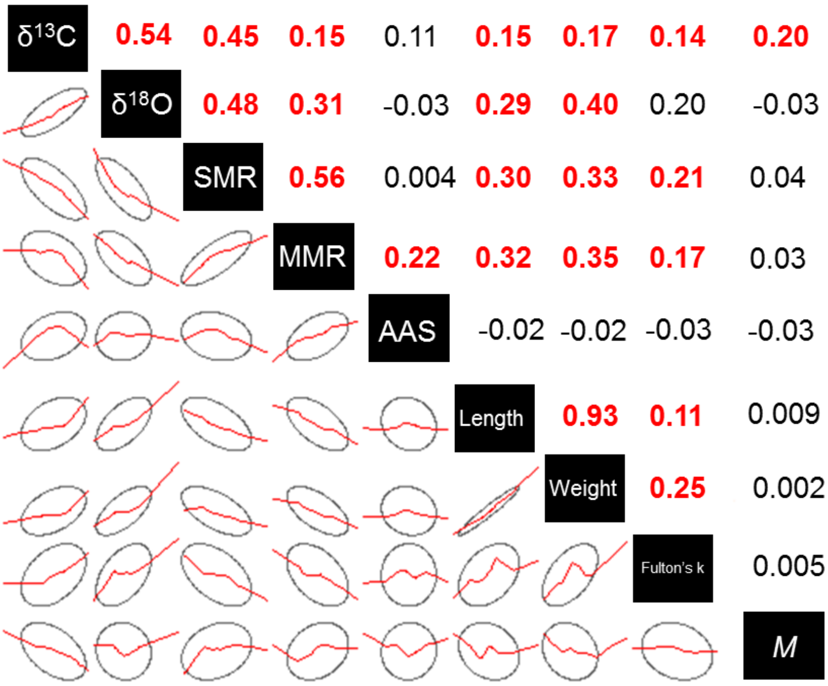

Figure S4.3 - Proportional contributions of metabolic carbon (*M*) to otolith $\delta^{13}C$ in juvenile snapper reared in different temperatures.

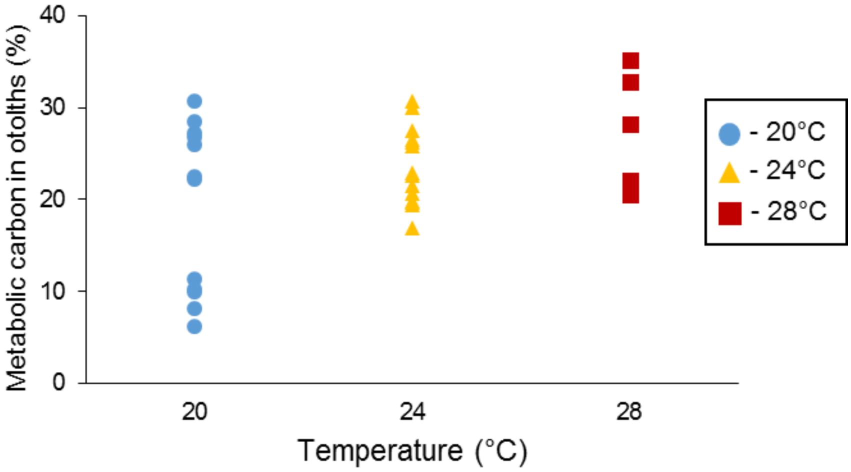

SUPPLEMENTARY INFORMATION S5

Chapter 5 - Linking chemical chronologies and physiology in a wild fish

SUPPLEMENTARY INFORMATION S5 – TABLES

Table S5.1 - Selection of optimal random effects structures (highlighted in **bold**) in lifetime carbon ($\delta^{13}C$) and oxygen ($\delta^{18}O$) isotopes in snapper otoliths. Random slope term designated with x | y.

	AICc	
	$\delta^{13}C$	$\delta^{18}O$
RANDOM EFFECTS		
1|FishID	**609.89**	**377.13**
Age|FishID	616.05	383.1
1|FishID + 1|Cohort	612.12	379.5
Age|FishID2 + 1|Cohort	613.9	382.48
1|FishID + Age|Cohort	616.65	379.49
Age|FishID + Age|Cohort	618.56	382.43
1|FishID + 1|Region	611.74	379.49
Age|FishID2 + 1|Region	613.66	382.43
1|FishID2 + Age|Region	613.57	381.91
Age|FishID2 + Age|Region	616.91	384.96
1|FishID2 + 1|Region + 1|Cohort	614	379.50
Age|FishID + 1|Region + 1|Cohort	615.89	382.48

Table S5.2 - Selection of optimal random effects structures (highlighted in **bold**) in lifetime magnesium (Mg:Ca), strontium (Sr:Ca) and barium (Ba:Ca) concentrations in snapper otoliths. Random slope term designated with x|y. If there were errors in the optimum model (i.e. Singular Fit), AICc comparison tests were rerun without models with errors. Asterix indicates the best models in this instance.

			AICc		
RANDOM EFFECTS	**Mg:Ca**	**Sr:Ca**	**Ba:Ca**	**Mn:Ca**	**Li:Ca**
1|FishID	-157.90	-957.38	-70.52	-578.49	-458.00
Age|FishID	**-215.76***	**-1145.95***	**-379.05**	-837.52	**-474.46**
1|FishID + 1|iSeason	-165.53	-966.56	-68.52	-579.44	-455.95
sAge|FishID + 1|Season	-228.10	-1160.61	-376.99	-844.32	-472.40
1|FishID + 1|Region	-156.02	-955.33	-68.52	-576.91	-455.95
sAge|FishID2 + 1|Region	-209.75	-1140.11	-375.36	-831.47	-468.39
1|FishID +sAge|Region	-213.70	-1143.89	-377.81	-835.46	-472.40
sAge|FishID + sAge|Region	-155.56	-951.36	-82.48	-575.83	-452.76
1|FishID + 1|iSeason + 1|Region	-163.55	-964.51	-66.52	-577.78	-453.89
sAge|FishID + 1|iSeason + 1|Region	-226.03	-1158.54	-375.74	-842.26	-470.33
1|FishID2 + sAge|iSeason + 1|Region	-188.34	-970.16	-92.80	-629.39	-449.89
sAge|FishID2 + sAge|iSeason + 1|Region	-247.98	-1156.19	-373.69	**-883.25**	-466.66
1|FishID + 1|iSeason + sAge|Region	-175.72	-962.01	-80.42	-581.64	-450.67
sAge|FishID2 + 1|iSeason + sAge|Region	-223.10	-1154.97	-373.28	-838.34	-466.31
1|FishID + 1|iSeason + sAge|Region + sAge|Region	-176.54	-955.78	-74.18	-575.40	-444.45
sAge|FishID + sAge|iSeason + sAge|Region	-150.12	-1152.68	-375.60	-879.51	-462.58

Table S5.3 - Selection of optimal fixed effects structures (highlighted in **bold**) in lifetime carbon ($\delta^{13}C$) and oxygen ($\delta^{18}O$) isotopes, magnesium (Mg:Ca), strontium (Sr:Ca), barium (Ba:Ca), manganese (Mn:Ca) and lithium (Li:Ca) in snapper otoliths in snapper otoliths.

				AICc			
FIXED EFFECTS	**$\delta^{13}C$**	**$\delta^{18}O$**	**Mg:Ca**	**Sr:Ca**	**Ba:Ca**	**Mn:Ca**	**Li:Ca**
Otolith growth, Sex, Fish length	582.31	344.59	-237.51	-1171.36	-396.31	-869.28	-499.20
Otolith growth, Fish length	803.48	501.12	-232.30	-1178.7	-397.86	-875.95	-496.92
Otolith growth, Sex	582.04	343.16	137.50	-1534.27	-421.07	-930.80	**-607.31**
Sex, Fish length	580.46	342.42	**-239.52**	-1171.16	-395.46	-866.35	-499.99
Otolith growth	801.54	498.95	137.87	**-1541.43**	-423.68	-932.54	-601.90
Sex	579.92	**340.9**	-234.33	-1178.63	-397.13	-872.89	-497.33
Fish length	801.48	499	135.91	-1534.22	-421.99	-930.43	-607.11
Base Model	799.49	496.88	136.28	-1541.42	**-424.55**	**-933.19**	-601.20
Otolith growth x Sex	581.48	343.73	-237.49	-1172.25	-395.32	-864.32	-498.07
Fish length x Sex	**579.11**	344.22	-230.42	-1177.22	-398.07	-874.34	-495.03
Otolith growth x Sex, CFL	581.94	345.42	-235.55	-1172.48	-396.21	-867.24	-497.38
CFL x Sex, Otolith growth	580.97	346.45	-235.62	-1169.85	-396.83	-867.64	-497.50

Table S5.4 - Selection of optimal extrinsic structures (highlighted in **bold**) in lifetime carbon (δ^{13}C) and oxygen (δ^{18}O) isotopes, magnesium (Mg:Ca), strontium (Sr:Ca) and barium (Ba:Ca) in snapper otoliths. Environmental covariates assessed include linear sea surface temperature (SST) and curvilinear sea surface temperature (SST + SST^2). Base model indicates that an environmental term did not improve fit.

				AICc			
ENVIRONMENTAL COVARIATE	**δ^{13}C**	**δ^{18}O**	**Mg:Ca**	**Sr:Ca**	**Ba:Ca**	**Mn:Ca**	**Li:Ca**
Base model	579.11	340.9	-239.52	**-1541.42**	**-424.55**	**-933.19**	**-607.31**
SST	427.48	**239.17**	-268.95	-1184.50	-401.23	-592.65	-447.25
SST + SST^2	425.92	240.18	-266.88	-1184.50	-399.39	-592.12	-445.21
SST (lagged)	427.18	240.26	**-279.39**	-1182.52	-392.10	-627.15	-438.2
SST (lagged) + SST^2 (lagged)	**425.62**	240.46	-277.51	-1171.58	-390.09	-626.24	-438.19

Table S5.5 - Selection of optimal extrinsic structures (highlighted in **bold**) in lifetime carbon (δ^{13}C) and oxygen (δ^{18}O) isotopes, magnesium (Mg:Ca), strontium (Sr:Ca) and barium (Ba:Ca) in snapper otoliths. Environmental covariates assessed include linear sea surface temperature (SST) and curvilinear sea surface temperature (SST + SST^2). Base model indicates that an environmental term did not improve fit.

				AICc			
ENVIRONMENTAL COVARIATE	**δ^{13}C**	**δ^{18}O**	**Mg:Ca**	**Sr:Ca**	**Ba:Ca**	**Mn:Ca**	**Li:Ca**
Base model	579.11	340.9	**-239.52**	**-1541.42**	**-424.55**	**-933.19**	**-607.31**
Chl-*a*	**285.22**	**157.21**	-96.78	-489.06	-111.82	-276.87	-188.88
Chl-*a* + Chl-*a*^{2}	286.17	159.29	-94.66	-486.96	-116.34	-275.92	-187.82
Chl-*a* (lagged)	285.53	159.12	-131.86	-475.68	-107.14	-242.40	-175.46
Chl-*a* (lagged) + Chl-*a*^{2} (lagged)	286.30	159.12	-130.04	-475.68	-110.83	-241.97	-175.46

SUPPLEMENTARY INFORMATION S5 – FIGURES

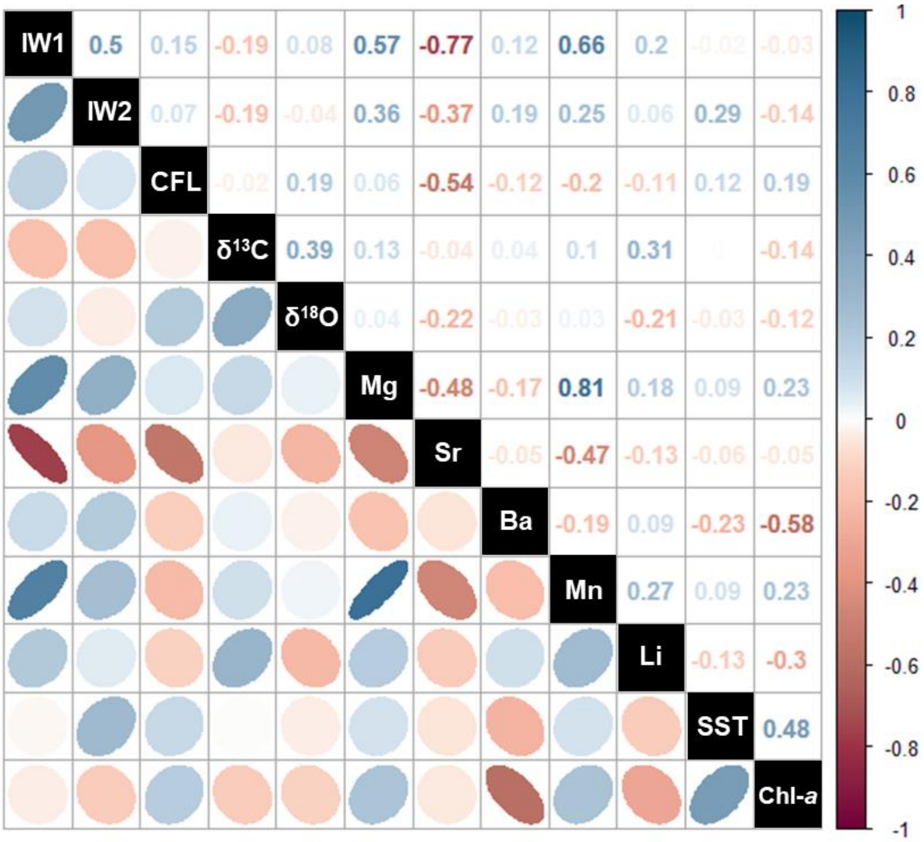

Figure S5.1 – Annual relationships in snapper otoliths between Axis 1 Increment Width (IW1; Figure 5.3), Axis 2 Increment Width (IW2; Figure 5.3), carbon isotopes (δ^{13}C), oxygen isotopes (δ^{18}O), magnesium (Mg), Strontium (Sr), Barium (Ba), Manganese (Mn), Lithium (Li), and extrinsic variables Sea Surface Temperature (SST) and Chlorophyll-*a* (Chl-*a*). Isotopes were analysed on the same axis as IW1 and elements were analysed on the same axis as IW2. Elements shown are ratioed to calcium. Spread of data and best fit line are indicated by the bottom panel, with narrower ellipses indicating stronger relationships. The top panel provides Pearson's correlation coefficients indicating the extent of correlation between the two variables. Correlation matrix were created using package *corrplot* in R.

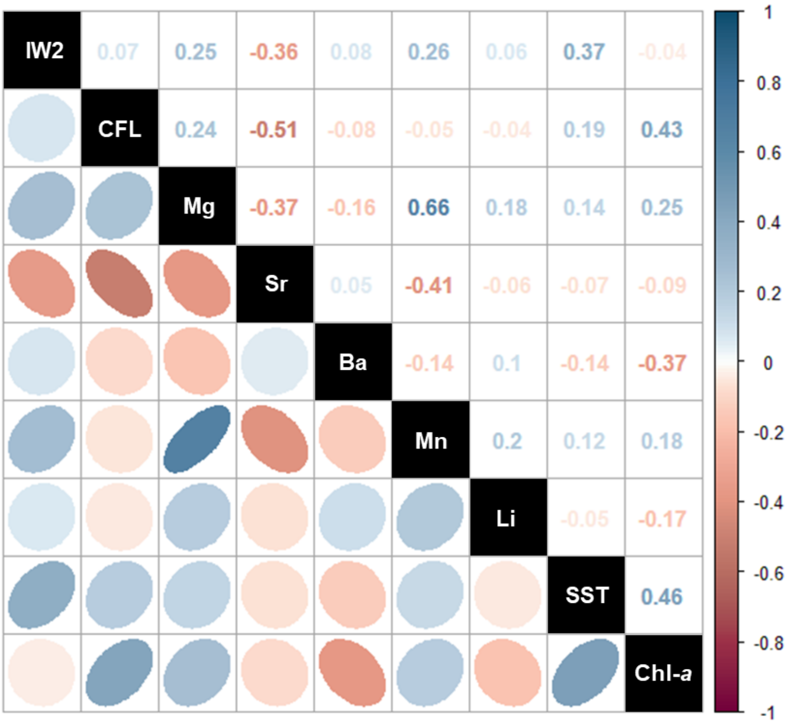

Figure S5.2 – Seasonal relationships in snapper otoliths between Axis 2 Increment Width (IW2; Figure 5.3), caudal fork length (CFL), magnesium (Mg), Strontium (Sr), Barium (Ba), Manganese (Mn), Lithium (Li), and extrinsic variables Sea Surface Temperature (SST) and Chlorophyll-*a* (Chl-*a*). Elements shown are ratioed to calcium. Spread of data and best fit line are indicated by the bottom panel, with narrower ellipses indicating stronger relationships. The top panel provides Pearson's correlation coefficients indicating the extent of correlation between the two variables. Correlation matrix were created using package *corrplot* in R.

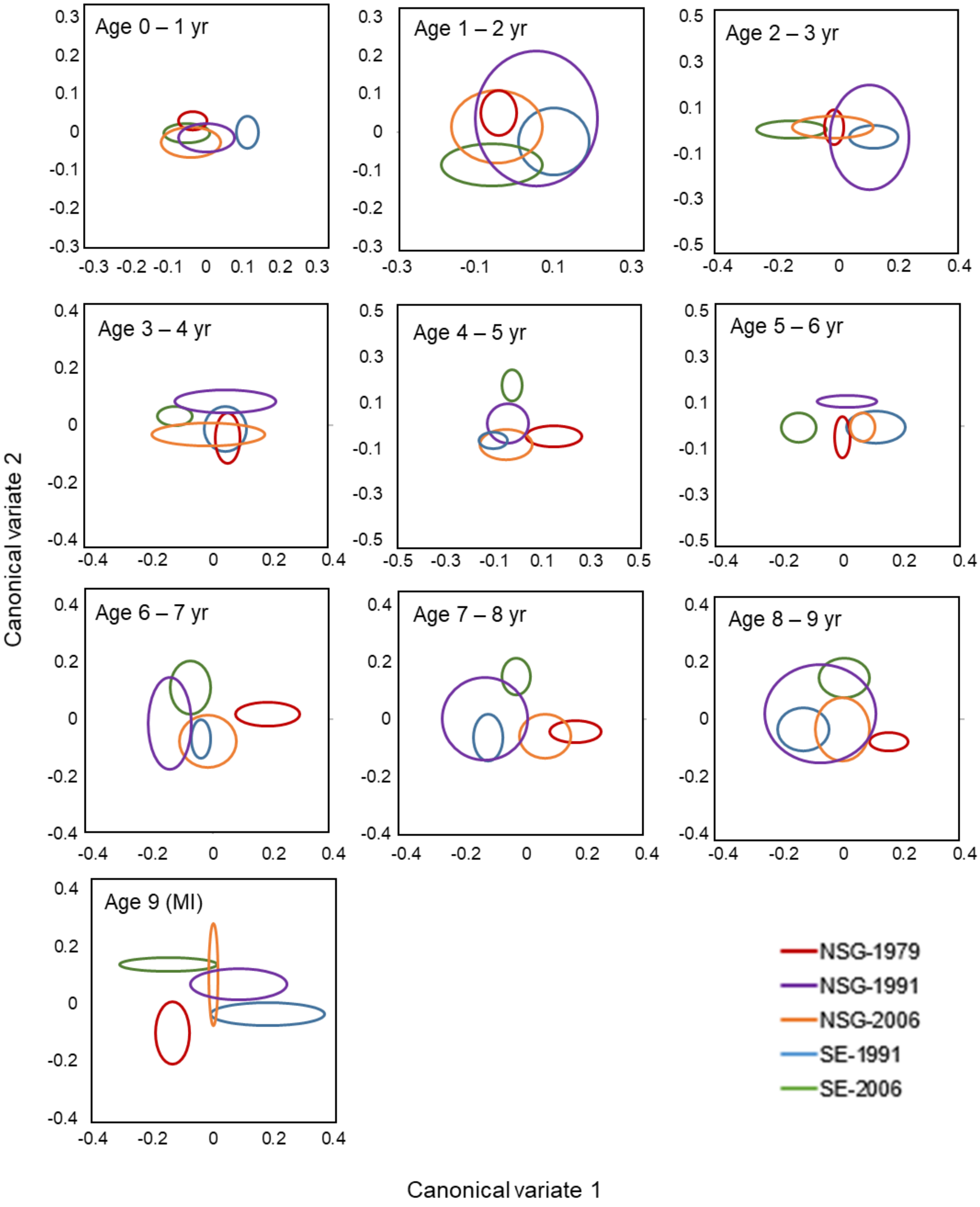

Figure S5.3 – Canonical analysis of principle coordinates (CAP) plot showing variation in chemical signatures in snapper otoliths for two regions (NSG, SE) and 3 cohorts (1979, 1991, 2006) in South Australia. Ellipses represent 95% confidence around group means. Vector diagrams show the direction and weight of individual chemical markers to sample distribution.